INFORMATION TO USERS

BIOSYNTHESIS OF
POLYKETIDES PRODUCED BY MARINE MICROBES

by

Gordon R. Macpherson

Submitted in partial fulfillment of the requirements
for the degree of Doctor of Philosophy

at

Dalhousie University
Halifax, Nova Scotia
September 2001

Canada

DALHOUSIE UNIVERSITY

FACULTY OF GRADUATE STUDIES

The undersigned hereby certify that they have read and recommend to the
Faculty of Graduate Studies for acceptance a thesis entitled "Biosynthesis of
Polyketides Produced by Marine Microbes" by Gordon R. Macpherson in partial
fulfillment of the requirements for the degree of Doctor of Philosophy.

Dated: _____October 18, 2001_____

External Examiner:

Research Supervisor:

Research Supervisor:

Examining Committee
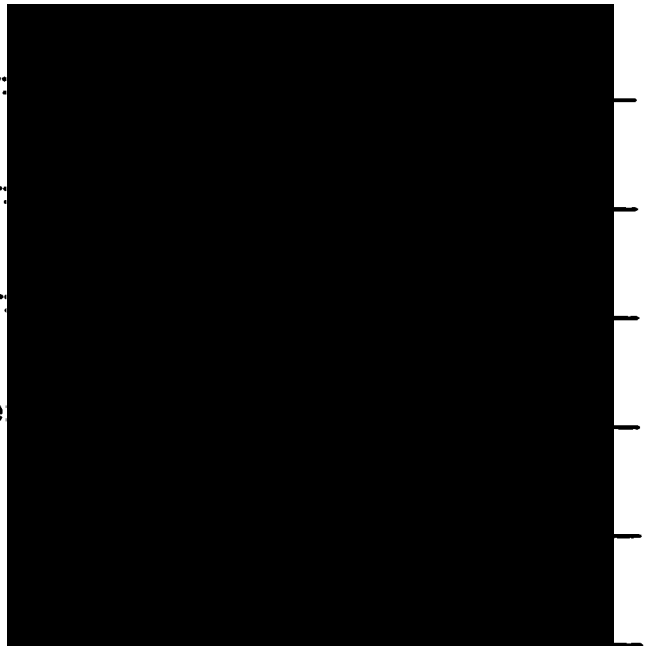
DALHOUSIE UNIVERSITY

DATE: October 29, 2001

AUTHOR: Gordon R. Macpherson

TITLE: BIOSYNTHESIS OF POLYKETIDES PRODUCED BY MARINE

  MICROBES

DEPARTMENT: Biology, Dalhousie University

DEGREE: Doctor of Philosophy   CONVOCATION: May   YEAR: 2001

↙ Gordon R. Macpherson

I dedicate this thesis to all of my family and friends whose love and support guided me during this challenging and fulfilling journey. To my mother and father, Francis and Gordon Macpherson, and to my two sisters, Lynne Anne LaFitte and Tanna Roxborough and their families. I love you all. I also dedicate this work to Dr. David McCorquodale, University College of Cape Breton, who inspired me to pursue a career in science.

TABLE OF CONTENTS

LIST OF FIGURES

xi

LIST OF TABLES

ABSTRACT

The most widely studied of all secondary metabolites, the polyketides (PKs), are low molecular weight compounds assembled via sequential condensations of small carboxylic acids. Biosynthetic and molecular genetic knowledge pertaining to PK production, mostly from studies of terrestrial microbes, have revealed the primary role of polyketide synthase (PKS) enzymes, which condense carboxylic acids to form highly functionalized metabolites. Studies on the biosynthesis of PKs produced by marine species revealed more complex pathways than those encountered in terrestrial species. In this study, we isolated PKS gene fragments from marine isolates of filamentous fungi via degenerate PCR. Phylogenetic comparison with corresponding sequences from terrestrial-derived fungi revealed a dichotomy, (consistent with a previous study involving terrestrial fungi only), between PKSs producing non-reduced (NR) PKs and those producing partially reduced (PR) PKs, but no clear division between sequences from marine and terrestrial fungi. PCR amplification of a PR-type gene fragment from a marine isolate of *Apiospora montagnei* is consistent with the production of an aromatic compound, papulacandin B (PapB) by this species. We have established that PapB is assembled via a PK pathway by way of experiments involving stable isotope precursor incorporation in conjunction with ^{13}C NMR spectroscopy. We extended the investigation to the biosynthesis of PKs of marine dinoflagellates. Although attempts to isolate PKS genes from dinoflagellate DNA or a constructed cDNA library were unsuccessful, stable isotope incorporation studies of DTX-5, a putative PK produced by the dinoflagellate *Prorocentrum maculosum*, 1) established the PK mechanism of its biosynthesis, 2) revealed a rare carbon deletion step and 3) demonstrated the incorporation of an intact amino acid into the structure. Mechanisms are proposed for the biosyntheses of PapB and DTX-5.

ABBREVIATIONS AND SYMBOLS

µg	microgram
µl	microlitre
^{13}C	carbon 13
^{15}N	nitrogen 15
^{18}O	oxygen 18
1D	one dimensional
COSY	correlation spectroscopy
TOCSY	total correlation spectroscopy
HMBC	heteronuclear multiple-bond correlation
HSQC	heteronuclear single quantum correlation
$^{1}J_{CC}$	one bond carbon 13-carbon 13 coupling constant
$^{1}J_{CN}$	one bond carbon 13-nitrogen 15 coupling constant
2D	two dimensional
$^{2}J_{COC}$	two bond carbon 13-carbon 13 coupling constant via oxygen
^{32}P	phosphorus 32
6dEB	6-deoxyerythronolide B
6MSA	6-methylsalycilic acid
6MSAS	6-methylsalycilic acid synthase
A	adenine
a.a.	amino acid
A_{260}	U.V. absorbence at 260nm
$A_{260/280}$	ratio of U.V. absorbence at 260nm and 280nm

Acetyl CoA	acetyl coenzyme A
ACP	acyl carrier protein
AF	aflatoxin
AFB_1	aflatoxin B_1
AIDS	acquired immunodeficiency syndrome
AQ	acquisition time
AT	acyl transferase
b	base
BLAST	basic local alignment search tool
bp	base pair
BTX-B	brevetoxin B
C	cytosine
ca	approximately
cDNA	complementary deoxyribonucleic acid
CoA	coenzyme A
d	days
D	deuterium
D1	delay between end of acquisition and next pulse in many sequences (specific to Bruker software)
dATP	deoxyadenosine triphosphate
DEBS	deoxyerythronolide B synthase
DEPC	diethylpyrocarbonate
DH	dehydratase

DMSO	dimethylsulfoxide
DNA	deoxyribonucleic acid
dNTP	deoxyribonucleoside triphosphate
DSP	diarrhetic shellfish poisoning
DTX	dinophysistoxin
EDTA	ethylenediaminetetraacetic acid
ER	enoyl reductase
ermE	erythromycin self-resistance gene
EST	expressed sequence tag
ExPASy	expert protein analysis system
FA	fatty acid
FAS	fatty acid synthase
G	guanine
h	hour
HGT	horizontal gene transfer
HMQC	heteronuclear multiple-quantum correlation
HPLC	high performance liquid chromatography
HR	highly reduced
Hz	hertz
i	resonance position i
I_0	integrated intensity of unshifted resonance
I_{CH2Cl2}	integrated resonance intensity of CH_2Cl_2 carbon resonance
I_d	intensity of doublet resonance

I_D	intensity of deuterium-retained resonance
I_i	integrated resonance intensity at position i
INADEQUATE	incredible natural abundance double quantum transfer experiment
IPTG	isopropyl-1-thio-β-D-galactopyranoside
I_s	integrated intensity of singlet resonance
kb	kilobase
KR	ketoreductase
KS	ketosynthase
LB	Luria-Bertani
M	molar
MA	malt agar
malonyl CoA	malonyl coenzyme A
MHz	megahertz
min	minute
ml	mililitre
mM	milimolar
MMLV-RT	moloney murine leukemia virus reverse transcriptase
mRNA	messenger RNA
N_2	nitrogen
NA	natural abundance
ng	nanogram
nm	nanometer

NMR	nuclear magnetic resonance
NOE	nuclear Overhauser enhancement
NR	non-reduced
NRPS	non-ribosomal peptide synthase
OKA	okadaic acid
oligo dT	oligo deoxythymidine
O-methyl ST	O-methylsterigmatocystin
ORF	open reading frame
PAGE	polyacrylamide gel electrophoresis
PAM	percent accepted mutation
PapB	papulacandin B
PapC	papulacandin C
PapD	papulacandin D
PCR	polymerase chain reaction
PK	polyketide
PKS	polyketide synthase
polyA$^+$	polyadenosine
PP1	protein phosphatase 1
PP2A	protein phosphatase 2A
PR	partially reduced
psi	pounds per square inch
R	molar ratio
R_{AV}	average retention

RNA	ribonucleic acid
RNaseA	ribonuclease A
RNaseH	ribonuclease H
rpm	revolutions per minute
rRNA	ribosomal RNA
rTaq	recombinant Taq
s	seconds
SAM	S-adenosylmethionine
SD	standard deviation
SDS	sodium dodecylsulfate
SSC	sodium chloride/sodium citrate
ST	sterigmatocystin
SW	spectral width
T	thymine
T4HN	1,3,6,8-tetrahydroxynaphthaline
TAE	tris/acetic acid/ethylenediaminetetraacetic acid
TBE	tris/borate/ethylenediaminetetraacetic acid
TCA	tricarboxylic acid
TE	tris/ethylenediaminetetraacetic acid
TE-SDS	tris/ethylenediaminetetraacetic acid/sodium dodecylsulfate
TLC	thin layer chromatography
U	units
U.V.	ultra violet

V	volts
V/cm	volts per centimeter
X-gal	5-bromo-4-chloro-3-indoyl-β-D-galactopyranoside

ACKNOWLEDGEMENTS

1.0 General Introduction

1.1 Polyketides

The term 'polyketide' (PK) is used to describe natural products assembled from units of small carboxylic acids such as acetate and propionate. Compared with other classes of natural products like the isoprenoids, alkaloids, and shikimate-derived compounds, PKs have arguably been studied the most intensely from several aspects of biology and chemistry. This is largely due to their vast diversity of chemical structures, their range of biological activities that impacts human health [1], and the mystery surrounding their presence in the biological systems that produce them [2]. From a chemical perspective, the most striking characteristic of the PK class of natural products is their structural diversity. The range of structures includes macrolides, macrocycles, aliphatic and alicyclic compounds, as well as simple or complex polycyclic aromatic compounds (Fig. 1). The structural diversity is further heightened by the existence of hybrids composed of PKs condensed with amino acids or peptides, which add further to the range of pharmacological and toxicological activity [3, 4] (Fig, 1).

PKs have been isolated from various sources including bacteria, fungi and to a lesser extent, plants. Many PKs are antibiotics isolated from the actinomycete bacteria, particularly members of the genus *Streptomyces* [5]. Actinorhodin (Fig. 1), for example, is an antibiotic isolated from *Streptomyces coelicolor* [6]. Other bacterial species produce macrolide PKs such as the aglycone of the antibiotic erythromycin, 6-deoxyerythronolide B [7] (Fig. 1).

1

6-methylsalicylic acid (single-ring, aromatic molecule)

Actinorhodin (polycyclic aromatic molecule)

6-deoxyerythronolide B (macrolide)

Lovastatin (reduced, complex molecule)

Myxalamid D (hybrid amino acid/polyketide molecule)

Avermectin B1b (macrocycle)

T-toxin (reduced, linear molecule)

Pristinamycin II$_B$ (hybrid peptide/polyketide molecule)

Example of a chalcone (aromatic polyketide produced by plant species)

Fig. 1: Structures of polyketides isolated from various marine and land-based organisms.

Filamentous fungi are also prolific producers of diverse PKs such as 6-methylsalicylic acid, lovastatin and T-toxin (Fig. 1), many of which exhibit interesting and important biological activity [8]. Chalcone (Fig. 1) and related PKs are a class of aromatic PKs produced by certain plant species [9]. Compared with bacteria and fungi, PK production in plants has been investigated to a lesser extent.

PKs are often described as secondary metabolites. The term "secondary metabolite" refers to compounds whose utility to the producing organism is unknown, since they do not appear to provide a function that is required for growth [2]. This is unlike primary metabolites such as sugars, peptides, proteins, fatty acids, and sterols, which are essential for growth and survival of the producing organism. The maintenance of secondary metabolic biosynthetic genes throughout lineages of taxa is largely unexplained because the selective pressures that determine their evolution are unclear [2]. Although the antimicrobial properties of many PKs implicate competition with other microbes to be the selective pressure required for maintenance of their biosynthetic genes in the population, this explanation cannot be extended to all examples. The evolution of secondary metabolism is a matter of great biological interest as microbes devote significant energy and resources to the biogenesis of products that often appear to have no obvious role for the organism's survival.

Research aimed at understanding the phenomenon of secondary metabolism has resulted in the discovery and characterization of unusual chemical structures and in many cases an understanding of the biosynthetic

pathways that are utilized in their production. Initially, experiments aimed at discerning the biosynthetic origin of secondary metabolites involved feeding labeled precursors to the producing organism in order to obtain labeled metabolites. The location and distribution of the incorporated label was determined either by a series of degradation experiments (for radiotracers) or by analysis of the ^{13}C nuclear magnetic resonance (NMR) spectrum (for magnetic labels) of the labeled metabolite [10, 11]. The latter approach employing stable isotopes and NMR spectroscopy has been particularly productive in uncovering new biosynthetic pathways [10, 11].

Such labeling experiments remain essential to characterize the biosynthetic pathway of a new metabolite. However, in the last number of years, biochemical and genetic approaches have been employed to identify the enzymes and genes involved in secondary metabolism and specifically to unravel the process of PK biosynthesis. Biochemical experiments on cell-free extracts of the patulin-producer *Penicillium patulum* resulted in the isolation of the first critical enzyme for patulin biogenesis, a polyketide synthase (PKS) [12]. This enzyme is responsible for sequentially linking acetate units to form the carbon skeleton of the PK metabolite [12]. More recently, attention has turned towards identification of the genes involved in biosynthesis of PKs, and such studies have resulted in the identification of complete sets of biosynthetic genes for a rapidly growing number of metabolites [13-15]. The identification of these genes, particularly those for the PKS, exposes an opportunity to create novel chemical

structures via engineering of PKS genes. Production of novel structures via manipulation of PKS genes is the focus of extensive review [16-21].

1.2 Polyketide biosynthesis

The term "polyketide" was first used in 1907 by J.N. Collie [22] to describe compounds formed using what he called "the ketide" group (-CH$_2$CO-), which he noted could form a variety of structural types by simple organic reactions. Birch and Donovan [23] later extended this idea into the 'polyacetate hypothesis', which describes the formation of compounds by linkage of acetate units as in fatty acid (FA) biosynthesis. Aromatic compounds could result from aldol-type cyclization of polyketones formed from linked units of acetate [23]. It is now known that PKs are indeed biosynthesized by sequential condensations of simple carboxylic acids such as acetate, propionate and sometimes butyrate [24, 25]. The biosynthetic mechanism is similar to that of FA biosynthesis (Fig. 2). The major differences between FA and PK biosynthesis are the greater variety of acyl precursors used to make PKs, as well as the greater potential for differential ketoreduction, dehydration and reduction after each new extender unit is added to the PK chain (Fig. 2) [2, 24].

The pioneering work by David Hopwood and his colleagues on the biosynthesis and genetics of the antibiotic actinorhodin (Fig. 1) [6, 26, 27] resulted in the cloning of the first PKS gene, along-with several other biosynthetic genes that are associated with actinorhodin production. Subsequent molecular
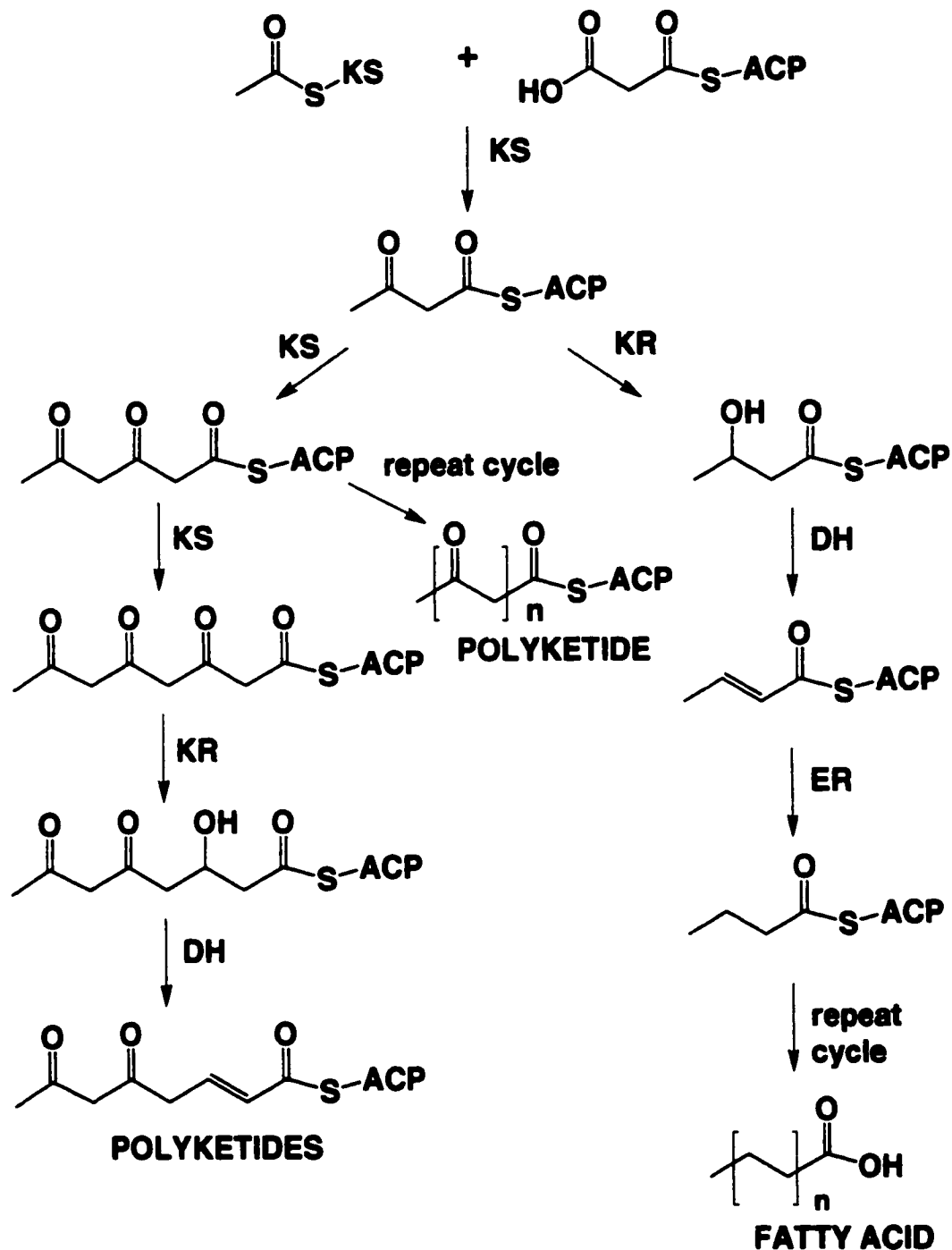
Fig 2: Initial steps in polyketide and fatty acid biosynthesis. Flexibility in the number of acyl condensations, ketoreductions and subsequent dehydration reactions yield a greater diversity of structures during polyketide assembly compared to fatty acid assembly. KS: ketosynthase; ACP: acyl carrier protein; KR: ketoreductase; DH: dehydratase; ER: enoyl reductase. This figure is modified from Bentley and Bennett [25].

genetic studies showed that PKS genes, like fatty acid synthases (FASs) [24], are divided into two main classes: In type I PKS systems, each new extender unit is added to the growing chain under the catalytic influence of separate domains on a series of connected multifunctional polypeptides. The 6-deoxyerythronolide B synthase of Saccharropolyspora erythrea (Fig. 3) is an example of a type I PKS and will be discussed in more detail later. In contrast, the condensation reactions in type II PKS systems are catalyzed by aggregates of individual monofunctional polypeptides that are used re-iteratively [24]. Actinorhodin (Fig. 1) is an example of a PK produced by a bacterial type II PKS [27]. Both type I and type II PKS systems catalyze the synthesis of polyacetates via extension of a starter unit, usually acetate or propionate, with malonyl units derived from acetate (Fig. 2). PK assembly begins when the acyl transferase (AT) transfers the starter acetyl from its CoA ester to the thiol group of the acyl carrier protein (ACP), then to the active site of the β-ketoacyl synthase (KS) where condensation with a malonyl extender unit, now attached to the vacated ACP, occurs. Thus, the chain grows on the ACP as further extender units are added, but is transferred to the KS for each successive chain extension reaction [24]. Depending on the synthase, other catalytic activities that influence the structure of the growing PK include ketoreductases (KR), enoyl reductases (ER), dehydratases (DH), and cylcases. FASs possess all necessary catalytic activities for complete reduction and dehydration of the newly introduced carbonyl groups, whereas PKSs can use none or a variety of these domains, resulting in a greater number of structures [1, 25] (Fig. 2). Further structural
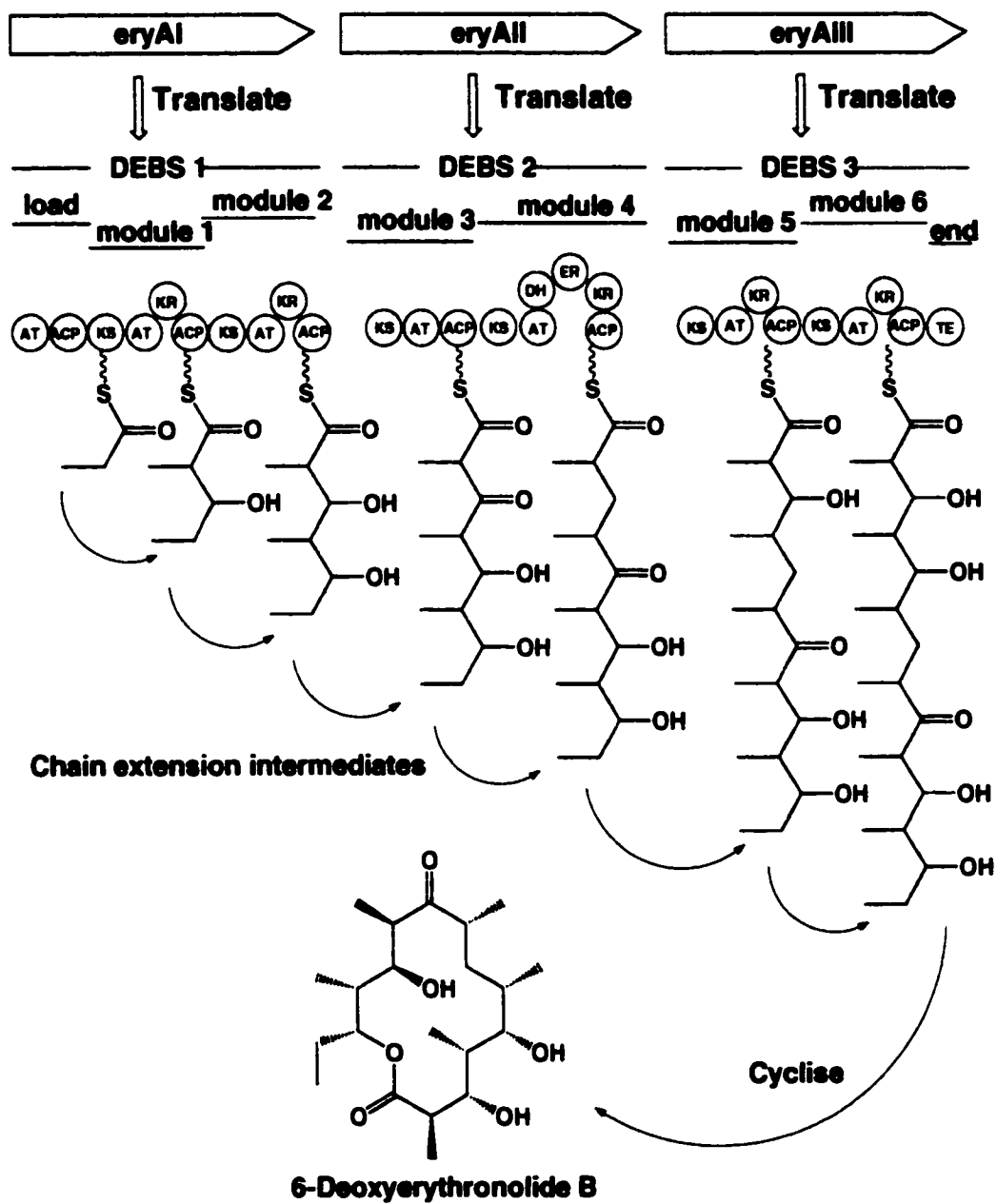
Fig. 3: Construction of 6-deoxyerythronolide B by 6-deoxyerythronolide B synthase. This figure is modified from Hopwood [119].

diversity is introduced by the action of enzymes that alter the nascent PKs. Post-PKS tailoring enzymes are present in many of the PK biosynthetic systems known, and each PK synthase pathway appears to have it's own suite of tailoring enzymes. Examples of PK modifying enzymes include cytochrome P-450s, monooxygenases, methyltransferases, reductases and dehydrogenases. The biosynthesis of sterigmatocystin (ST) (Fig. 4) in *Aspergillus nidulans* for example, requires fourteen post-PKS transformations catalyzed by a series of biosynthetic tailoring enzymes [28].

In addition to PKS systems, PK structural diversity is often augmented by the elaboration of PK structures containing amino acids or peptides within the backbone of the molecule. Such examples are myxalamid D of *Stigmatella aurantiaca* [29] and pristinamycin II_B of *Streptomyces pristinaespiralis* [4] (Fig. 1). Synthesis of these hybrid PK/peptide metabolites involves interaction of PKSs with Non-Ribosomal Peptide Synthases (NRPSs) either as hybrid synthases or as separate enzymes [4]. Hybrid synthases like the myxalamid S synthase, for example, extend an assembled PK chain with peptide or amino acid moieties by channeling the newly formed PK to a specific NRPS module that catalyzes the attachment of the peptide or amino acid to the PK [29] (Fig. 5). Synthesis of hybrid PK/peptide metabolites by separate PKS and NRPS enzymes require specific ligases to join the PK and peptide moieties that were assembled independently [4]. Individual modules of NRPSs catalyze modifications to the elongating peptide including epimerization, cyclization and N-methylation, producing a variety of PK/NRP structures depending upon which modules are
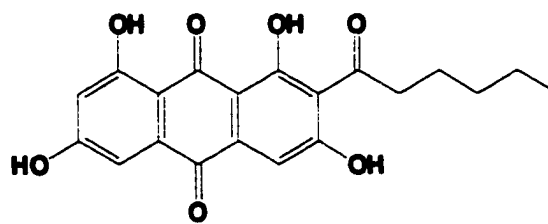
Norsolorinic acid
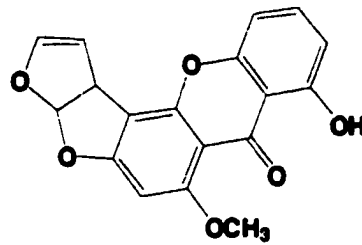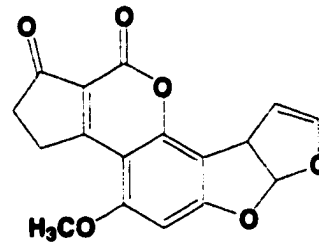
Sterigmatocystin

Aflatoxin B₁

Fig. 4: Structures of norsolorinic acid, sterigmatocystin and aflatoxin B₁.
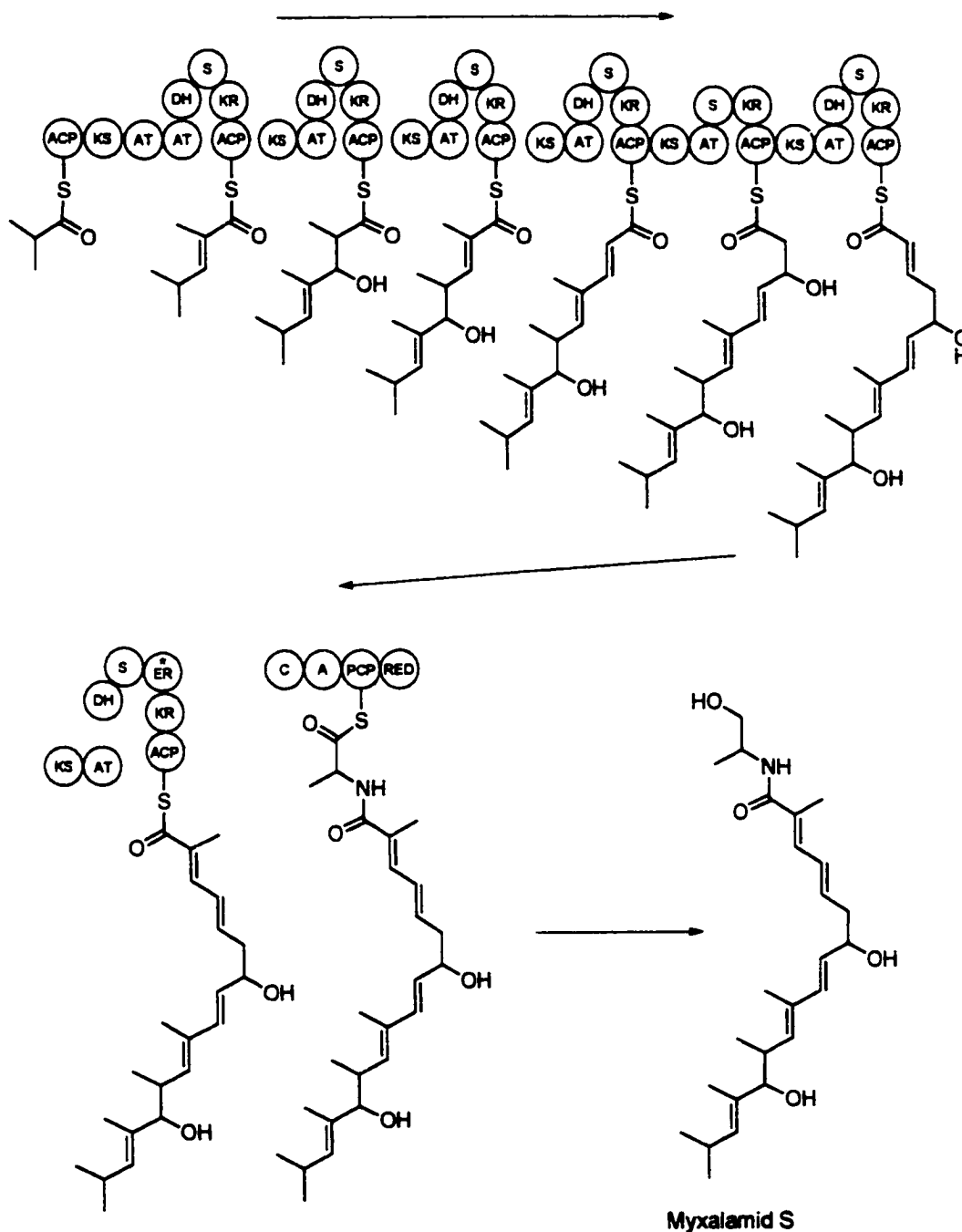
Fig. 5: Biosynthesis of the hybrid polyketide/non-ribosomal peptide metabolite myxalamid S. Domain abbreviations are ACP: acyl carrier protein; KS: ketosynthase; AT: acyltransferase; DH: dehydratase; KR: ketoreductase; C: condensation domain; A: adenylation domain; PCP: peptidyl carrier protein; RED: terminal reductase domain. Arrows indicate the direction of chain growth. This figure is modified from Silakowski *et al*. [29].

present [30]. NRPSs have even been adapted for the production of hybrid PK-peptide structures via co-expression of PKS/NRPS gene hybrid constructs in heterologous host organisms [3, 4, 31].

Although many PKS genes have been isolated and identified, the review presented here is not intended to be comprehensive and only a few representatives from fungi and bacteria will be considered.

1.3 Fungal Polyketide Synthases

The fungal metabolite 6-methylsalicylic acid (6MSA) (Fig. 1) is a precursor to the PK mycotoxin and antibiotic patulin [32] produced by some species of *Penicillium*. It is among the simplest PKs studied to date and is biosynthesized by a type I PKS which uses one molecule of acetyl-CoA and three molecules of malonyl-CoA [12] to assemble the metabolite. The 6MSA synthase was purified by Dimroth *et al.* [12] making it the first microbial PKS purified to homogeneity. Subsequently, a DNA fragment containing the 3' terminus of the 6MSAS gene from *Penicillium urticae* was isolated by Wang *et al.* [33]. This was achieved by hybridization of a mixed oligonucleotide probe derived from the amino acid sequence of the purified synthase to a *Penicillium urticae* genomic DNA library and isolation of clones containing the PKS gene. The 6MSAS gene was the first reported PKS gene sequence from a fungus. As was the case with the PKS gene for erythromycin (*vide infra*) [34], the predicted amino acid sequence of the fungal PKS suggested a domain arrangement as evident from the presence of

KR and ACP regions in close proximity. The amino acid sequences of these domains are more similar to vertebrate FASs than to fungal FASs. It is unlikely, therefore, that the 6MSAS gene evolved from FAS genes in the same species. Concurrently, Beck et al. [35] observed the greater similarity of the 6MSAS gene to vertebrate rather than fungal FAS genes. They isolated the 6MSAS gene by screening a Penicillium patulum genomic DNA expression library with a specific polyclonal MSAS antiserum. Sequencing of the recombinant DNAs in phage that gave a positive immunological response led to the assembly of the 6MSAS gene sequence from overlapping DNA fragments. The 6MSAS protein sequence was deduced from a single open reading frame and contained specific domains that could be matched with sequenced fragments of the intact 6MSAS obtained from a peptidic digest of the pure protein. This confirmed that all active sites required for 6MSA biosynthesis are present on a single multifunctional polypeptide. Beck et al. [35] have proposed a scheme for 6MSA biosynthesis that involves eleven reaction steps catalyzed by seven different enzyme components. Characterization of the 6MSA biosynthetic pathway and the corresponding PKS paved the way for heterologous expression of the 6MSA PKS gene in a bacterial host [36]. Significant amounts of 6MSA were produced in the bacterial host using this approach. The heterologous expression of the 6MSAS gene in a bacterium by Bedford et al. [36] was the first experiment involving the expression of a functional eukaryotic PKS in a prokaryotic host. Production of 6MSA in a host organism that normally does not produce this metabolite supports the idea that new PKs and their synthases from slow growing or low producing organisms

could potentially be mass-produced in model host organisms such as *S. coelicolor* or *E. coli*. More recently, Fujii *et al.* [37] achieved *in vivo* synthesis of the multi aromatic ring fungal PK, 1,3,6,8-tetrahydroxynaphthalene (T4HN), by overexpression of the biosynthetic genes in a heterologous fungus.

Species of filamentous fungi produce the carcinogenic mycotoxins sterigmatocysitin (ST) and aflatoxin B_1 (AFB_1) from the PK precursor molecule norsolorinic acid (Fig. 4) [38]. Because these compounds pose a medical and economic threat to humans, the biological mechanisms governing their biosynthesis are of great interest to scientists involved in agricultural and medical research [39]. Early research on aflatoxins focused on structural characterization and tracer experiments that determined the PK mode of AFB_1 assembly [40]. These isotope incorporation experiments firmly established the PK origin of AFB_1 and its pathway intermediates, while the identification of AFB_1 biosynthetic enzymes and the genes that encode them occurred later. Efforts to purify AFB_1 biosynthetic enzymes from *Aspergillus parasiticus* yielded an O-methyltransferase that converts ST to O-methyl ST, which in turn led to the characterization of the corresponding gene [41]. To date, many genes responsible for ST/AF biosynthesis have been identified by experiments involving mutagenesis of pathway genes. Recombinant clones either expressed the product of a reporter gene, or accumulated AF/ST biosynthetic pathway intermediates, allowing for detection and isolation of the mutated gene [42-49]. As in the case for actinorhodin and other PKs, the AF biosynthetic genes were found to be clustered [43]. Two AFB_1 genes (KS and AT) are located within a 35

kb stretch of the *A. parasiticus* genome, and similarly Yu *et al.* [50] found at least

9 genes involved in AFB₁ biosynthesis within a 60 kb genomic DNA fragment

from *A. parasiticus*. The cluster included genes that encoded a PKS, reductase,

FAS, two dehydrogenases, a methyltransferase and an oxoreductase. Later,

Brown *et al.* [28] sequenced a 60 kb DNA fragment from the ST producer,

Aspergillus nidulans. Twenty-five genes that comprise the entire ST biosynthetic

cluster in this fungus were present on a single stretch of genomic DNA, including

those that encode a PKS, FAS, monooxygenases, dehydrogenases, an esterase,

an oxidase and a DNA binding protein [28]. The reactions catalyzed by enzymes

encoded by post-PKS modification genes in the PKS gene cluster illustrate the

significant role of such reactions in AFB₁ biosynthesis. Post-PKS tailoring

enzymes can therefore modify a relatively simple PKS product, in this case

norsolorinic acid (Fig. 4), to produce a more complex metabolite.

1.4 Bacterial polyketide synthases

Studies of bacterial PKSs are more numerous than those of fungal PKSs

[31]. Biosynthetic and genetic studies involving the antibiotic erythromycin from

Saccharopolyspora erythraea contributed substantially to our understanding of

how PKS systems function, and illustrated the ability to manipulate a PKS in

order to produce compounds of specific design [7, 51, 52]. The first enzyme-free

erythromycin precursor, 6-deoxyerythronolide B (6dEB) (Fig. 1), is assembled by

giant multifunctional polypeptides (type I PKS) in a mechanism that requires six

consecutive cycles of condensation and reduction of small carboxylic acids [34]. Part of the 6-deoxyerythronolide B (DEBS) biosynthetic gene cluster was isolated by screening a *S. erythrea* genomic DNA library with part of the erythromycin self-resistance gene (ermE) which is clustered with the PKS [34]. Sequencing of regions flanking ermE identified an open reading frame (ORF A) that encoded the catalytic domains required for cycles 1 and 2 of 6dEB chain elongation. Bevitt *et al.* [53] later demonstrated that the DEBS cluster encodes three large multidomain polypeptides, each of which catalyzes two cycles of PK chain extension. Surprisingly, the erythromycin biosynthetic genes showed high sequence similarity to vertebrate rather than bacterial FAS genes.

The modular organization of the erythromycin PKS as outlined by Donadio *et al.* [51] is shown in Figure 3. Mutagenesis of specific DEBS KR and ER domains resulted in the production of new 6dEB analogues of predicted structure and provided support for the proposed modular organization of DEBS [51, 54]. Perhaps more significantly, production of a new compound of predetermined structure via mutagenesis of a PKS gene demonstrated the potential of PKS gene manipulation for rational drug design [51, 52]. The ability to design new PKs was augmented by the discovery of the broad substrate specificity of the thioesterase (TE) domain [55, 56], which permitted premature ring closure of the growing 6dEB PK when transferred from DEBS 3 to DEBS 1 [56].

The robustness of DEBS for engineering new analogues was further demonstrated with the construction of a combinatorial library of 6dEB analogues via simultaneous manipulation of multiple catalytic centers of the PKS [57]. In

addition, multiple transformations of a bacterial host with DEBS gene constructs resulted in large libraries of 6dEB analogues [58]. Modifications included the replacement of AT and β-carbon processing domains with heterologous domains from the rapamycin PKS of *Streptomyces hygroscopicus*. In combination, various approaches involving modifications of the DEBS gene have yielded almost 100 analogues of the erythromycin aglycone [58]. The demonstration by Roberts *et al.* [59] that a fully functional 6dEB PKS domain (DEBS 3) can be overproduced in *E. coli* further underscores the potential use of PKS genes for the construction of desired products in heterologous hosts. Expression of engineered PKS genes in heterologous hosts, however, typically results in low yields of the desired metabolite(s). Methods are now being developed to circumvent the problem of low metabolic yields of engineered metabolites. For example, Lombo *et al.* [60] reported a 300% increase in 6dEB yield upon co-expression in *Streptomyces coelicolor* of the DEBS gene with plant enzymes that convert carboxylic acid precursors into their respective CoA thioesters at high efficiency. Until recently, the mechanism by which the growing PK is transferred between the different DEBS proteins during 6dEB biosynthesis was unknown. Tsuji *et al.* [61] recently identified short linker peptides at the carboxy and amino termini of individual modules of modular PKSs, which facilitate transfer of the growing metabolite between modules. Synthesis of new PKs by directed mutagenesis of individual PKS domains, and overexpression of mutant genes in novel hosts are exciting accomplishments for natural products chemistry and drug discovery. Further understanding the structure and function of microbial

PKS genes has profound implications for the characterization, overproduction and manipulation of PKs from organisms that are difficult to isolate and/or culture, such as many marine species.

1.5 Polyketide synthesis by marine organisms

The search for natural products has extended to the oceans, which cover more than 70% of the earth and represent the largest habitat on the planet [62]. Because of their potential as new leads for the pharmaceutical industry, PKs from marine organisms have recently become the focus of considerable attention [63, 64]. Putative PKs have been isolated from a variety of marine macroorganisms including sponges [65-67], molluscs [68], bryozoans [64, 69] and nudibranchs [70, 71] (Fig. 6). However, it is strongly suspected that the PKs isolated from macroorganisms, particularly sponges, are likely of microbial origin [64]. Macroorganisms may acquire PK compounds through associations with PK-producing microbes, either by feeding on them or through symbiotic relationships [64]. The phosphatase inhibitor okadaic acid (Fig. 6), for example, was originally isolated from a sponge [65] and later found to be produced by a dinoflagellate species [72].

Many PKs from marine organisms are implicated in toxic events worldwide [73] while others are showing potential as anticancer, anti-inflammatory, immunostimulatory, antiviral and antimicrobial agents [74]. The structural variety of PKs produced by marine species is an indication that more complex

Okadaic acid (65)(Polyketide from the sponge *Halichondria okadai*).

Baconipyrone D (68)(isolated from the mollusc *Siphonaria baconi*).

Diaulusterol A (71)(Polyketide from the nudibranch *Diaulula sandiegensis*).

Triophamine (77) (isolated from the nudibranch *Triophia catalinae*).

Bryostatin 2 (69)(anticancer compound from the bryozoan *Bagula neritina*).

Altohyrtin A (67)(Potent cytotoxins from the sponge species *Hyrtios* and *Spongia*).

Fig. 6: Putative polyketides isolated from marine macroorganisms.

secondary metabolic enzyme systems operate in these organisms. The structural complexity and medical importance of PKs produced by marine species are generating interest in the enzymatic systems that govern their biosynthesis. However, the necessary isotope labeling experiments to establish a biosynthetic pathway in a marine organism is difficult to perform for several reasons. These include the low yield of metabolites, culturing difficulties, and the uncertainty of efficient precursor uptake – particularly in organisms that are phototrophic. The structural complexity of some marine PKs also presents a challenge in correctly discerning the isotope incorporation patterns. To a large degree these difficulties explain why studies on the biosynthesis of marine PKs are few [75].

Of the marine species studied to date, marine bacteria, fungi and dinoflagellates have been shown to be fruitful sources of PKs, often producing unique chemical structures [76-85] (Fig. 7). The identification of a growing number of unique, biologically active marine bacterial PKs has raised industrial and academic interest in marine microorganisms [86], resulting in discoveries of diverse PKs such as the antibiotic halowanone C [76], and the antiviral compound macrolactin A [77, 78] (Fig. 7). PK diversity within the marine bacteria has also inspired biosynthetic studies on an increasing number of metabolites [75]. For example, the PK oncorhyncolide (Fig. 7), is produced by an unidentified marine bacterial species [83]. Labeling experiments to establish the fate of acetate in the biosynthesis of oncorhyncolide demonstrated the incorporation of seven intact acetate units, confirming its identity as a PK [87] (Fig. 8).
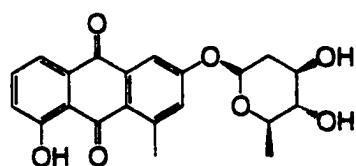
Halowanone C (76)(antimicrobial agent from a *Streptomyces* marine isolate).
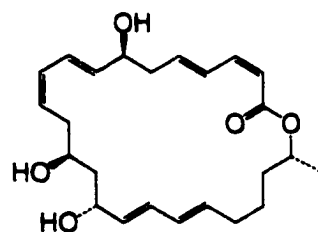
Macrolactin A (77)(antiviral agent from an unidentified deep sea bacterium).
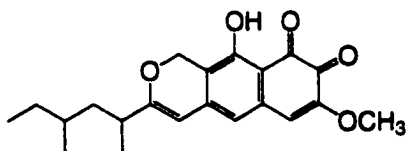
Obionin A (79)(metabolite from the marine fungus *Leptosphaeria obiones*)
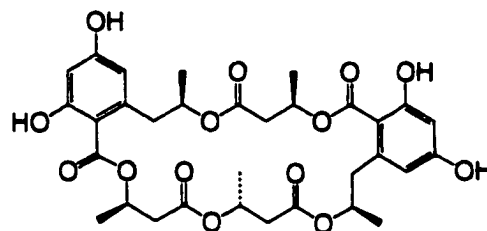
15G256d (80)(antifungal agent from the marine fungus *Hypoxylon oceanicum*).
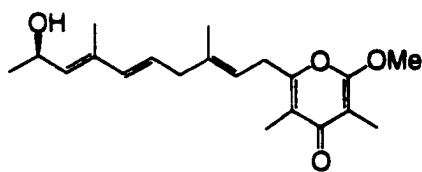
Kalkipyrone (81)(toxin from the cyanobacterium *Lyngbya majuscula*).
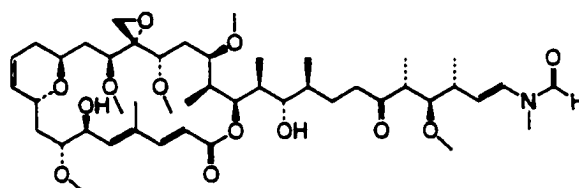
Tolytoxin (82)(polyketide from the cyanobacterium *Scytonema mirabile*)
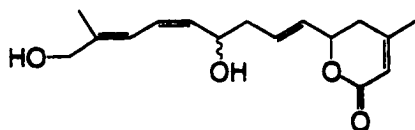
Oncorhyncolide (83)(polyketide from an unidentified marine bacterium)
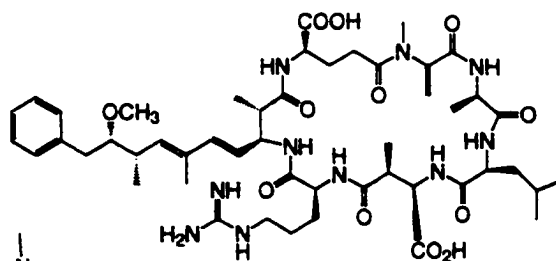
Microcystin (84)(hybrid polyketide/peptide from the cyanobacterium *Microcystis aeruginosa*)
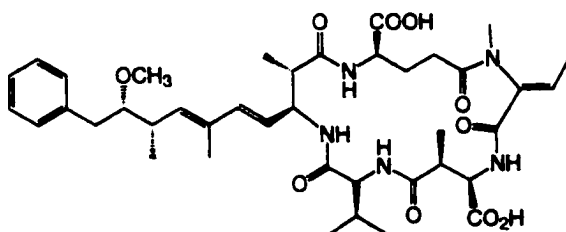
Motuporin (85)(hybrid polyketide/peptide isolated from the sponge *Theonella swinhoi*)

Fig. 7: Examples of polyketides produced by various marine microbes.
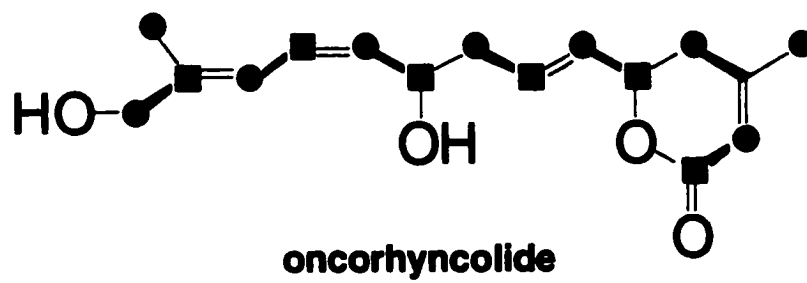
oncorhyncolide

●—■ intact acetate unit

● methyl carbon of acetate

Fig. 8: Incorporation of [2-^{13}C] acetate and [1,2-^{13}C$_2$] acetate stable isotopes into the bacterial polyketide oncorhyncolide.

Interestingly, the pendant methyl groups of oncorhyncolide are derived from the methyl group of acetate. This is unusual, since such methyl groups are generally derived from S-adenosylmethionine (SAM) or by incorporation of a propionate unit in the PK chain. Despite the success with fungal PKs from terrestrial hosts, the effort devoted to the biosynthetic study of marine fungal products is modest, and to the author's knowledge no biosynthetic data are reported at the time of writing. However, the increasing interest in the biology and chemistry of marine fungi isolated from substrates such as marine sediments, submerged wood, sponges and the surface of macroalgae [88] will undoubtedly add to our knowledge and interest of marine microbial products.

Marine and freshwater cyanobacteria produce a variety of PKs, though once again biosynthetic studies have been few. In one notable example, the brackish water cyanobacterial metabolite microcystin (Fig. 7) was shown to be assembled as a hybrid PK/NRP [89]. The microcystin biosynthetic operon of *Microcysitis aeruginosa* was eventually sequenced and shown to encode a hybrid modular PKS/NRPS [90]. Motuporin (Fig. 7), a metabolite structurally related to microcystin, was isolated from a marine sponge and is thought to originate from a marine cyanobacterium [85]. Labeling studies on the biosynthesis of tolytoxin produced by the cyanobacterium *Scytonema mirabile* implicate the unusual involvement of a glycine starter unit subsequently extended by 15 acetate units [82] (Fig. 9). The pendant methyl groups of tolytoxin originate from the tetrahydrofolate C_1 pool in a manner more typical of generating such groups. Though few in number, biosynthetic studies of cyanobacterial
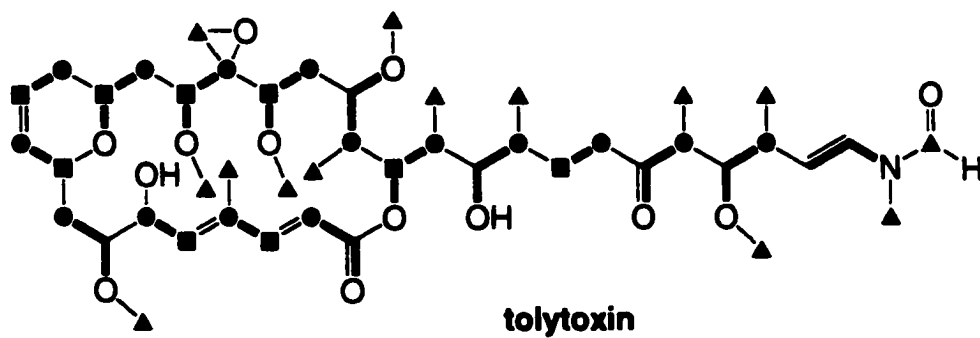
tolytoxin

N‿‿‿ intact glycine unit

▲ methyl carbon from [methyl-^{13}C] methionine

●—■ intact acetate unit

Fig. 9: Incorporation of acetate, glycine and methionine stable isotopes into the cyanobacterial product tolytoxin.

metabolites indicate that production of hybrid PK/amino acid and PK/NRP compounds represent a common event in the secondary metabolism of these organisms.

Another group of marine microbes, the dinoflagellates, are an extremely diverse taxon with the numbers of described species in the thousands [91]. Dinoflagellates are prolific producers of diverse natural products, many of them unique and complex PKs that include polyether ladders, linear polyethers and macrocycles [92]. Putative PKs of various structural types have been isolated from dinoflagellates [93-96], their complexity and unique chemistry surpassing all known PKs from other taxa (see Fig. 10). Though many putative PKs have been isolated from various marine organisms, those from dinoflagellates have received the most scrutiny, both for their bioactivity and their biosynthesis. For toxic species, biosynthetic interest stems from their implication in toxic events resulting in public health and economic effects worldwide [73].

Biosynthetic studies conducted on dinoflagellate PKs have uncovered some unusual trends. Incorporation of ^{13}C-labeled acetate in brevetoxin B, a neurotoxin produced by the dinoflagellate Ptychodiscus brevis [97], resulted in a labeling pattern that is inconsistent with typical PK biosynthesis [98-100] (Fig. 11). For example, pendant methyl groups of BTX-B derive from two different precursors, S-adenosylmethionine (SAM) and the C2 position of acetate (Fig. 11). As mentioned earlier, the derivation of methyl groups from the C2 position of acetate is unusual in PK biosynthesis, but seems to be a trend in dinoflagellate PKs [92, 101]. Also, sequential incorporation of backbone carbons derived from
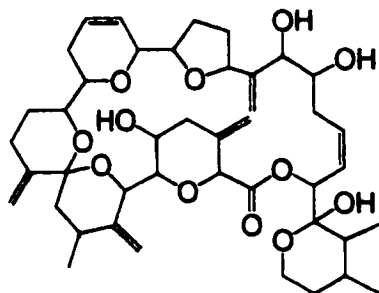
Goniodomin A (93)(potent antifungal agent from the dinoflagellate *Alexandrium hiranoi*).
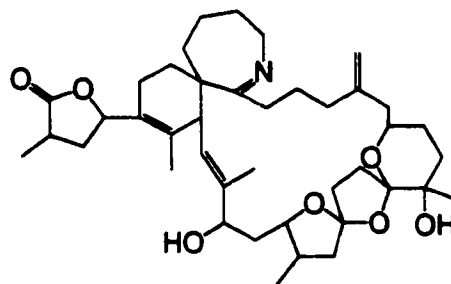
Spirolide B (94)(toxin isolated from shellfish but known to be of dinoflagellate origin).
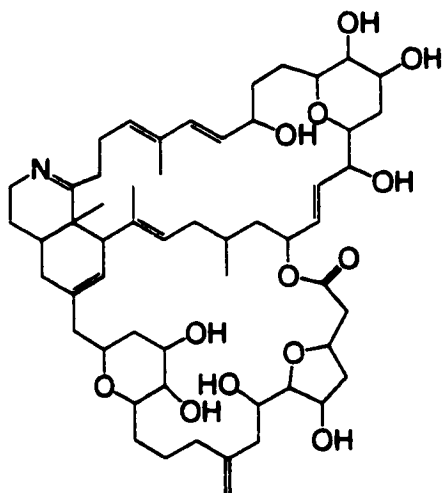
Prorocentrolide A (95)(potent toxin from the dinoflagellate *Prorocentrum lima*).
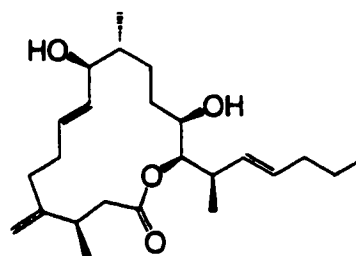
Amphidinolide J (96)(from the dinoflagellate *Amphidinium sp*. This metabolite is toxic against human colon tumor cells).

Fig. 10: Examples of putative polyketide metabolites from dinoflagellates.
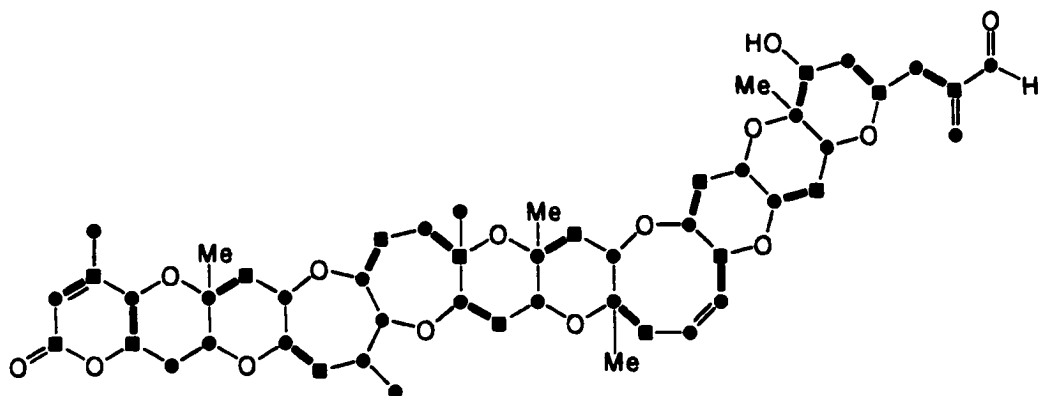
brevetoxin B

● methyl carbon of acetate

■ carboxyl carbon of acetate

●—■ intact acetate unit

Me methionine-derived methyl

Fig. 11: Incorporation of acetate stable isotopes into brevetoxin B.

the C2 position of acetate apparently interrupts the usual PK pattern of intact acetate condensation during BTX-B assembly [98-100] (Fig. 11). The latter labeling pattern was suggested to result from incorporation of acetate methyl-derived precursors from the tricarboxylic acid (TCA) cycle [99, 100]. Labeling patterns similar to that of BTX-B were also obtained in studies of the dinoflagellate metabolites amphidinolides [102, 103] (Fig. 12) and okadaic acid [104-106] (Fig. 13). However, in the case of OKA, loss of C1 acetate derived carbons from the backbone was explained by intervention of Favorski-type rearrangements [107]. Such rearrangements could result in the interruption of intact acetate unit sequences with single carbons from C2 of acetate, and are likely responsible for the labeling patterns observed for BTX-B [99, 100] (Fig. 11) and the amphidinolides [102, 103] (Fig. 12). Deviations from 'typical' PK biosynthetic mechanisms suggest that a unique variety of enzyme systems function to elaborate PK metabolites in certain marine organisms.

While the knowledge of PK biosynthesis and genetics gained by researching terrestrial species has extended our understanding of secondary metabolism, the under-representation of species from marine environments in such studies begs further investigation. The lack of research on marine PK biosynthesis and molecular genetics is surprising in view of the diversity of chemical structures isolated from marine organisms. Although several reasons can be offered to account for this, the fact remains that compared to terrestrial organisms, few marine organisms have been studied directly for the PKs that they produce. Marine species have usually been examined for their ability to
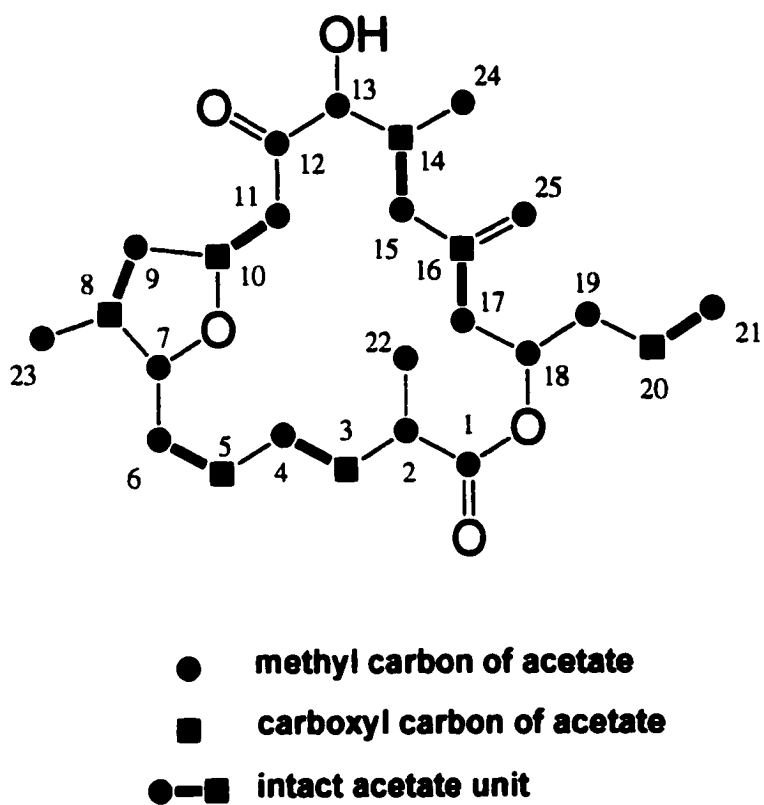
Fig. 12: Incorporation of [1-^{13}C], [2-^{13}C] and [1,2-^{13}C$_2$] acetate into amphidinolide T1. This figure is modified from Kobayashi *et al.* [103].
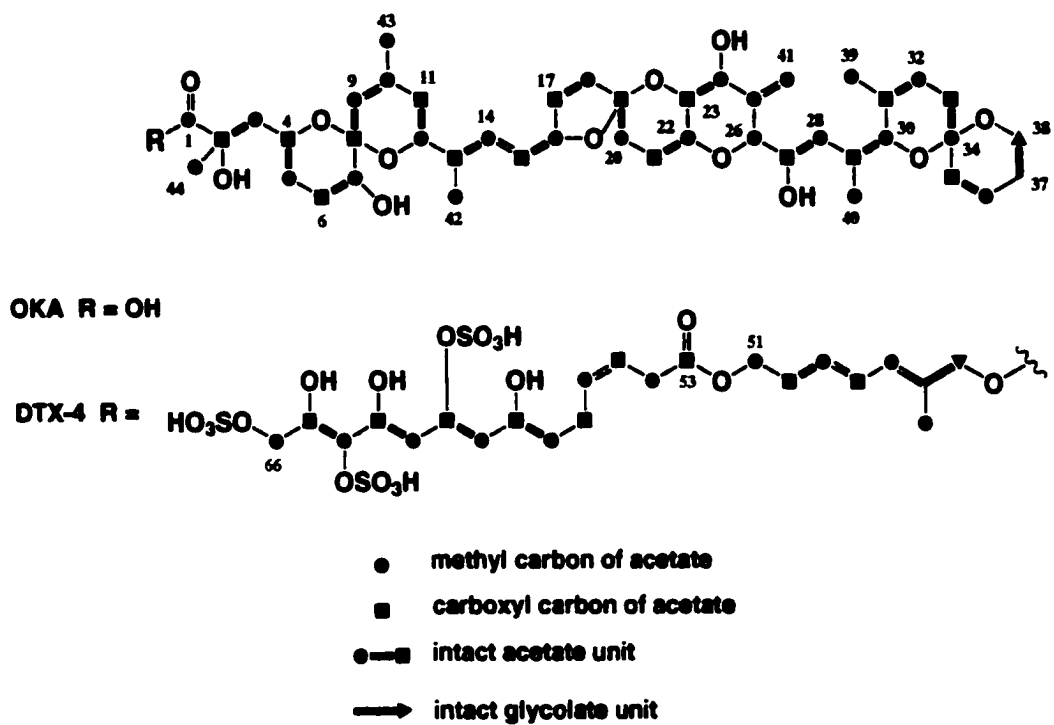
Fig. 13: Incorporation of acetate and glycollate stable isotopes into okadaic acid and DTX-4.

produce biologically active compounds [64 and other reports in this series] rather than to explore how they are made.

The application of molecular genetic techniques to identify and eventually harness the biosynthetic potential of marine organisms is also lacking. Despite the success of this approach with terrestrial microbes, there are few studies on the genetics of marine microbe secondary metabolism, much less PK production. At the time of writing, PK biosynthetic gene sequences have been reported only from two marine bacterial species [13, 108], a cyanobacterium [109] and a marine protist [108]. Clearly there is an opportunity to explore the potential of marine bacteria and fungi for their ability to over-produce new compounds with novel properties or biological activities, as well as the manipulation of genes from marine microbes to produce additional analogues. Despite the promise of novel structural diversity in marine environments, less than an estimated 5% of PK-producing marine species are known [88] or can be cultivated, so this resource remains essentially untapped [86]. Cloning of biosynthetic genes that code for the production of PKs in marine microbes could lead to the heterologous expression of important compounds from organisms that are difficult to culture, as is the case with many marine species. Many of the techniques already developed to study biosynthesis of terrestrial PKs could be successfully applied to marine bacteria or fungi.

Natural products chemists and biologists who are interested in the evolution of secondary metabolism in marine organisms eagerly await the isolation and sequencing of genes responsible for the assembly of complex

marine PKs. A major point of interest from an evolutionary perspective is whether the PKS genes of marine bacteria, fungi and dinoflagellates will more closely resemble those of terrestrial fungi or bacteria, perhaps providing clues with respect to their chemical heritage and their utility to the species that produce them. Recent comparative analysis of marine bacterial and protist PKS genes showed that they share regions of high sequence similarity, indicating lateral gene transfer between these prokaryotic and eukaryotic marine species [108].

Isolation of PKS genes from certain marine taxa is likely to be difficult. Indeed, the genetic diversity between PK-producing marine species is itself a source of difficulty when looking for new PKS genes. Techniques such as polymerase chain reaction (PCR) and molecular hybridizations require that the target DNA sequence is sufficiently similar to a molecular probe or set of PCR primers to permit hybridization to occur. Dinoflagellates are an example of a PK-producing marine taxon for which PKS molecular genetics holds great promise of novel PKS gene discovery. Dinoflagellate genetic organization, however, is enigmatic [110] and characteristics that are seemingly unique to this taxon have precluded the isolation and characterization of their PKS genes [111]. These primarily include the lack of an efficient transformation system, extreme polyploidy and atypical nucleotides that hinder restriction digests [101, 111].

Intimate knowledge of the biosynthesis of a metabolite followed by molecular genetic characterization of the associated biosynthetic tailoring enzymes, may be a useful strategy for isolating PK biosynthetic genes from marine species. Since PKS genes from different species are often too diverse in

structure to allow for detection of dinoflagellate PKS genes using known DNA sequence, it may be necessary to use our knowledge of the tailoring enzymes involved in modification of the pre-formed PK. If one or more of the dinoflagellate PK tailoring enzymes have precedents in systems that are already characterized at the genetic level, their corresponding genes may be more useful as probes or as templates for PCR primer construction. Experiments involving the use of tailoring enzyme genes as probes to isolate PKS genes must be conducted with the assumption that the tailoring genes are clustered with the PKS genes. Also, the degree of sequence diversity between species must be low enough to allow for the construction of useful primer sets and/or molecular probes. Alternatively, purification of PK biosynthetic enzymes may lead to the production of specific probes and/or PCR primers via reverse translation of the amino acid sequence. It may also be possible to generate mutants deficient in production of a particular metabolite and to isolate the mutated locus by detection of a selectable marker produced from a reporter gene. Mutagenesis by recombination would require an efficient transformation system, a technique successfully employed in fungal and bacterial genetics, but not yet available for dinoflagellates [101]. However in this regard, recent progress toward genetic transformation of *Amphidinium* and *Symbiodinium* species is encouraging [112]. Although not a direct approach to identify specific genes, randomly sequencing expressed sequence tags (ESTs) derived from cDNAs of PK producers could result in the isolation of PKS related cDNAs. For example, PKS-related ESTs were isolated from the human parasite *Cryptosporidium parvum* during an EST survey of its genome [113].

In summary, the structural complexity of marine PKs and the unique biosynthetic pathways employed to produce them, underscore the need to identify and characterize the biosynthetic genes. This would offer the possibility that such bioactive compounds could be produced more efficiently in other hosts and add further to the possibility of creating novel PK structures by combinatorial biosynthesis. Hastening the discovery of new PKS genes and their products, would reduce the need to develop and maintain cultures of PK-producing marine species and the necessity of harvesting quantities of scarce wild-type marine species. This thesis compares the biosynthesis of representative PKs from terrestrial and marine species, and discusses the potential for isolating marine PK biosynthetic genes using known PKS gene sequence data derived from terrestrial species.

2.0 Ketosynthase Gene Fragments from Marine Isolates of Filamentous Fungi: Phylogenetic Comparison to Terrestrial Fungal PKS Genes

2.1 Introduction

Interest in polyketide synthase (PKS) gene evolution has increased with the discovery of new PKS gene sequences from diverse taxa. The sequence data help explain why polyketide (PK) production does not correspond with phylogenetic relationships. The discrepancy between taxonomy and PK production in various species has long been noted over the last century by natural products chemists who have isolated PKs from morphologically distinct fungal species [114-116] and from members of even more diverse taxa such as fungi and bacteria [37]. On the other hand, separate isolates of the same species can produce different PKs presumably due to the occurrence of different PKS genes in their genomes [8]. These observations, which seem inconsistent with a vertical mode of PKS gene inheritance in these species, underscore the need to explore other possible mechanisms of PKS gene acquisition such as horizontal gene transfer (HGT) [117, 118]. The large number of available sequences from bacterial sources has facilitated comparative PKS gene analyses in this group, the results of which suggest their origin from duplicated fatty acid synthase (FAS) genes and subsequent distribution via HGT [2, 119]. Since the first PKS gene was sequenced [27], the subsequent explosion of PKS genetic information has mainly been obtained from actinomycetes, with relatively few PKS genes being reported from eukaryotes [8]. This is somewhat surprising considering the

tremendous diversity of secondary metabolites that have been isolated from eukaryotes such as the filamentous fungi [118] and dinoflagellates [101].

Comparative analyses of the few available fungal PKS genes have nevertheless uncovered some noteworthy data. For example, Bingle *et al.* [120] performed phylogenetic analyses of fungal ketosynthase (KS) fragments from 16 terrestrial fungi, the results of which revealed an interesting dichotomy within this group of PKS condensing domains. The dichotomy is between KSs involved in the biosynthesis of PKs such as aflatoxins [38] and spore pigments [37, 121], whose post-PKS carbon structures are non-reduced (NR), and those involved in the biosynthesis of the partially reduced (PR) polyketide 6-methylsalicylic acid [12]. More recently, this analysis was extended [122] to include KSs involved in the biosynthesis of PKs whose post-PKS carbon structure is highly reduced (HR). Examples of HR PKs include the squalestatins [123], lovastatin [124] and T-toxin [125]. Sequence analysis of the biosynthetic genes that code for the production of HR PKs supports a correlation between KS gene sequence and PK backbone structure. This information could potentially be used to predict the nature of the carbon backbone of PK structures produced by PKS genes for which no function has yet been assigned. Likewise, given a PK structure, it may be possible to predict the type of KS responsible for assembly of its carbon backbone.

Using this data, we can begin to examine the distribution of different types of PKSs in various taxa and investigate why apparently morphologically identical fungal species produce different PK metabolites and why different fungal species

often produce the same metabolite. In order to properly assess the affect of environmental diversity on PKS gene evolution, more PKS genes must be isolated and sequenced from species inhabiting diverse environments such as the oceans. To investigate the relationship between PK production and phylogenetic position across environmental boundaries, we have undertaken an analysis of PKS genes from marine fungi. An increasing variety of unique PKs have been isolated from marine species of fungi [88] as well as bacteria [86] and dinoflagellates [101]. Isolation of PKS gene sequences from marine fungi would increase the representation of available eukaryotic PKS genes to ultimately establish a more complete understanding of PKS gene evolution. Marine fungi are good candidates for studying PKS gene evolution because they are known producers of diverse PKs (often with unique chemistry [88]), and genetic data (molecular probes and polymerase chain reaction (PCR) primers [120, 122]) have been generated for PKS genes from their terrestrial counterparts. The ocean represents a vastly different type of environment from land, likely providing selective pressures for inhabiting organisms that are not encountered by terrestrial species. It has been suggested that such different environmental pressures would result in the synthesis of a greater variety of secondary metabolites in marine bacteria [86]. It is reasonable to extend this assumption to marine fungi, particularly in light of their ability to produce unique PKs [88]. Analysis of such genes from marine fungi would reveal whether NR, PR and HR-type PKSs also exist in ocean species and help to establish the effect (if any) that marine environments may have on PKS gene evolution. It may be possible to

predict the type of gene involved in biosyntheses of individual PKs of known structure and/or biosynthesis.

To this end, we have used existing information available for terrestrial fungal PKS genes to isolate new PKS gene fragments from filamentous fungi taken from marine environments. Phylogenetic analyses of these genes and corresponding genes from terrestrial fungi did not reveal a clear dichotomy between marine and terrestrial fungal KSs, but did result in the isolation of KSs of both NR and PR types, which formed distinct clades in constructed phylogenetic trees. Reasons for the existence of KSs of similar sequence in fungi from both environments as well as for the presence of both PR and NR KS forms are suggested. Addressing these questions effectively will help elucidate the evolutionary processes that determine the mode of PKS gene transmission within and/or between lineages.

2.2 Materials and methods

KS gene fragments were amplified by PCR from the DNA of various fungal species isolated from marine environments. Initially, two fungal species known to produce PKs, *Apiospora montagnei* and *Microsphaeropsis olivacea*, were cultured in liquid media. Later, 58 fungal species were grown on solid media and PCR screened for the presence of KS gene fragments as described below.

2.2.1 Culturing of *Apiospora montagnei* and *Microsphaeropsis olivacea*

Small portions of fungal mycelia were removed from the surface of 5 ^{0}C

MA (2 % malt extract, 2 % agar in water) slant cultures and inoculated onto fresh

MA plates. Portions of each freshly grown species were transferred into UC1

(0.14 M glucose, 2.5 %w/v Pharmamedia in distilled, deionized water) medium (6

x 100 ml) and shaken (25 ^{0}C, 200 rpm for 72 h). Aliquots (50 ml) of each UC1

culture were used to inoculate UC2 (2 %w/v molasses, 3 %w/v dextrin white, 1.5

%w/v fish meal, 1.5 %w/v Pharmamedia in distilled, deionized water) broth (1 L).

The cultures were shaken (200 rpm, 25 ^{0}C) for 8 days, harvested by

centrifugation and the wet biomass stored (-80 ^{0}C).

2.2.2 Isolation of DNA from *Apiospora montagnei* and *Microsphaeropsis olivacea*

For each DNA isolation reaction, fungal biomass obtained from either

liquid culture or solid media was ground to a fine powder in liquid nitrogen and a

small portion resuspended in TE-SDS (Tris-HCl, pH 8.0, 10 mM, EDTA 10 mM,

SDS 0.5%, 600 μl). Proteinase K (16.6 U) was added to each reaction prior to

overnight incubation (37 ^{0}C). Excess undigested biomass was removed from

each isolation reaction by centrifugation (15000 x g, 5 min). To eliminate RNA,

RNaseA (3.2 U) was added to each reaction supernatant and these reactions

incubated (37 ^{0}C, 30 min). Each DNA preparation was extracted with 100 %

Tris-saturated phenol (600 µl), centifuged (5000 x g, 5 min) and the aqueous phase collected and extracted with 50 % phenol: 50 % chloroform (600 µl). The aqueous phase from this extraction (containing the DNA) was collected and extracted with 100 % chloroform (200 µl) to remove contaminating protein, carbohydrates and phenol from the previous extraction. The aqueous phase was then isolated and the DNA precipitated with 100 % isopropanol (600 µl). The reactions containing the precipitated DNA were centrifuged (15000 x g, 10 min) and the supernatant discarded. 70 % ethanol (700 µl) was used to wash the pelleted DNA from the previous step. Each DNA pellet was dried and resuspended in sterile distilled, deionized water (50 µl). DNA samples were stored at 5 °C. Presence of DNA was assessed by electrophoresis through a 1 % agarose (USB chemicals) gel at 6.7 V/cm in 1 X TAE (0.04 M Tris-acetate, 0.001 M EDTA) running buffer. 1 µg of 1 kb DNA Ladder (Gibco/BRL) was co-electrophoresed as a DNA size standard.

2.2.3 PCR amplification of ketosynthase gene fragments from *A. montagnei* and *M. olivacea* DNA

Two sets of degenerate PCR primers [120] designed around the enzyme active sites encoded by known fungal KS genes were used to amplify PKS gene fragments from *A. montagnei* and *M. olivacea* DNA. These were LC3 (5'-GCIGARCARATGGAYCCICA-3') and LC5c (5'-GTIGAIGTIGCRTGIGCYTC-3'),

which specifically amplify PR-type genes such as the 6-MSAS gene, and LC1 (5'-GAYCCIMGITTYTTYAAYATG-3') and LC2c (5'-GTICCIGTICCRTGCATYTC-3') which specifically amplify NR-type genes such as those which code for the biosynthesis of spore pigments [120]. Primers were used at the following concentrations: 1 µM (LC1), 0.75 µM (LC2), 1 µM (LC3) and 1.25 µM (LC5c). For each template DNA tested, four reactions were prepared. These included a reaction containing all necessary reagents and both primers, two single-primer control reactions, and a control reaction which included both primers and all other necessary reagents but no template DNA. Reactions (including single-primer and non-template control reactions) were prepared simultaneously as a master mix of the required reagents with the exception of primers and template, which were added separately to the appropriate reaction tubes. Addition of the appropriate volume of master mix, primers and template DNA provided each reaction with 2.5 U of rTaq DNA polymerase (Pharmacia), 0.4 mM dNTPs, the appropriate concentration of each primer and 1 µl of template DNA (concentration not determined). Reactions were prepared using water from aliquots of autoclaved sterile distilled, deionized water that had been stored at -20 ^{0}C in 1.5 ml Eppendorf tubes for single use and disposal. Reactions were cycled in a Perkin-Elmer GeneAmp PCR System 2400 Thermal Cycler starting with an initial denaturation at 94 ^{0}C for 5 min followed by 34 cycles of 94 ^{0}C for 1minute, 55 ^{0}C annealing phase for 1 min and 72 ^{0}C extension for 3 min. A final 10 min incubation step at 72 ^{0}C was included following completion of the 34 cycles.

2.2.4 Agarose gel electrophoresis of PCR reaction products

1 µl of 10 X DNA loading dye (0.25 % bromophenol blue, 0.25 % xylene cyanol FF, 30 % glycerol in water) and sterile, distilled and deionized water (4 µl) were added to aliquots (5 µl) of each PCR. These preparations were electrophoresed through a 1 % agarose gel (1 X TAE buffer, 1h electrophoresis, 6.7 V/cm). 1 µg of 1 kb DNA Ladder (Gibco/BRL) was included on the gel as a DNA size standard. Following electrophoresis, the gel was stained by immersion in ethidium bromide (0.001 M), visualized by U.V. illumination and photographed using a BioRad (Gel Doc) imaging system.

2.2.5 Culturing of 58 fungal species isolated from marine environments

Isolation of PKS genes from *A. montagnei* and *M. olivacea* prompted an investigation of other marine fungal isolates that are maintained at the Institute for Marine Biosciences, Halifax microbial collection. Portions (approximately 1 cm^2) of 58 randomly selected fungal MA slant cultures were used to inoculate separate MA plates that were subsequently incubated at 25 ^{0}C. A control MA plate that was not inoculated with fungi was included. For most cultures, fungal growth was evident after two days. To allow slow-growing isolates to accumulate fungal biomass, DNA was isolated after seven days of growth. To obtain DNA

samples of each fungal species, a small portion of the growing fungal biomass was removed into cell lysis solution (600 µl)(PureGene DNA Isolation Kit, Gentra Systems). DNA was isolated by a protocol designed for extraction of genomic DNA from plant tissue (PureGene DNA Isolation Kit, Gentra Systems) which involved an overnight cell digestion with proteinase K (16.6 U), an RNA degradation step with RNaseA (3.2 U) and selective precipitation of protein and carbohydrates. DNA samples were stored at 5 °C.

2.2.6 PCR screening of fungal DNA samples for ketosynthase gene fragments

Fungal DNA samples were PCR-screened in groups of six for the presence of PKS genes using both LC primer sets. Each set of six PCRs was prepared as a master mix containing all required PCR reagents with the exception of template DNA, which was added separately to each reaction tube. Each individual reaction received *Taq* DNA polymerase (2.5 U, Pharmacia), dNTPs (0.4 mM), the appropriate concentration of each primer and template DNA (10 to 40 ng as estimated by ethidium bromide plate assay) in 1 X Taq DNA polymerase buffer (50 µl). Positive and negative control reactions were prepared along with the other reactions from the same master mixes. Positive control reactions used a previously-amplified PCR product (of known sequence identity as assessed by BLASTx query) as the DNA template. These were amplified from *Penicillium thomii* or *Apiospora montagnei* DNA screened with the

LC1/LC2c (NR) primer set and *Phoma* sp. or *Apiospora montagnei* DNA with the LC3/LC5c (PR) primer set. A template sample obtained by following the DNA extraction protocol using a small portion of media from the control MA plate (not inoculated with fungi) served as a negative control template (hitherto referred to as a "media only" control). Control reactions contained the same concentration of reagents as the non-control reactions with the exception of the change in template.

2.2.7 Agarose gel electrophoresis of fungal PCR products

Aliquots (5 µl) of each PCR reaction were electrophoresed through 1% agarose gels (1 h, 6.7 V/cm). Gels were stained by immersion in ethidium bromide (0.001 M) and visualized/photographed under U.V. light (BioRad Gel Doc system). All reactions prepared and run at the same time were electrophoresed on the same gel, including the positive and negative control reactions for both primer sets. Where PCR product yield was poor, a 1:1000 dilution of the post-PCR reaction in sterile water was prepared and used as a template in a repeat reaction to generate more product. Aliquots of PCR reactions that yielded products in the expected size-range were purified and sequenced.

2.2.8 Purification and sequencing of PCR products

PCR products were purified by centrifugation (30 min, 1000 x g) through size-exclusion columns (Centricon-100, Millipore) to eliminate protein, dNTP and primer dimer/multimer contaminants. DNA concentrations in the purified reactions were determined by U.V. absorbance (A) at 260 nm and purity both by observation of the $A_{260/280}$ ratio which equals 1.8 for pure DNA [126] and by agarose gel electrophoresis. PCR products were sequenced in both forward and reverse directions using the degenerate forward and reverse PCR primers from the initial amplification reaction. Each 20 μl sequencing reaction consisted of 100 ng template DNA and 50 ng of the appropriate primer in cycle sequencing reactions (PE Applied Biosystems) using the buffer and BigDye Terminator PCR reagents supplied by the manufacturer. Cycle sequencing parameters consisted of a 96 ^{0}C initial denaturation followed by 25 cycles of 96 ^{0}C for 10 s, 50 ^{0}C for 5 s and 60 ^{0}C for 4 min prior to a final incubation at 4 ^{0}C. The DNA in each reaction was precipitated with ethanol, resuspended in STOP solution (10 mM EDTA, 83.3 % formamide, 3 μl) and denatured at 96 ^{0}C for 2 min. Samples were electrophoresed (20 hours, 2500 V) through a 6 % polyacrylamide (Longranger, Mandel) gel in 0.5 X TBE (0.045 M Tris-borate, 0.001 M EDTA, pH 8) on an Applied Biosystems 373 DNA sequencer. Quality of the sequence was determined by observation of the sequencing chromatogram (Sequencher software) and where possible, ambiguities corrected. Sequences were identified

by query against the GenBank database using the Basic Local Alignment Search Tool (BLASTx) algorithm [127].

2.2.9 Phylogenetic analysis of conceptual translations of ketosynthase gene sequences from terrestrial and marine fungi

The DNA fragments obtained in this study were analyzed for similarity to other fungal KS sequences of terrestrial fungal origin previously submitted to the databases. Potential encoded protein sequence was deduced from DNA sequence using the ExPASy translation tool (Canadian Bioinformatics Resource, Canada). Deduced protein sequences for each reading frame were queried against GenBank to identify which reading frame coded for KS. Presence of the known KS active site motif GPxxxxxxxCxSxL [34] was required for acceptance of a reading frame in deducing the protein sequence. To ensure all sequences used in phylogenetic analyses were of equal length (342 bases/114 a.a.), each sequence was clipped at a distance of 210 bases upstream of the 5' end of the active site and 90 bases downstream of the 3' end. This was done to prevent bias in the phylogenetic analyses that might be generated by sequence length differences. This sequence length covers the maximum sequence available for the products obtained in this study. ClustalW [128] was used to generate a local alignment of sequences obtained in this study along with available terrestrial fungal KS protein sequences obtained from sequence databases using the

Sequence Retrieval System (Canadian Bioinformatics Resource, Canada). Subsequent phylogenetic analyses were generated using the Phylip software package (J. Felsenstein, University of Washington). Bootstrap resampling was used to generate 100 data sets using the program SEQBOOT. Each data set was converted into a distance matrix using the program PROTDIST via the PAM distance method. Neighbor-joining trees were generated from the distance matrices using the program NEIGHBOR and these assembled into a consensus tree using the program CONSENSE. Parsimony analysis of the bootstrapped data sets was performed using the program PROTPARS and the resulting data sets assembled into a consensus tree using CONSENSE. TREEVIEW (R.D.M Page, University of Glasgow) was used to display the resulting trees. For both neighbor-joining and parsimony trees, the *Streptomyces coelicolor* ActI protein sequence was chosen as an outgroup to root the tree since actinomycete PKS genes are assumed to be ancestral to eukaryotic PKS genes [119].

2.2.10 Dot blot analyses of fungal PCR products

Dot blot experiments were performed to test for hybridization between KS PCR products and various fungal genomes that yielded KS PCR products in this study. Fungal DNA dot blots were prepared by denaturing aliquots (10 µl) of each fungal DNA sample (10-40 ng as estimated by ethidium bromide plate assay) at 95 ^{0}C for 10 min, addition of 20 X SSC (3 M sodium chloride, 0.3 M sodium citrate, 10 µl) and spotting aliquots (6 µl) of each denatured sample on

Hybond N+ (Amersham) membrane. DNA was fixed to the membrane by immersion in sodium hydroxide (0.4 M, 20 min) and washing in 5 X SSC as recommended in the Hybond N+ DNA Dot Blot protocol (Amersham). Between 8 ng and 46 ng of probe DNA were included as a positive control and λ DNA or 1 kb DNA Ladder (Gibco/BRL) (1 μg) was spotted on the same membrane to serve as a negative control. Fluorescently labeled KS probes (AlkPhos Direct DNA Labeling Kit, Amersham/Pharmacia Biotech) were prepared from fungal KS-related PCR products following the protocol recommended by the manufacturer. Blots were hybridized in a Techne Hybridizer (Mandel Scientific) at various temperatures ranging from 70 °C to 50 °C in separate hybridization reactions and the blots exposed to film (Labscientific Inc.) for 30 min, 60 min and several hour time intervals.

2.3 Results

2.3.1 Amplification of A. montagnei and M. olivacea KS gene fragments

Single PCR products in the expected 700-800 bp size-range [120] were amplified from A. montagnei and M. olivacea DNA with KS gene-specific primers (Fig.14). PCR with A. montagnei DNA using the LC3/LC5c primer pair, which is known to amplify PR-type KS fragments such as the KS involved in 6-MSAS biosynthesis [35, 120], yielded a single product of approximately 700 bp. This primer pair did not amplify a product from the DNA of M. olivacea. The LC1/LC2c
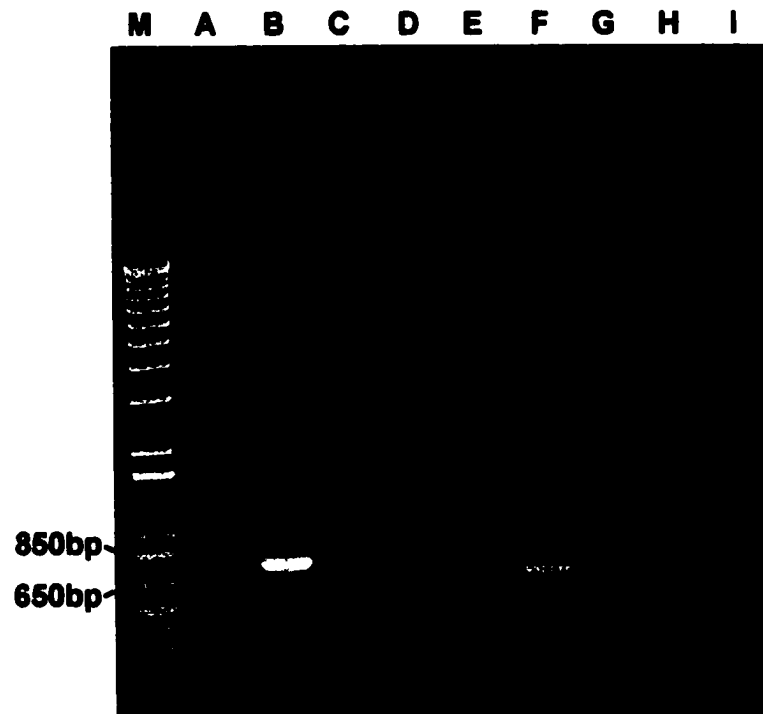
Fig.14: 1% agarose gel showing PCR products amplified from
Apiospora montagnei and *Microsphaeropsis olivacea* DNA. M) DNA size
markers; A) empty lane; B) LC1/LC2c primers + *M. olivacea* DNA; C) LC1
primer only + *M. olivacea* DNA; D) LC2c primer only + *M. olivacea* DNA;
E) LC1/LC2c primers no template control; F) LC3/LC5c primers +
A. montagnei DNA; G) LC3 primer only + *A. montagnei* DNA; H) LC5c primer
only + *A. montagnei* DNA; I) LC3/LC5c primers no template control.

primer pair, which is known to amplify NR-type KS fragments such as the KS responsible for spore pigment and aflatoxin biosynthesis [120], amplified gene fragments (700 bp) from the DNA of *A. Montagnei* (not shown) and *M. olivacea* (Fig. 14). No product was amplified in any of the single primer or template-free control reactions for either primer set, suggesting that the products from the double primer reactions are not single-primer artifacts or the result of contamination from a source other than the fungal DNA tested. The products amplified from the DNA of *A. montagnei* and *M. olivacea* were sequenced from both ends and each product queried against sequences in GenBank using the BLASTx algorithm. Each product had high sequence similarity to fungal KS sequences in GenBank. As expected, the LC3/LC5c product amplified from *A. montagnei* DNA had highest similarity to the 6MSAS KS (PR-type) (E value = 2e-69) while the LC1/LC2c products from *A. montagnei* and *M. olivacea* DNA had highest similarity to KSs involved in spore pigment (NR-type) biosynthesis (E value = 3e-93).

2.3.2 PCR screening of fungal DNA for ketosynthase genes

Of 58 marine fungal isolates obtained for screening, 50 were successfully cultured as summarized in Table 1. Fig. 15 is an example of the agarose gel electrophoresis results from one set of six species whose DNA was screened by PCR with both LC primer sets. PCR screening of DNA from available species with the LC primer sets yielded products in the expected 700-800 bp size range

Table 1: Ketosynthase-related DNA fragments amplified from marine isolates of filamentous fungi.

FUNGAL ISOLATE	GROWTH (Y/N)	LC1/2C PROD (Y/N)	LC3/5C PROD (Y/N)	FUNGAL ISOLATE	GROWTH (Y/N)	LC1/2C PROD (Y/N)	LC3/5C PROD (Y/N)
Acremonium strictum	Y	N	N	Mortierella isabellina	Y	N	N
Acremonium/Verticillum sp.	Y	Y	N	Mucor sp.	Y	N	N
Alternaria alternata	Y	Y	N	Nigrospora oryzae	N	NA	NA
Alternaria tenuissima	Y	Y	N	Nodulisporium sp.	Y	N	N
Apiospora montagnei	Y	Y	Y	Penicillium commune	Y	Y	N
Arthrinium sp	Y	Y	N	Penicillium helicum	Y	Y	N
Ascophyllum restricus	Y	N	N	Penicillium thomii	Y	Y	N
Aspergillus fumigatus	N	N	N	Periconia minutissima	Y	Y	N
Aspergillus niger	Y	Y	N	Pestalotia sp.	Y	Y (2 products)	N
Aureobasidium pullulans	Y	N	N	Pestalotiopsis sp.	Y	N	N
Bipolaris sp	Y	N	N	Phialophora fastigata	Y	N	N
Botrytis cinerea	N	NA	NA	Phoma sp.	Y	N	Y
Botryophaephora sp.	Y	Y	N	Pithomyces chartarum	N	NA	NA
Chaetomium globosum	N	NA	NA	Pseudeurotium zonatum	Y	Y	N
Cladosporium sp	Y	Y	N	Pycnidia	Y	N	N
Cunninghamella sp	Y	Y	N	Scolecobasidium sp.	Y	N	N
Cylindrocloeum sp.	Y	Y	N	Sordaria fimicola *	Y	Y	N
Dendryphiella sp.	N	NA	NA	Sporormia sp.	Y	N	N
Dicholomyces cepae	Y	Y	N	Sporormiella minima	Y	N	N
Didymosphaeria enata	Y	N	N	Stemphylium sp.	Y	Y	N
Eladia saccula	N	NA	NA	Tolypocladium cylindros	Y	N	N
Endoxyla sp.	Y	Y	N	Tolypocladium nivea	Y	N	N
Fusarium oxysporum	Y	N	N	Tolypocladium niveum	Y	N	N
Geotrichum/Candida sp	Y	Y	N	Trichoderma hamatum	Y	N	N
Gliocladium roseum	Y	N	N	Trichoderma polysporum	Y	N	N
Gymnoascus sp.	Y	Y	N	Truncatella engustata	Y	N	N
Microascus longirostris	N	NA	NA	Ulocladium chartarum	Y	N	N
Microsphaeropsis olivacea isolate 1	Y	Y	N	Westerdykella sp.	Y	Y	N
Microsphaeropsis olivacea isolate 2	Y	Y	N				

Footnote: * terrestrial derived species obtained from Edna Staples, Dalhousie University, Halifax, Nova Scotia.
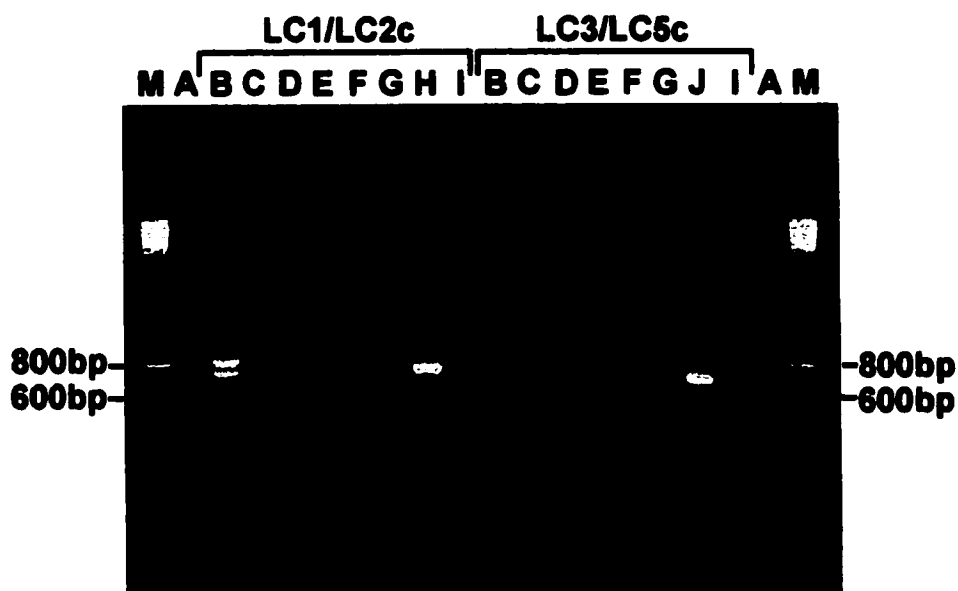
Fig. 15: 2% agarose gel showing the results of PCR-screening of DNA from six marine fungal isolates using ketosynthase-specific primers. DNA from all six fungal isolates were screened with both primer sets in separate reactions as indicated above the gel. M) DNA size markers; A) empty lane;

B) *Pestalotia* sp.; C) *Mucor* sp.; D) *Geotrichum/Candida* sp.;

E) *Tolypocladium nivea*; F) *Trichoderma polysporum*; G) *Microsphaeropsis olivacea*; H) *Penicillium thomii* amplified KS fragment (sequence verified positive control); I) media only (no template) negative control; J) *Phoma* sp. amplified KS fragment (sequence verified positive control).

from a total of 26 fungi (Table 1). Sequencing reactions using these products as templates and the appropriate LC primer as the sequencing primer resulted in quality data of various read lengths for 24 templates. All 24 sequences were compared to sequences in Genbank via the BLASTx algorithm and all had high sequence similarity to known fungal KS sequences. For eight of these, the read length was below the previously established sequence length cut-off of 342 bases (114 a.a. when translated) for phylogenetic analyses and therefore were not investigated further. Sequencing reactions which did not work at all or gave short sequence reads may be due to the presence of impurities left over from the template purification protocol. In some cases, the presence of two or more templates of similar length was evident from the sequencing chromatogram. These are assumed to either originate from distinct loci within the genome or from different alleles at individual loci. This is not surprising as individual fungi have been reported to produce more than one structurally distinct PK [129] whose biosyntheses are likely coded for by distinct PKS genes. Likewise, biosynthesis of the fungal PK lovastatin involves two distinct PKS genes [124].

2.3.3 Phylogenetic comparison of marine fungal KS sequences to known fungal KS sequences isolated from terrestrial environments

A local alignment of conceptual translations of PCR product sequences obtained from marine fungal isolates in this study with fungal KS sequences in

the databases was prepared using ClustalW (Fig. 16). This alignment demonstrates that the sequences form two major groups, PR-type KS and the NR-type KS, with varying degrees of variation within groups. The active site consensus sequence is highly conserved throughout all groups with the active site cysteine present in all sequences. Variable residues within the active site differ to various degrees between species. Phylogenetic analyses were performed to further establish relationships between the sequences. Neighbor-joining and parsimony methods were used to analyze multiple bootstrapped data sets of the deduced protein sequence data of KS sequences from 18 marine-isolated fungal species. These represent the total number of sequences obtained that were of sufficient length as established previously. Both the neighbor-joining (Fig. 17) and parsimony (Fig. 18) analyses group the sequences into two major clades consistent with the occurrence of the two major groups observed in the sequence alignment (Fig. 16) and from similar analyses reported previously for terrestrial fungal KSs [120]. Neither analytical method resulted in a clade containing marine fungal products exclusively. Rather, the marine species' KSs formed clades with KSs from various terrestrial fungi. All sequences obtained in this study with the exception of the A. montagnei PR-type sequence (AmontLC35c) branched with the NR clade. Some species' sequences branched with KSs from different genera rather than with members of their own genus. Interestingly, on both neighbor-joining (Fig. 17) and parsimony (Fig. 18) trees, a sub-clade occurred within the NR clade that contains five marine fungal species' KSs branching together with low bootstrap support. On the neighbor-joining tree

Fig. 16: Alignment of conceptual translations of ketosynthase (KS) gene sequences from marine (shown in uppercase letters) and terrestrial (shown in lowercase letters) fungal isolates. Residues are boxed if 85% or higher of the sequences compared have the same amino acid at this position. The active site is indicated with a line and the active site cysteine with an asterisk. Database accession numbers are given where sequences not analyzed by Bingle *et al.* [120]. Terrestrial fungal sequence identities are as follows: ppatulmsas (*Penicillium patulum* MSAS); penicifrei (*Penicillium frei* KS); aterremsas (*Aspergillus terreus* MSAS); aparapksp1 (*Aspergillus parasiticus* pksP1); phomalc35c (*Phoma* sp. MSAS-type); ppatulpks2 (*P. patulum* PKS2, EMBL U89769); anidupksst (*Aspergillus nidulans* pksST); aparapksl1 (*A. parasiticus* pksL1); sordarfimi (*Sordaria fimicola*, terrestrial isolate, Dalhousie University, Halifax, Canada); clagpks1ks (*Colletotrichum lagenarium* PKS1); phosplc12c (*Phoma* sp. LC1/LC2c product); aparasitic (*A. parasiticus* Genbank accession AJ132275); aparamajor (*A. parasiticus* major product); pgriseoful (*Penicillium griseofulvum* KS EMBL AJ132274); ppatuLC12c (*Penicillium patulum* LC1/LC2c product); anidulanwa (*A. nidulans* WA); aparaminor (*A. parasiticus* minor product); afumialb1p (*Aspergillus fumigatus* alb1); cheterpks1 (*Cochliobolus heterostrophus* PKS1); ScoeliAct1 (*Streptomyces coelicolor* act1 KS). Marine fungal sequence identities are as follows: AMONTLC35c (*Apiospora montagnei* LC3/LC5c PR type KS); DICHOTOCEJ (*Dichotomyces cejpii* NR type KS); PENICOMMU (*Penicillium commune* LC3/LC5c PR type KS); PERICONMIN (*Periconium minutissima* LC3/LC5c PR type KS); CLADIOSPSP (*Cladiosporium* sp. LC3/LC5c PR type KS); PENICHELIC (*Penicillium helicum* LC3/LC5c PR type KS); PENICTHOMI (*Penicillium thomi* LC3/LC5c PR type KS); APIOSPMONT (*Apiospora montagnei* LC3/LC5c PR type KS); ARTHRINISP (*Arthrinium* sp. LC3/LC5c PR type KS); ENDOXYLASP (*Endoxyla* sp. LC3/LC5c PR type KS); PSEUDERZON (*Pseudeurotium zonatum* LC3/LC5c PR type KS); STEMPHYLSP (*Stemphylium* sp. LC3/LC5c PR type KS); ASPERGNIG (*Aspergillus niger* LC3/LC5c PR type KS); MOLIVLC12c (*Microsphaeropsis olivacea* LC3/LC5c PR type KS); WESTERDYSP (*Westerdykella* sp. LC3/LC5c PR type KS).

```
ppsumass        1   - S L E V A S E A L E D A G I - P A K S L S G S D - - - T A V F W G V
penctd          1   - S L E V A S E A L E D A G I - P A K C L S G S D - - - T A V F W G V
stmemass        1   - S L E V T W E A L E D A G I - P P Q S L S G S E - - - T A V F M G V
apsadsp1        1   - A L E V T W E A L E N A G I - P L S S L S G S D - - - A A V F M G V
AMONTLC35C      1   - S L L R R G K P S R T R V Y - D P K S L S G S D - - - T A V F M G V
phomat35c       1   - G L E V T W E A L Q N P G I - N P K S L A G S D - - - T A V Y I G V
ppsulpis2       1   - A L E V A W E A L E N A G I - S P S R L A G S D - - - T S V Y M G V
PERICONMIN      1   - - S L P L M R L W K C L A M C Q T E L A L H S S T E L V H F M D R P
PENICCOMMU      1   G X W R L L M K H W R W Q A S F L T P R L P H R K T A L E F S M A - P
antdupksst      1   - - L M S T Y E A M E R G G I - V P D T T P S T Q R N R I Q V F H G V
apsmipksi1      1   - - L M S T Y E A M E R A G L - V P D T T P S T Q R D R I Q V F H G V
CLADIOSPSP      1   - - - F S V P Q K L S I K P V S V P D R S S S T Q K P R V G V Y F G C
ENDOXYLASP      1   - - L X T A Y X A L E M S G Y - X P N R T P S T K L D R I G T F Y G Q
sordarimi       1   - - P Q Q P T R H W R C L D T - V P N R T P S T K L D R I G T F Y G Q
ARTHRINISP      1   - - L T T A Y E A L E M S G Y - V P N R T P S T R L D R I G T F Y G Q
APIOSPMONT      1   - - L T T A Y E A L E M S G Y - V P N R T P S T R L D R I G T F Y G Q
dagpis1ks       1   - - L T T A Y E A L E M C G Y - V P N R T P S T R L D R I G T F Y G Q
phospic12c      1   - - L T T A Y E A L E M S G Y - V P N R T A S T R L D R I G T F Y G Q
STEMPHYLSP      1   - - L T T A Y E A L E M S G Y - V P N R T P S T K L E R I G T F Y G Q
PSEUDERZON      1   - - L T T A Y E A L E M S G Y - V P N R T P S T K L H R I G T F Y G Q
ASPERGINIG      1   - - L T T A Y E A L E M S G Y - V P N R T P S S K L E R I G T F Y G Q
MOLIVLC12C      1   - - L T T A Y E A L E M S G Y - V P N R T P S S K L E R I G T F Y G Q
WESTERDYSP      1   - - L V T A Y E A L E S S G Y - V P N R T P S T Q L N R I G T F Y G Q
apsmstic        1   - - L V T A Y E A L E M S G Y - V G N R T R S T T L S R I G T F Y G Q
apsamajor       1   - - L V T A Y E A L E M S G Y - V G N R T R S T T L S R I G T F Y G Q
ppsesotu        1   - - L L T A Y E A L E M A G F - I P D S T P S T Q K N R V G V F Y G M
ppsuLC12c       1   - - L L T A Y E A L E M A G F - I P D S T P S T Q K N R V G V F Y G M
PENICTHOMI      1   - - L L T A Y E A L E M A G F - I P D S T P S T Q K N R V G V F Y G M
PENICHELIC      1   - - L L T A Y E A F E M A G F - I P D S T P S T Q K N R V G V F Y G M
antdulamwa      1   - - L L T A Y E A L E G A G F - V P D S T P S T Q R D R V G I F Y G M
apsaminor       1   - - L L T A Y E A L E M A G F - I P D S T P S T Q R D R V G L F Y G M
alumsib1p       1   - - L L S A Y E A L E M A G F - V P N S S P S T Q R D R V G I F M G M
DICHOTOCEJ      1   - - - H T I N S L A S S R D F L W A D K R R L S R - - Q F G A R H R D
chsterpis1      1   - - - E C S Y E A F E N S G T - P M S K I V G T D - - - T S V F V S S
ScosiAct1       1   - L D P D T L D P A R V G V S L G S A V A A A T S L E R E Y L L L S D

ppsumass       31   N S D D Y S K L V L E D L P N V E A W M G I - - G T A Y C G V P N R I
penctd         31   N S D D Y S K L V L E D L P N V E T W M G I - - G T A Y C G V P N R I
stmemass       31   N S D D Y S K L L L E D I P N V E A W M G I - - G T A Y C G V P N R I
apsadsp1       31   N S D D Y G K L L L E D L P H V E P W M G I - - G T A Y C G V A N R I
AMONTLC35C     31   N S D D Y N K L L L E D L P N V D A W M G I - - G T A Y C G V P N R I
phomat35c      31   H S D D Y S R L L L E D I P N I E A W M G I - - G T T A H G I P N R I
ppsulpis2      31   N S D D Y G K L V L E D L T G V G A H M G V - - G T A Y C G I P S R I
PERICONMIN     34   A T I G V R S M P R R - - M W T P T L S L V - - A S A P - L D Q G R I
PENICCOMMU     35   V M I I V R T A V R - - - T L T H T L F L A - - A I V R - S H P G R I
antdupksst     33   T S N D W M E T N T A - - Q N I D T Y F I T - - G G N R G F I P G R I
apsmipksi1     33   T S N D W M E T N T A - - Q N I D T Y F I T - - G G N R G F I P G R I
CLADIOSPSP     33   T S N D W M E T N S A - - Q D I D T Y F I P - - G G N R A F I P G R I
ENDOXYLASP     33   T S D D W R E I N A X - - Q E V D T Y F I T - - G G V R A F G P G R I
sordarimi      33   T S D D W R E I N A A - - Q E V D T Y F I T - - G G V R A F G P G R I
ARTHRINISP     33   T S D D W R E I N A A - - Q E V D T Y Y I T - - G G V R A F G P G R I
APIOSPMONT     33   T S D D W R E I N A A - - Q E V D T Y Y I T - - G G V R A F G P G R I
dagpis1ks      33   T S D D W R E I N A A - - Q E V D T Y Y I T - - G G V R A F G P G R I
phospic12c     33   T S D D W R E I N A A - - Q E V D T Y F I T - - G G L R A F G P G K I
STEMPHYLSP     33   T S D D W R E I N A A - - E N I D T Y F I T - - G G V R A F A P G R I
PSEUDERZON     33   T S D D W R E I N A A - - E N I D T Y F I T - - G G V R A F A P G R I
ASPERGINIG     33   T S D D W R E I N A A - - E N V D T Y F I T - - G G V R A F A P G R I
MOLIVLC12C     33   T S D D W R E I N A A - - Q N V D T Y F I T - - G G V R A F A P G R I
WESTERDYSP     33   T S D D W R E I N A A - - E N V D T Y F I T - - G G V R A F A P G R I
apsmstic       33   T S D D Y R D V N A A - - Q D I G T Y F I T - - G G I R A F G P G R I
apsamajor      33   T S D D Y R D V N A A - - Q D I G T Y F I T - - G G I R A F G P G R I
ppsesotu       33   T S D D Y R E V N S G - - Q D I D T Y F I P - - G G N R A F T P G R I
ppsuLC12c      33   T S D D Y R E V N S G - - Q D I D T Y F I P - - G G N R A F T P G R I
PENICTHOMI     33   T S D D Y R E I N S G - - Q D I D T Y F I P - - G G N R A F T P G R I
PENICHELIC     33   T S D D Y R E I N S G - - Q D I D T Y F I P - - G G N R A F T P G R I
antdulamwa     33   T S D D Y R E I N S G - - Q D I D T Y F I P - - G G N R A F T P G R I
apsaminor      33   T S D D Y R E I N S G - - Q D I D T Y F I P - - G G N R A F T P G R I
alumsib1p      33   T S D D Y R E I N S G - - Q D I D T Y F I P - - G G N R A F T P G R I
DICHOTOCEJ     31   L L H W W H S C F W P C K S V A A L L T R - - L R L T K S E K G R I
chsterpis1     29   F A T D Y T O M L W R D P E S V P M Y O C T N S G F S R S N L A N R I
ScosiAct1      35   S G R D W E V D A A W L S R H M F D Y L V P - - - - S V - - M P A E V
```

Fig. 16

```
                    *
          ┌──────────────────────────┐
ppeaumeas   64  S Y H L N L M G P S T A V D A A C A S S L V A I H H G V Q A I R L G E
penicfial   64  S Y H L N L M G P S T A V D A A C A S S V V A I H H G V Q A V R L G E
aternemes   64  S Y H L N L M G P S T A V D A A C A S S L V A I H L G R Q A I L Q G E
asparadsp1  64  S Y H L N L M G P S T A V D A A C A S S L V A I H H G R Q A I L S G E
AMONTLC35C  64  S Y H L N L M G P S T A V D A A C A S S L V A I H H G R Q A I M M G E
phomacc35c  64  S Y H L N L M G P S A A V D A A C A S S L V A V N S G Q Q A I L A G K
ppeauips2   64  S Y L L D L M G P S V A L D A A C A S S L V A V H H A R Q A I R A G E
PERICONMIN  64  N Y H F G F S G P S F N I D T A C S S S M A A I Q L A C T S L W A K D
PENICCOMMU  64  N Y H F K F S G P S V S V D T A C S S S L S A I H M A C N S L W K N D
anduplast   64  N F C F E F S G P S Y S N D T A C S S S L A A I H L A C N S L W R G D
asparaps1   64  N E C F E F A G P S Y T N D T A C S S S L A A I H L A C N S L W R G D
CLADIOSPSP  64  N Y H F K F S G P S Y T I D T A C S S S L T A I H L A C N A L W R G E
ENDOXYLASP  64  N Y H F G F S G P S L N I D T A C S S S A A A L Q V A S T A L W A R D
sordarimi   64  N Y H F G F S G P S L N V D T A C S S S A A A L Q V A S T A L W A R D
ARTHRINISP  64  N Y H M G F S G P S L S I D T A C S S S A A A L Q V A C T S L W V K D
APIOSPMONT  64  N Y H M G F S G P S L S I D T A C S S S A A A L Q V A C T S L W V K D
asgpks1ks   64  N Y H F G F S G P S L N I D T A C S S S A A A L N V A C N S L W Q K D
phospic12c  64  N Y H F G F S G P S L N I D T A C S S S A A V L Q I A C T S F W A K D
STEMPHYLSP  64  N Y Y F K F S G P S Y S V D T A C S S S I L A A I Q L A C T S L W A G D
PSEUDERZON  64  N Y Y F K F S G P S Y S I D T A C S S S I L A A I Q L A C T S L W A G D
ASPERGINIG  64  N Y Y F K F S G P S Y S I D T A C S S S I L A A I Q L A C T S L W A G D
MOUVLC12C   64  N Y Y F K F S G P S F S I D T A C S S S I L A A I Q L A C T S L W A G D
WESTERDYSP  64  N Y Y F K F S G P S F S I D T A C S S S I L A A I Q L A C T S L W A G D
aparastic   64  N Y Y F K F S G P S F S I D T A C S S S I L A A I Q L A C T S L W S G D
aparamajor  64  N Y Y F K F E G P S F S V D T A C S S S L A A I Q L A C T S L W S G D
pgrieoti    64  N Y Y F K F S G P S V S V D T A C S S S I L A A I H V A C N S L W R N E
ppeauLC12c  64  N Y Y F K F S G P S V S V D T A C S S S I L A A I H V A C N S L W R N E
PENICTHOMI  64  N Y Y F K F S G P S V S V D T A C S S S I L A A I H V A C N S L W R N E
PENICHELIC  64  N Y Y F K F S G P S V S V D T A C S S S I L A A I H I A C N S L W K N D
anduanva    64  N Y Y F K F S G P S V S V D T A C S S S I L A A I H L A C N S I W R N D
aparaminor  64  N Y Y F K F S G P S V S V D T A C S S S I L A A I H M A C N S I W R N D
alumabi1p   64  N Y Y F K F S G P S V S V D T A C S S S I L A A I H L A C N A I W R N D
DICHOTOCEJ  64  N Y F F K F S G P S Y S V D T A C S S S I L A A I Q L A C T A I W N G E
cheterpis1  64  S Y S F D L K G P S V L V D T A C S G L T A L H L A C Q S L L V G D
ScoelAct1   64  A W A V G A E G P V T M V S T G C T S G L D S V G N A V R A I E E G S


ppeaumeas   99  S K V A I V G G V N A L C G P G
penicfial   99  S Q V A I V G G V N A L C G P G
aternemes   99  S E V A I V G G V N A L C G P G
asparadsp1  99  S K V A I V G G V N A I F G P G
AMONTLC35C  99  S K V A I V G G V N A L L G P G
phomacc35c  99  S R V A I V G G V N V C L S P A
ppeauips2   99  T D L A I A G G V N A L L G P G
PERICONMIN  99  C D T A V V G G L S C M T N S D
PENICCOMMU  99  C D T A I I A G G T N V L T N P D
anduplast   99  C D T A V A G G T N M I F T P D
asparaps1   99  C D T A V A G G T N M I Y T P D
CLADIOSPSP  99  V D T A I I G G T N V L T N P D
ENDOXYLASP  99  C D T A I V G G L S C M T N P D
sordarimi   99  C D T A I I V G G L S C M T N P D
ARTHRINISP  99  C D T A I I G G L S C M T N S D
APIOSPMONT  99  C D T A I I G G L S C M T N S D
asgpks1ks   99  C D T A I V V G G L S C M T N P D
phospic12c  99  C D T A V V G G L S C M T N P D
STEMPHYLSP  99  C D T A C A G G L N V L T N P D
PSEUDERZON  99  C D T A C A G G L N V L T N P D
ASPERGINIG  99  C D T A C A G G L N V L T N P D
MOUVLC12C   99  C D T A C A G G L N V L T N P D
WESTERDYSP  99  C D T A C A G G L N V L T N P D
aparastic   99  C D T A V T G G L S V L T S P D
aparamajor  99  C D T A V T G G L S V L T S P D
pgrieoti    99  S D S A V A G G V N I L T N P D
ppeauLC12c  99  S D S A V A G G V N I L T N P D
PENICTHOMI  99  C D S A V A G G V N I L T N P D
PENICHELIC  99  C D S A V A G G V N I L T N P D
anduanva    99  C D T A I T G G V N I L T N P D
aparaminor  99  C D A A I A G G V N I L T N P D
alumabi1p   99  C D T A I S G G V N L L T N P D
DICHOTOCEJ  99  C D T A V A G G L S I L T S P D
cheterpis1  99  V R Q A L A A G S S L I L G P E
ScoelAct1   99  A D V M F A G A A D T P I T P I
```

Fig. 16

58

ScoeliActl — *Streptomyces coelicolor*
70 ┌ PpatulPKS2 — *Penicillium patulum*
├ AterreMSAS — *Aspergillus terreus*
23 ┌ AMONTLC35c — *Apiospora montagnei*
19 ┌ PhomaLC35c — *Phoma sp.*
24 └ AparapksPl — *Aspergillus parasiticus*
16 Penicifrei — *Penicillium frei*
49 PpatulMSAS — *Penicillium patulum*

PR type KS

ChaterPKSI — *Cochliobolus heterostrophus*
63
61 DICHOTOCEJ — *Dichotomyces cejpii*
42 PENICCOMMU — *Penicillium commune*
PERICONMIN — *Periconia minutissima*
62 CLADIOSPSP — *Cladosporium sp.*

NR type KS

94 ┌ AnidupksST — *Aspergillus nidulans*
└ AparapksL1 — *Aspergillus parasiticus*
33
32 95 PENICHELIC — *Penicillium helicum*
89 PENICTHOMI — *Penicillium thomii*
85 88 PpatulC12c — *Penicillium patulum*
Pgriseoful — *Penicillium griseofulvum*
40 Aparaminor — *Aspergillus parasiticus*
43 AnidulanWA — *Aspergillus nidulans*
AfumiAlb1p — *Aspergillus fumigatus*
37 96 Aparamajor — *Aspergillus parasiticus*
Aparasitic — *Aspergillus parasiticus*
78 45 ClagPKS1KS — *Colletotrichum lagenarium*
97 APIOSPMONT — *Apiospora montagnei*
87 ARTHRINISP — *Arthrinium sp.*
28 PhospLC12c — *Phoma sp.*
88 Sorderfimi — *Sordaria fimicola*
60 ENDOXYLASP — *Endoxyla sp.*
24 PSEUDEURZON — *Pseudeurotium zonatum*
50 STEMPHYLSP — *Stemphylium sp.*
66 42 ASPERGNIG — *Aspergillus niger*
MOLIVLC12c — *Microsphaeropsis olivacea*
WESTERDYSP — *Westerdykella sp.*

10

Fig. 17: Phylogenetic analysis of ketosynthase fragments from various marine and terrestrial fungal isolates by neighbor-joining. Abbreviations are as described in the legend to Fig. 16. Boxes indicate sequences obtained from marine isolates in this study. Putative PR and NR-type KSs group into distinct clades indicated above and below the dividing line respectively.
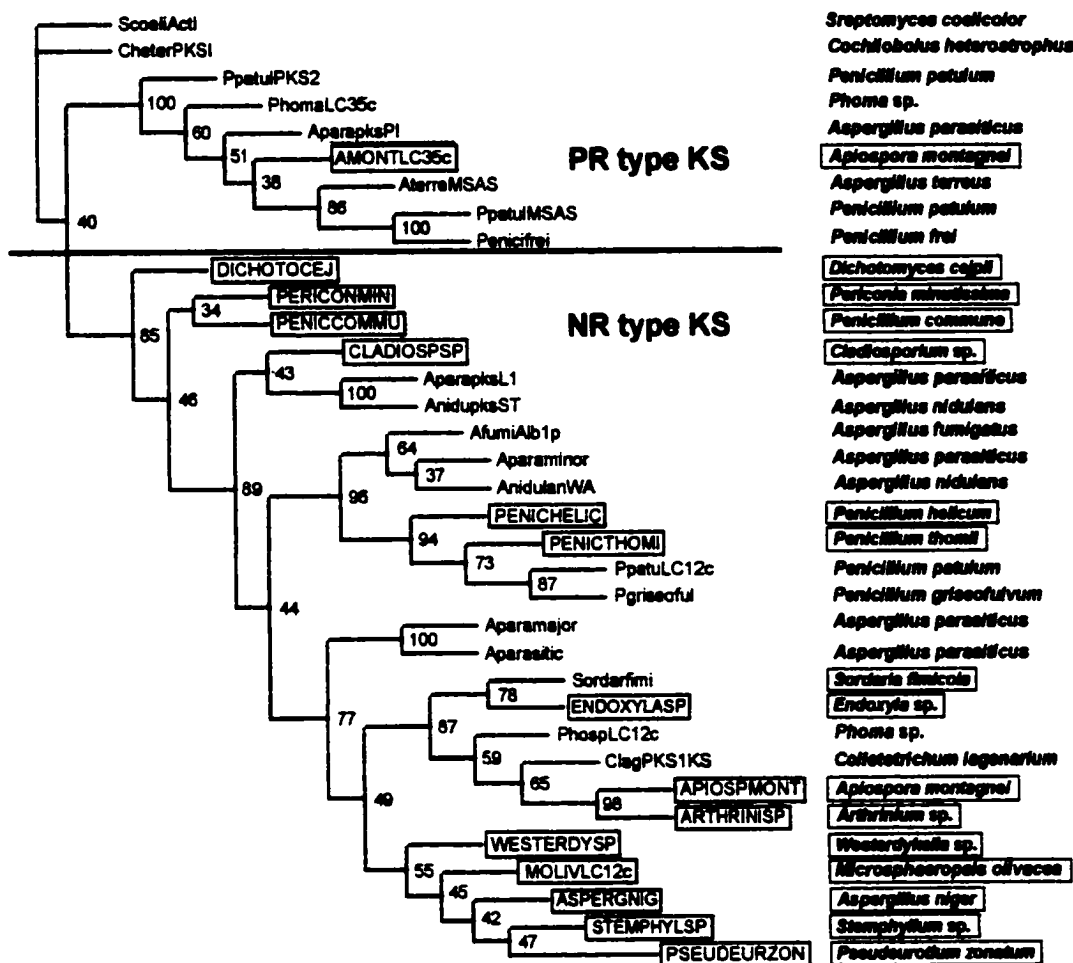
Fig. 18: Phylogenetic analysis of ketosynthase fragments from various marine and terrestrial fungal isolates by parsimony. Abbreviations are as described in the legend to Fig. 16. Boxes indicate sequences obtained from marine isolates during this study. Putative PR and NR-type KSs group into distinct clades shown above and below the dividing line respectively.

(Fig. 17), bootstrap support values between nodes within the PR clade were lower on average (33.5 +/- 21.4 S.D.) than those within the NR clade (62.5 +/- 24.7 S.D.). On the parsimony tree (Fig. 18), bootstrap support values were slightly higher on average between nodes of the PR clade (72.5 +/- 26.5 S.D.) than between nodes of the NR clade (67.8 +/- 22.5 S.D.).

2.3.4 Dot blot hybridization of fungal KS gene probes to fungal DNA

Fluorescently labeled probes prepared from fungal KS-related PCR products were hybridized to various fungal DNAs from which KS PCR products were amplified (see Fig. 19). Most of these reactions resulted in hybridization between the probe and several fungal DNA samples at various intensities. Optimum hybridization temperature was between 50 ^{0}C and 55 ^{0}C. Below 50 ^{0}C, negative control DNA samples bound probes resulting in faint signals due to non-specific hybridization. In most cases, 3 h to overnight exposure of the film was required for detection of signal in all samples except for positive controls (short exposures of less than 1 h were sufficient in these cases). Unequal amounts of fungal DNA were spotted on the membrane because of difficulty determining DNA concentrations by absorbance measurement. Agarose gel electrophoresis of the fungal DNA samples revealed differential quantities of DNA in each sample spotted (not shown). Probes prepared from Periconia minutissima, Verticillium sp., Sordaria fimicola and Apiospora montagnei (PR and NR-type respectively) PCR products hybridized at 50 ^{0}C to several of the fungal DNAs tested, including
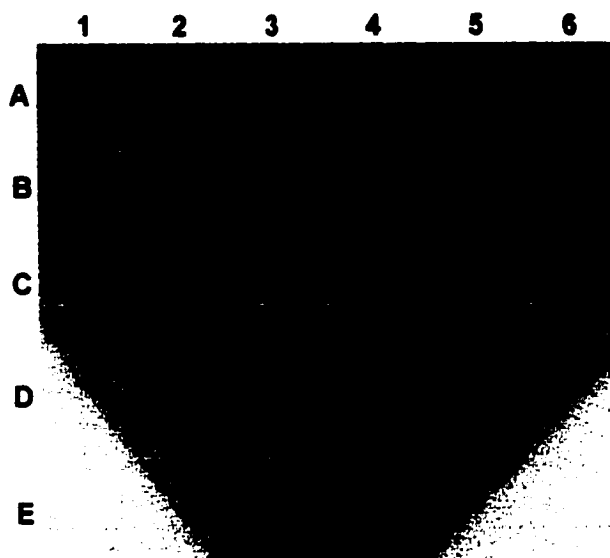
Fig. 19: Dot blot hybridization of *Apiospora montagnei* LC3/LC5c PCR product probe (MSAS-type) to genomic DNA from various marine fungal isolates at 50°C. A1) *Cladiosporium* sp.; A2) *Periconia minutissima*; A3) *Endoxyla* sp.; A4) *Alternaria tenussima*; A5) *Alternaria alternata*; A6) *Aspergillus nidulans*; B1) *Phoma* sp. B2) *Westerdykella* sp.; B3) *Phoma* sp.; B4) *Verticillium* sp; B5) *Pseudeurotium zonatum*; B6) *Microsphaeropsis olivacea*; C1) *Apiospora montagnei*; C2) *Penicillium helicum*; C3) *Cylindrogloem* sp.; C4) *Gymnoascus* sp.; C5, C6, D1, D2, D3, D4 and D6 are blank (no DNA spotted); D5) 1μg 1kb DNA ladder (negative control), E3 and E4) *A. montagnei* LC3/LC5c PCR product DNA (positive control). 6μl of each DNA sample (concentration not determined) was spotted except for the positive control DNA of which 28ng were spotted. The blot was exposed to film overnight in order to visualize faint signals.

those from which they were originally amplified (Fig. 19). These very faint signals, however, were often difficult to distinguish from background noise. Other probes tested were those prepared from PCR products amplified from *Alternaria alternata*, *Microsphaeropsis olivacea* and *Phoma* sp. DNA. The *Alternaria alternata* product hybridized only to *Periconia minutissima* and to *A. montagnei* DNA. The *Microsphaeropsis olivacea* product (MolivLC12c) did not hybridize to *M. olivacea* DNA but rather hybridized only to that of *Gymnoascus* sp. This is likely due to insufficient *M. olivacea* DNA on the membrane given the low DNA concentration in this sample as observed by agarose gel electrophoresis (not shown). The *Phoma* sp. product hybridized to *Phoma* sp. DNA and to various other fungal DNAs, but also to the negative control sample which, while visible only after overnight exposure, indicates non-specific hybridization due to low hybridization and/or post hybridization wash stringency.

2.3.5 Dot blot Hybridization of marine fungal KS gene probes to fungal KS-related PCR products

Three KS PCR products were used to probe the other 26 fungal KS PCR products in separate hybridization reactions (see Fig. 20). Two of these probes, corresponding to *Dichotomyces cejpii* and *Alternaria tenussima* PCR products, are of the NR type as determined by multiple sequence alignment and phylogenetic analyses. Hybridization of the *Alternaria tenussima* probe at 70 °C to a dot blot of 25 other PCR products resulted in signals from *A. tenussima* and
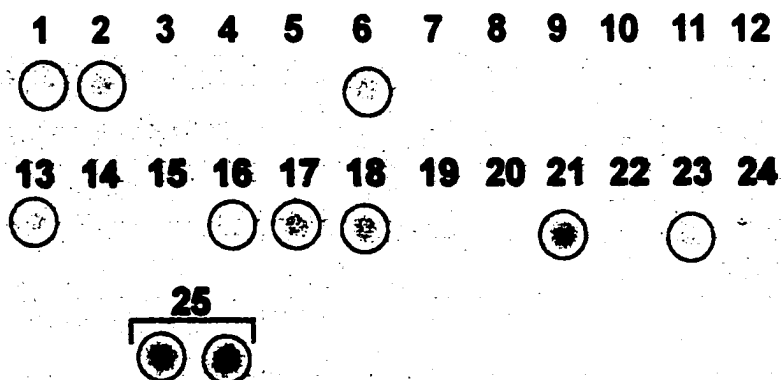
Fig. 20: Dot blot hybridization of *Alternaria tenussima* LC1/LC2c PCR product to PCR products amplified from various marine fungal isolates. Visible signals due to hybridization to the *A. tenussima* probe are encircled. Unless otherwise stated, the PCR products amplified from the fungal isolates listed were amplified using the LC1/LC2c primers. 1) *Alternaria alternata*; 2) *Alternaria tenussima*; 3) *Apiospora montagnei*; 4) *Penicillium thomii*; 5) *Phoma* sp. (LC3/LC5c); 6) *Aspergillus niger*; 7) *Phoma* sp. (LC3/LC5c) PCR product (from a separate reaction); 8) *Cylindrogloem* sp; 9) *Westerdykella* sp; 10) *Gymnoascus* sp; 11) *Stemphylium* sp; 12) *Endoxyla* sp; 13) *Cladosporium* sp; 14) *Cunninghamella* sp; 15) *Dichotomyces cejpii*; 16) *Periconia minutissima*; 17) *Botryophialphora* sp; 18) *Pseudeurotium zonatum*; 19) *Penicillium helicum*; 20) *Geotrichum/Candida* sp; 21) *Microsphaeropsis olivacea*; 22) *Penicillium commune*; 23) *Arthrinium* sp; 24) *Apiospora montagnei* (isolate 2). 24) *Alternaria tenussima* probe DNA (positive control). Quantity of PCR products spotted range from 8ng to 46ng. The blot was hybridized at 70°C and exposed to film for two hours.

nine other NR type products after a 2 h exposure (Fig. 20). Three other signals from NR-type products were detected following overnight exposure, but no signal from PR-type PCR products resulted. Hybridization of the *Dichotomyces cejpii* probe to an identical blot at 70 $^{\circ}$C resulted in strong signals from *D. cejpii*, *Cunninghamella* sp. and *Sordaria fimicola* NR-type PCR products after a 1 h exposure (data not shown). Strong signals appeared from *Cladiosporium* sp. and *Pseudeurotium zonatum* products, and weak signals from several other NR-type products following overnight exposure, but no signals from PR-type products were evident even after overnight exposure. Hybridization of the *A. montagnei* PR-type probe (AmontLC35c) to a similar blot resulted in signals only from the *A. montagnei* PR-type PCR product as well as *A. montagnei* and *Verticillium* sp. PCR products of unknown sequence that were amplified using the LC1/2c primer set (not shown).

2.4 Discussion

2.4.1 Isolation of new KS gene fragments from marine isolates of filamentous fungi

Degenerate PCR primers [120] constructed using known terrestrial fungal KS genes were used in this study to amplify similar genes from fungi that had been isolated in marine environments. DNA sequencing and Genbank comparison determined that these sequences are highly similar to fungal KS

genes. Table 1 summarizes the results of these experiments. *A. montagnei* and *M. olivacea* were the first marine fungal isolates screened for the presence of KS genes and both yielded KS-related products (Table 1). PK compounds have been isolated from marine isolates of *M. olivacea* [88] and other *Microsphaeropsis* sp. [129], indicating the presence of PKS genes. Likewise, experiments conducted in our lab have resulted in the isolation of various suspected PKs from a marine isolate of *A. montagnei* (unpublished results). We then screened 48 other marine isolates of filamentous fungi resulting in the amplification of KS-related gene fragments from 24 for a total of 26 (including the *A. montagnei* and *M. olivacea* KS gene fragments)(Table 1). We can speculate on the potential products of these genes based on which primers were successfully used to amplify them and on their similarity to known KSs. Bingle *et al.* [120] have described the relationship between KS genes that were amplified using these primers and the degree of ketoreduction introduced during biosynthesis of their PK products. The LC1/LC2c primers are specific for KSs involved in the biosynthesis of non-reduced (NR) PKs such as spore pigments and aflatoxins while the LC3/LC5c primers are specific for KSs involved in partially reduced (PR), 6-MSAS-like PKs [120, 122]. This may reflect a fundamental structural requirement at this part of the PKS in order to accommodate synthesis of PKs of different basic carbon backbone structure. If a common fundamental reductive constraint determines which type of KS will be involved in the biosynthesis of a particular PK, we can assume a direct relationship between primary a.a. sequence and product structure. This may be

difficult in some cases, however as PKs are often drastically modified post-PKS by tailoring enzymes [24], masking the structure of the nascent compound. Nevertheless, since the *M. olivacea* product obtained in this experiment, for example, was amplified with the LC1/LC2c primer set, we suggest that it is likely involved in the biosynthesis of a spore pigment or aflatoxin-like (NR) PK. For *A. montagnei*, from which products were obtained using both primer sets (Table 1), we suggest that the LC1/LC2c-amplified KS gene fragment is involved in the biosynthesis of a NR PK. The LC3/LC5c-amplified KS gene fragment is probably involved in the biosynthesis of a 6MSA-related (PR) PK. Papulacandin B (see Fig. 21), a suspected PK isolated in our lab from the same *A. montagnei* isolate, has an aromatic moiety that resembles 6-MSA (unpublished results, see section 2.0 of this thesis). It is interesting to speculate that the LC3/LC5c product of *A. montagnei* originated from a gene involved in the biosynthesis of this compound. Of the 26 PCR products obtained from marine fungal isolates during this study, only two were amplified using the LC3/LC5c primer set (Table 1). The rest were amplified using the LC1/LC2c primers, suggesting a more widespread occurrence of NR compared to PR PKs throughout the marine fungi. Although this is consistent with the more frequent occurrence of aromatic PKs in terrestrial fungi [8], more PKS genes must be isolated from marine fungi to determine the magnitude of this trend in marine environments.

2.4.2 Phylogenetic analyses of marine and terrestrial fungal KS gene fragments

Phylogenetic comparison of KS gene sequences obtained from marine fungal isolates in this study to available terrestrial fungal KS gene fragments in the databases via neighbor-joining (Fig. 17) or parsimony based analyses (Fig. 18) did not result in a dichotomy between terrestrial-derived KSs and those from marine fungi. As noted by Bingle et al. [120] for terrestrial fungi, the division between KSs of NR type and those of PR type is maintained in both the neighbor-joining (Fig. 17) and parsimony-based (Fig. 18) phylogenies prepared from KSs from marine fungal isolates. Though no exclusively marine versus terrestrial dichotomy resulted in either phylogeny, the marine-derived sequences tend to branch together at the exclusion of the terrestrial KSs on both trees. Three sub-clades within the NR clade were exclusively comprised of KSs of marine fungal origin on both neighbor-joining (Fig. 17) and parsimony (Fig. 18) trees. In most cases, nodes of these clades branched together with low bootstrap support, suggesting a high level of structural diversity between their putative coded PKs. This is consistent with the remarkable structural diversity of PK compounds that have been isolated from marine fungi in recent years [62, 63, 88, 129-131]. Within the NR clade of both the neighbor-joining (Fig. 17) and parsimony (Fig. 18) trees, KS phylogeny does not correspond with the morphology-based taxonomic species identification. The *Penicillium commune* sequence, for example, branches with the *Periconia minutissima* sequence at 42% bootstrap support on the neighbor-joining tree (Fig. 17) and 34% on the

parsimony tree (Fig. 18), but not with sequences from its congeners *P. helicum* or *P. thomii*. Likewise, the *Aspergillus niger* KS branches with the *Microsphaeropsis olivacea* sequence at 42 % bootstrap support on the neighbor-joining tree (Fig. 17) and with a clade containing KSs from *Stemphylium* sp. and *Pseudeurotium zonatum* at 42 % on the parsimony tree (Fig. 18) rather than with its several (albeit terrestrial) congeners. Though a fundamental difference between marine and terrestrial KSs could be invoked to account for the latter example, this would not explain the separate branching of sequences from marine isolates of *Penicillium*.

Production of identical or similar PKs by different fungal species has been observed previously. The pigment melanin, for example, is produced by *Alternaria alternata*, *Colletotrichum lagenarium* and *Verticillium dahliae* [8]. The PK citrinin is also produced by multiple fungal species [116]. Thus, the various producers of PK compounds are not always close relatives (as determined by morphology) and close relatives (or different isolates of a species) often produce different PKs [8]. It is not surprising, therefore, to find very similar or identical KSs in morphologically distinct fungal species' genomes. As for many primary metabolic genes of scattered distribution throughout the major domains of life [117], the scattered distribution of PKS genes throughout fungal species is inconsistent with a vertical mode of gene inheritance, suggesting horizontal gene transfer (HGT) has played a major role in fungal PKS evolution. "Dispensable" biosynthetic genes are more likely to be transferred by HGT than primary metabolic genes [117]. Fungal natural product pathways have been referred to

as "dispensable" since they are either not required for growth, or are only required under a limited range of conditions [132]. Several lines of evidence support a major role of HGT in the evolution of secondary metabolism in fungi. Examples from terrestrial fungi include a) differential occurrence of *PKS1* gene homologues in closely related strains of *Cochliobolus heterostrophus* [8] while a different fungal genus has such a homologue [133], b) functional and physical conservation of sterigmatocystin biosynthetic gene clusters that differ in gene order and direction of transcription between various fungi [115] and c) higher G + C content of fungal β-lactam biosynthetic genes compared with the rest of the genome [134]. Thus, it is likely that HGT is a major evolutionary force with respect to fungal PKS evolution. Walton [118] has hypothesized a selective mechanism which may drive horizontal transfer of fungal secondary metabolic genes. This hypothesis, which is an extension of the "selfish operon" hypothesis of Lawrence and Roth [135], suggests that selection at the level of the gene cluster favors the lateral transfer of fungal secondary metabolic genes. The "selfish operon" hypothesis is also consistent with the observation that secondary metabolic genes are usually clustered together [2]. Whatever the selective pressure, if HGT determines the distribution of PKS genes in filamentous fungi, species identifications based on secondary metabolite production would generate misleading taxonomic conclusions, and phylogenies constructed using secondary metabolic genes would be unstable.

Misidentification of fungal species may also contribute to the apparently scattered distribution of KSs in fungi. Identification of fungal species, which is

usually based inadequately on morphological characteristics [136] or even on single gene phylogenetics, are likely not representative of true phylogeny as morphology-based phylogenies conflict with gene phylogenies. Furthermore, phylogenies based on some genes conflict with those based on other genes [137]. Peterson and Hughes [138] doubt that a unified fungal species concept is even possible. The weight of evidence, therefore, suggests that HGT and species misidentification both compound problems associated with fungal taxonomy. Under these circumstances, fungal taxonomy based on secondary metabolite biosynthesis [139] should be strictly utilitarian.

2.4.3 Dot blot hybridizations of marine fungal KS gene probes to fungal DNA and PCR products

Several fungal KS PCR products were used to construct probe DNAs that were subsequently used in dot blot hybridizations with the genomic DNAs of several randomly selected fungal genomes that were screened for KS genes in this study, including the genomes from which the KSs were originally amplified (see Fig. 19). Of these, *Periconia minutissima*, *Verticillium* sp., and *Apiospora montagnei* (PR and NR-type respectively) PCR products hybridized to several of the fungal DNAs tested, including those from which they were originally amplified (see Fig. 19). This is not surprising as similar PKS genes are known to occur throughout a variety of filamentous fungi [8]. Differences in signal intensity and/or the absence of signal may be due to variation in levels of sequence similarity

between the various genes and the probe DNAs. Also, differential amounts of the various DNAs spotted on the membrane due to difficulty encountered with fungal DNA quantitation or low DNA yield likely influenced signal intensity. Hybridization of probe DNAs to the DNA of multiple isolates, however, reinforces the conclusion reached from the sequence data, phylogenetic analyses and the occurrence of PKs from diverse fungal species [62, 63, 88, 129-131] that PKS genes are widespread among marine fungi.

NR-type KS PCR products from various marine fungal DNAs were able to hybridize to several other NR-type PCR products but not to PR-type products (see Fig. 20). This suggests that probe DNAs generated using these primers would not be useful for detection of PKS genes involved in the biosynthesis of PR PKs. Lack of NR-type probe hybridization to PR-type PCR products is consistent with similar observations of terrestrial fungal KS gene probes [120, 122]. Hybridization of the A. montagnei PR-type probe (AmontLC35c) to an identical dot blot resulted in signals from the A. montagnei PR-type PCR product and A. montagnei and Verticillium sp. PCR products of unknown sequence that were amplified using the LC1/2c primer set. These multiple template PCR products may be a mix of NR and PR-type products. If a PR type product is present, linear PCR from the LC2c primer may amplify it since LC2c is 70 % identical in sequence to the LC5c primer and 100 % identical at the first three residues of the 3' end. This result is consistent with the presence of NR and PR-type sequences in A. montagnei. For Verticillium sp., if both types are present in the genome, one would expect to amplify a PR-type product with the LC3/LC5c

primers. This did not occur, suggesting that the LC3 primer site was absent in the *Verticillium* genome. Our experiments with marine fungi are consistent with the observation from terrestrial fungi [122] that the utility of KS probe DNAs for isolation of homologous sequences in other fungi is probably limited to those involved in the biosynthesis of PKs that share common PKS-level assembly mechanisms.

The search for new sources of PK diversity is expanding to include the marine environment. Metabolites of unique chemistry are taken from marine species at an increasing rate, underscoring the need for follow-up molecular genetic studies involving their biosynthetic genes. An important part of this endeavor includes comparison of these genes to their terrestrial counterparts in order to obtain a more complete understanding of PK chemical heritage across environmental boundaries. The marine fungi represent a useful starting point for this given their impressive ability to produce PK diversity and precedent molecular genetic knowledge from their terrestrial counterparts. Our results demonstrate the utility of terrestrial fungal molecular genetic knowledge for isolating new PKS genes from marine fungal isolates. Consistent with production of increased PK diversity by marine fungi as compared to terrestrial fungi, phylogenetic comparisons between the terrestrial and marine derived KS sequences suggest that they are different from one another, but that they maintain the fundamental sequence constraints that determine the structure of their respective nascent PKs. Furthermore, the scattered distribution of PKS genes throughout the fungi (likely due to lateral gene transfer) appears to be a

factor with marine fungal PKS genes as well. To the best of our knowledge, the KS gene fragments obtained during the course of this study are the first PKS-related sequences obtained from marine fungi, and they should facilitate isolation of new PK biosynthetic gene clusters from these taxa.

3.0 Biosynthetic studies of the polyketide Papulacandin B produced by a marine isolate of the ascomycetous fungus *Apiospora montagnei*.

3.1 Introduction

The papulacandins (Fig. 21) are a group of glycolipid antibiotics first isolated from the deuteromycetous fungus *Papularia sphaerosperma* [140, 141]. The most bioactive of these compounds, papulacandin B (PapB), has been shown to inhibit cell wall synthesis in *Candida albicans* [142, 143], *Geotrichum lactis* [144, 145] and *Saccharomyces cerevisiae* [142, 146, 147]. It is largely inactive against filamentous fungi, bacteria and protozoa [141]. The molecular target for PapB is (1,3)-β-D-glucan synthase. Enzyme inhibition assays indicate that PapB binds irreversibly to (1,3)-β-D-glucan synthase thereby preventing uptake of glucose in the biosynthesis of glucan [144]. Glucan is one of two major polysaccharide structural components of yeast cells, and therefore an important target for antifungal activity. Interestingly, the assembly of mannan, another major fungal cell wall glycoprotein, is only slightly affected by PapB [142]. As is the case with many secondary metabolites, potential medical applications of papulacandins have prompted interest in their isolation [148], structural elucidation [149], chemical synthesis [150-153] and investigations into their bioactivity [154]. Specifically, this interest in bioactivity has focused on their potential value as therapeutic agents to combat certain human fungal infections, a problem that is particularly severe for immunocompromised hosts such as AIDS patients [148]. Compounds that can effectively treat fungal infections by mechanisms that do not interfere with metabolic pathways in mammals are
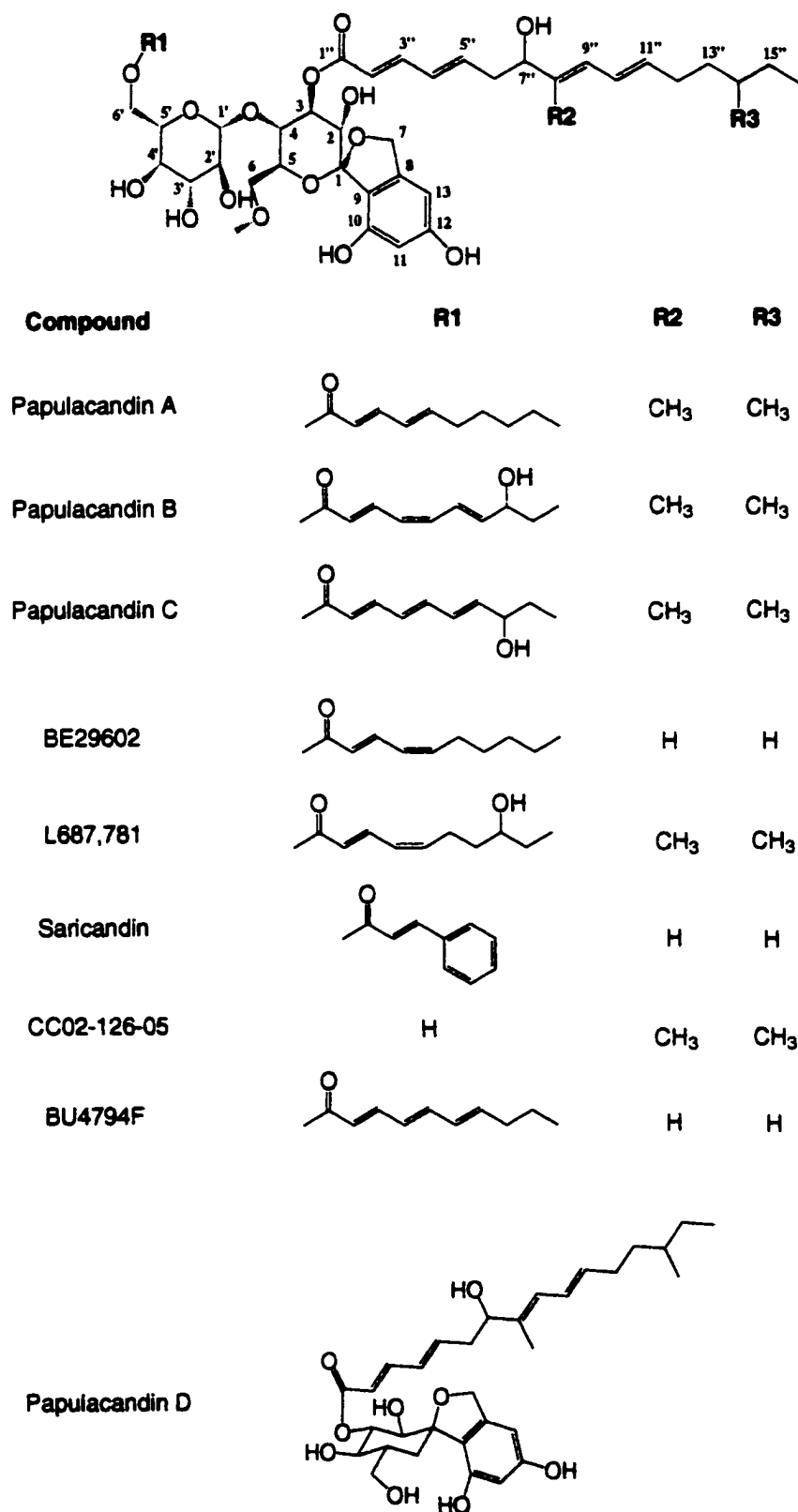
Fig. 21: Structure of papulacandin B and various related compounds.

especially rare [155, 156], and so the discovery of such new antifungal agents is of great importance to human health.

In this regard, PapB is a candidate for drug development because the molecular target, (1,3)-β-D-glucan synthase, is not a component of the cells of higher eukaryotes. Thus it has the potential for development as an antifungal drug with limited human toxicity [157]. This potential has stimulated the ongoing search for new papulacandin derivatives and other inhibitors of fungal cell wall synthesis. Inspection shows that PapB is a complex molecule, composed of an aromatic moiety resembling the terrestrial fungal polyketides 6-methylsalycylic acid (6MSA) [158] or orsellininc acid, linked by a spirocyclic structure to a lactose diglycoside with two linear aliphatic acyl side-chains that resemble modified fatty acids (Fig. 21). Several new compounds, many of which are structurally related to the papulacandins [159-164] (Fig. 21), have also been isolated. Most PapB-related compounds vary with respect to the degree of saturation and hydroxylation of the shorter C_{10} acyl chain, and the degree of methylation of the longer C_{16} acyl chain. However, some analogues display more drastic modifications to the overall papulacandin structural organization (see Fig. 21). Papulacandins B and C [165], BE29602 [166], L687781 [161] and BU4794F [164] (Fig. 21) vary only with respect to the methylation, saturation and/or hydroxylation of the acyl chains (Fig. 21). The inhibitory effect of these analogues on glucan synthesis in yeast is similar to that of PapB. This indicates that slight modifications to the acyl chains do not have a significant effect on the antifungal activity of papulacandins. However, more drastically modified

papulacandin analogues display markedly reduced antifungal activity. Saricandin (Fig. 21), a papulacandin-related compound possessing a cinnamyl ester in place of the C_{10} acyl chain, displays much less antifungal activity compared to other papulacandins [167]. This may be due to a reduced affinity of saricandin for the active site of (1,3)-β-D-glucan synthase compared with other papulacandin derivatives. However, the effect of saricandin on (1,3)-β-D-glucan synthase has not been tested directly by enzyme inhibition assay. Another papulacandin analogue, papulacandin D (PapD) (Fig. 21), lacks both the C_{10} acyl chain and the galactose residue present in most papulacandins [165]. Traxler et al. [154] reported that the antifungal activity of PapB is lost when it is converted to PapD. Rommele et al. [165], however, observed that PapD has a similar inhibitory effect as PapB on glucan biosynthesis, but a reduced inhibitory affect on yeast growth. Thus, absence of the short acyl chain and/or galactose residues may inhibit uptake or penetration of the compound into yeast cells [165], but does not reduce its effect on (1,3)-β-D-glucan synthase. It is unknown whether the low level of antifungal activity observed for saricandin is also due to its inability to penetrate yeast cells. If saricandin, which has an intact diglycoside (Fig. 21), was shown to inhibit (1,3)-β-D-glucan synthase in an enzyme inhibition assay, it would be consistent with the hypothesis that the C_{10} acyl chain is specifically required for penetration or uptake into the host cell.

Elucidation of papulacandin structures and their respective bioactivities can provide clues as to the biological mechanisms that govern their biosynthesis. Stable isotope feeding experiments can establish the precursor units required in

the biosynthesis of papulacandins, which in turn could lead to the isolation and characterization of the biosynthetic enzymes involved as well as their corresponding genes. Of interest to evolutionary biologists and chemical ecologists are the selective pressures that govern secondary metabolic gene maintenance and transmission in microorganisms. On the other hand, through knowledge of their biosynthesis, it may one day be possible to generate new papulacandin derivatives by expressing papulacandin biosynthetic genes in heterologous host organisms. In the short term, biosynthetic and molecular genetic analyses of PapB production by *Apiospora montagnei* would contribute to our understanding of secondary metabolism in this marine-derived fungal species. In addition, determination of the PapB biosynthetic pathway would increase the representation of fungal secondary metabolites from the marine environment that have been investigated in this way.

The fatty acid and aromatic residues of PapB, which are both essential for antifungal activity [154], appear to be polyketide (PK) in origin. The different reductive organization of the suspected PK moieties indicate that they are synthesized independently from each other, probably by separate enzymes. While PK aromatic compounds are common fungal metabolites, highly reduced PKs such as the linear aliphatic side chains of PapB are less frequently encountered in fungi, and data on their biosynthesis is limited [8]. Terrestrial filamentous fungi are known to produce a diverse array of PK metabolites [118], though considerably fewer species from the marine environment have been studied. In the following section, the isolation of PapB from a marine isolate of

Apiospora montagnei is described together with investigations into the biosynthesis of the compound using $[1,2-{}^{13}C_2]$ acetate as a precursor in conjunction with ${}^{13}C$ NMR spectroscopy.

3.2 Materials and methods

3.2.1 Culturing of *Apiospora montagnei* for construction of a papulacandin B production curve

A portion (approximately 1 cm^2) of *A. montagnei* maintained at 5 °C on a MA (malt agar) slant, was transferred to a fresh MA plate and stored at 25 °C for 72 h. A small portion of the freshly grown mycelium was used to inoculate UC1 medium (100 ml) (2.5 %w/v glucose, 2.5 %w/v Pharmamedia in distilled, deionized water) and the culture shaken (200 rpm) at 25 °C for 72 h. An aliquot (5 ml) of this culture was transferred to each of five flasks containing sterile UC2 broth (100 ml) (2 %w/v molasses, 3 %w/v dextrin white, 1.5 %w/v fish meal, 1.5 %w/v Pharmamedia in distilled, deionized water) and the UC2 cultures shaken (200 rpm) for 8 days. Aliquots (5 ml) of each UC2 culture were removed daily to separate centrifuge tubes (14 ml vol.) during the eight-day growth period. The biomass was collected by centrifugation and sonicated vigorously in 100 % methanol (4 ml). Aliquots (15 µl) of each methanol extract were analyzed by analytical high performance liquid chromatography (HPLC) (HP 1090 Liquid Chromatograph with DAD; Zorbax RXC8 2 mm x 10 cm column; flow rate 0.3

ml/min) and elution with aqueous methanol mixtures containing 0.1 % trifluoroacetic acid as follows: 60 % H_2O: 40 % acetonitrile (10 min); 50 % H_2O: 50 % acetonitrile (10 min); 100 % acetonitrile (5 min). PapB was eluted 7 min following injection. The average level of PapB production for each day was calculated from measured U.V. absorption levels of the peak eluting at 7 min, and these figures plotted against time to generate a PapB production curve (Fig. 22).

3.2.2 Administration of [1,2-$^{13}C_2$] sodium acetate to *A. montagnei* cultures

Portions of freshly grown mycelia were transferred from an MA plate to 6 flasks containing UC1 media (100 ml) and shaken at 200 rpm for 72 h at 25 °C. Aliquots (50 ml) of each UC1 culture were used to inoculate UC2 broth (6 x 1 L), and the cultures shaken at 200 rpm for 8 d at 25 °C.

Precursor feeding was as follows: Separate aliquots (40 ml) of the labeled precursor in distilled, deionized water were drawn from a stock solution of [1,2-$^{13}C_2$] sodium acetate (480 ml; 62 mM) and sterilized by autoclaving. These aliquots were added to each of the six UC2 cultures of *A. montagnei* on day 3 following inoculation (giving a precursor concentration of 2.3 mM) and again on day 4 (final precursor concentration 4.6 mM). The *A. montagnei* biomass was harvested by centrifugation on day 8.
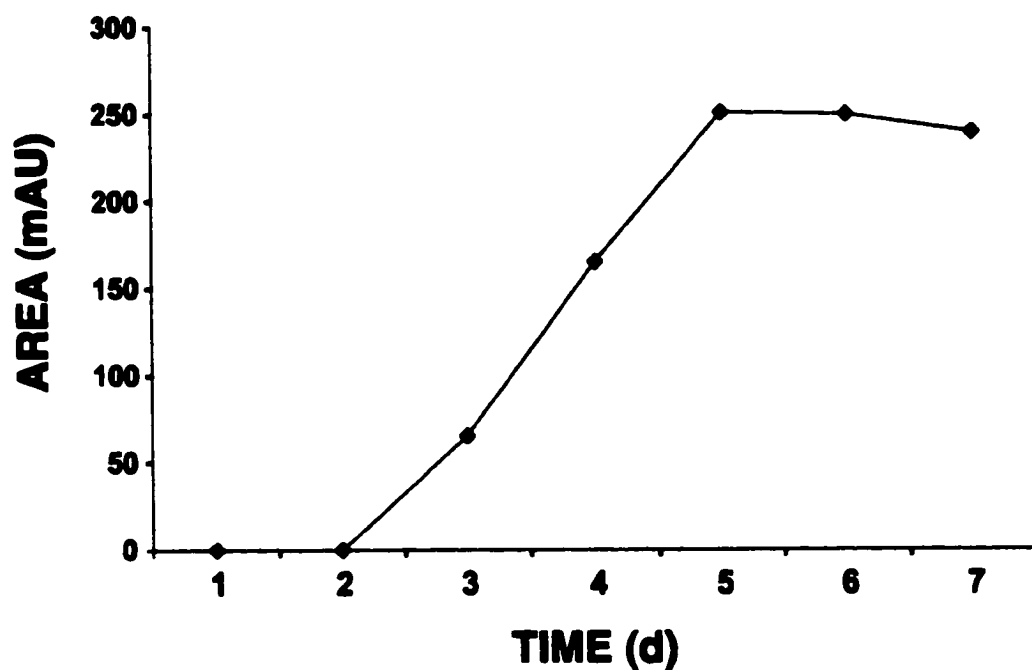
Fig. 22: Average production of papulacandin B by five *Apiospora montagnei* cultures over a seven day period. Levels of PapB are measured in terms of the analytical HPLC peak area in mAU (milliampere units) at the 7.7 minute PapB elution interval (average area = 138.93 mAU with a standard deviation of 115.43 mAU).

3.2.3 Purification of [1,2-^{13}C$_2$] sodium acetate-labeled papulacandin B

The harvested *A. montagnei* biomass was sonicated vigorously (10 min) in an excess of 100 % methanol (900 ml) and the extract evaporated to dryness (Büchi RE III Rotovapor). The remaining biomass was resuspended in the same volume of methanol, sonicated and the extract evaporated to dryness. This was repeated until the color of the methanol was unchanged following sonication (four times in this case). The methanol extracts were combined, evaporated to dryness and residue dissolved in 80 % methanol: water (500 ml). The aqueous methanol solution was partitioned three times against hexane. The aqueous phase was collected, evaporated to dryness and the weight recorded (17.57 g). The extract was then absorbed onto C18 powder (LiChroprep RP-C18; 40-63 μm) and applied atop a C18 vacuum liquid chromatography column which had been pre-conditioned with 100% methanol and then equilibrated with water containing 1 % acetic acid. Aqueous methanol mixtures containing 1 % acetic acid were passed through the column and fractions (2 L) collected as follows: water; 70 % water: methanol; 50 % water: methanol; 30 % water: methanol; 20 % water: methanol; 10 % water: methanol; 100 % methanol; and the column washed with dichloromethane. Each fraction was examined by analytical HPLC for the presence of papulacandins, which appeared in the 20 % water: methanol fraction. This fraction was evaporated to dryness and dissolved in 50 % water (0.5 % acetic acid): methanol (1 ml) and applied atop a Flash C-18 column (LiChroprep 15 μm C-18) previously equilibrated with 50 % water: methanol

(containing 0.5 % acetic acid). The following solutions (500 ml batches, each containing 0.5 % acetic acid) were run through the column under N_2 pressure: 50 % water: methanol; 40 % water: methanol; 30 % water: methanol; 20 % water: methanol; 10 % water: methanol; and 100 % methanol. Aliquots (15 µL) of each fraction were analyzed by both analytical HPLC (Fig. 23) and thin layer chromatography (TLC) (5 cm high C18 plates; 20 % water: methanol (1 % acetic acid) mobile phase; visualized under short wave U.V. light, sprayed with anisaldehyde and heated). Fractions containing papulacandins were combined and PapB (34 min retention time) and PapC (30 min retention time) purified by semi-preparative HPLC (Capcell Pak C-18, SG120A, 5 µm 10 mm x 250 mm column; 54.3 % water: 45.7 % acetonitrile mobile phase; 2.0 ml/min flow rate; U.V. detection at 235 nm) by collecting peaks from multiple injections (50 µl). Yield of PapB was 1.5 mg.

3.2.4 NMR recording conditions

PapB (1.5 mg) obtained from the $[1,2-^{13}C_2]$ acetate-labeling experiment was dissolved in methanol-d_4 (700 µl) for NMR spectroscopy at 500.13 MHz (^{1}H) (Fig. 24) or 125.7 MHz (^{13}C) (Fig. 25) using a Bruker DRX-500 spectrometer at 20 °C. One-dimensional (1D) ^{1}H single-pulse and ^{13}C {^{1}H}-decoupled single-pulse spectra were recorded, as well as two-dimensional (2D) double-quantum-filtered ^{1}H COSY (Fig. 26), ^{1}H TOCSY (mixing time 160 ms, Fig. 27) and ^{1}H/^{13}C HSQC (Fig. 28) spectra. Standard spectra (apart from HMQC instead of HSQC), plus a ^{1}H/^{13}C HMBC spectrum, were recorded previously using a Bruker AMX-
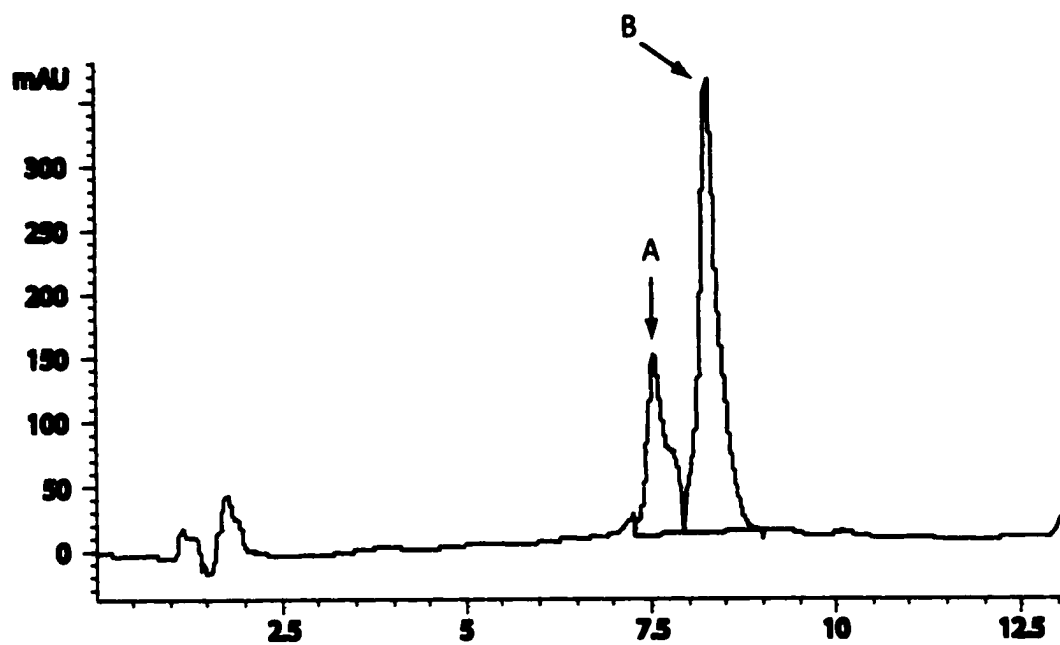
Fig. 23: Analytical HPLC chromatogram of post-flash C18 combined column fractions containing papulacandins. A: unidentified papulacandin-type compound, B: papulacandin B.
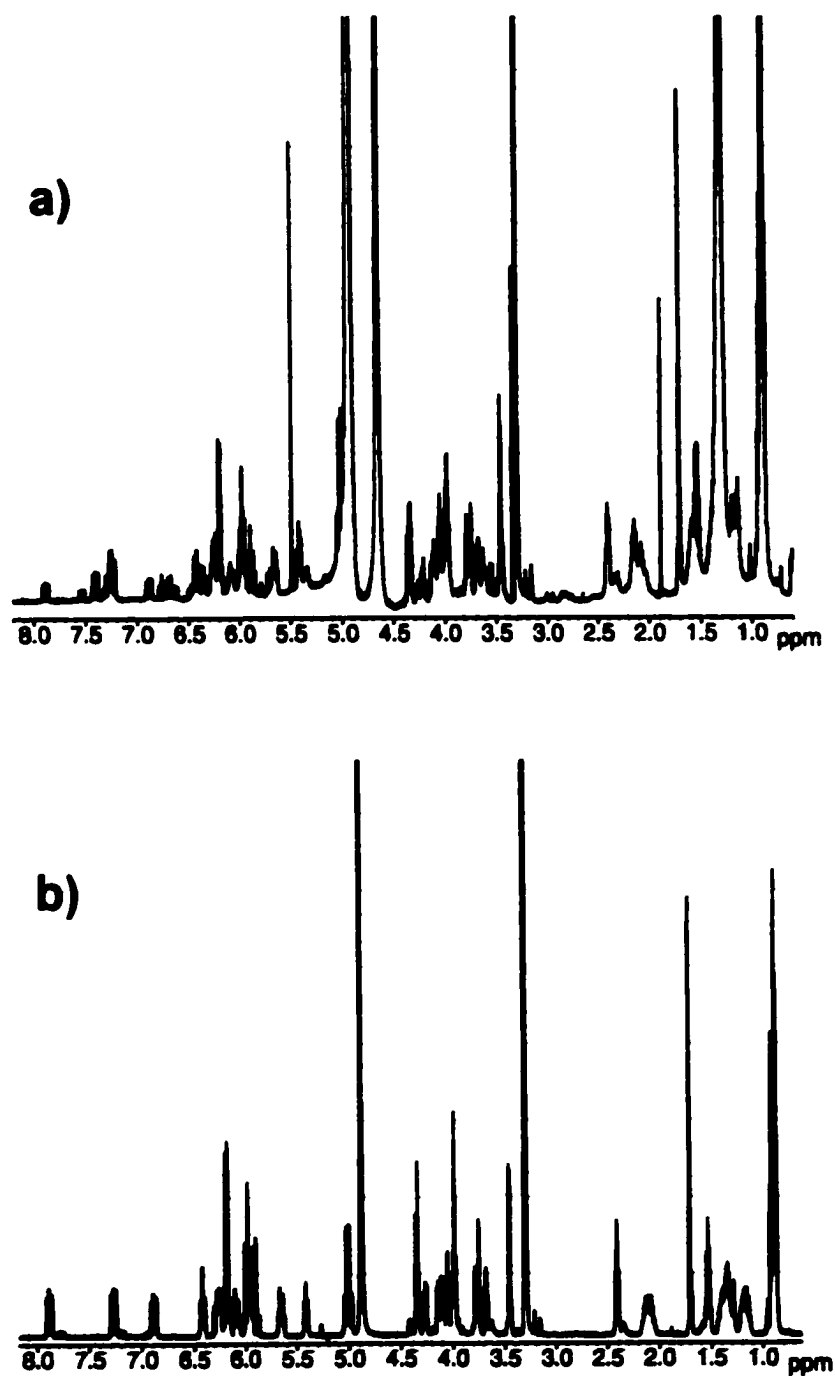
Fig. 24: ¹H spectra of papulacandin B. a) ¹H spectrum of [1,2-¹³C₂] acetate-enriched fraction containing papB and related compounds. b) ¹H spectrum of unlabeled, pure papB. Resonances in the ¹H spectrum of pure papB are present in that of the [1,2-¹³C₂] acetate-enriched fraction.
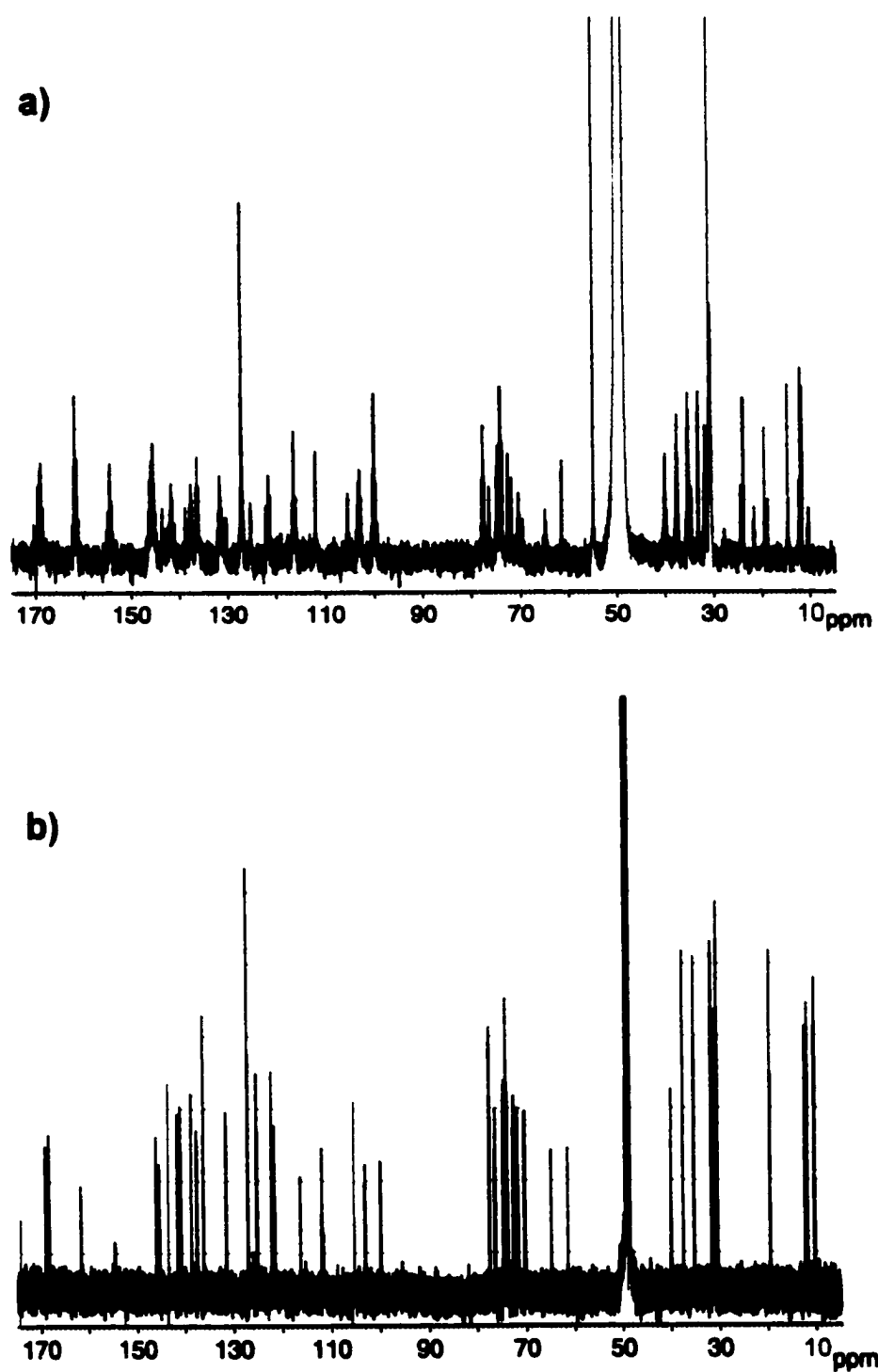
Fig. 25: [13]C spectra of a) [1,2-[13]C$_2$] acetate-enriched fraction containing papB and related compounds and b) unlabeled, pure papB. [13]C resonances of pure papB are present in the ^{13}C spectrum of [1,2-[13]C$_2$] acetate-enriched fraction.
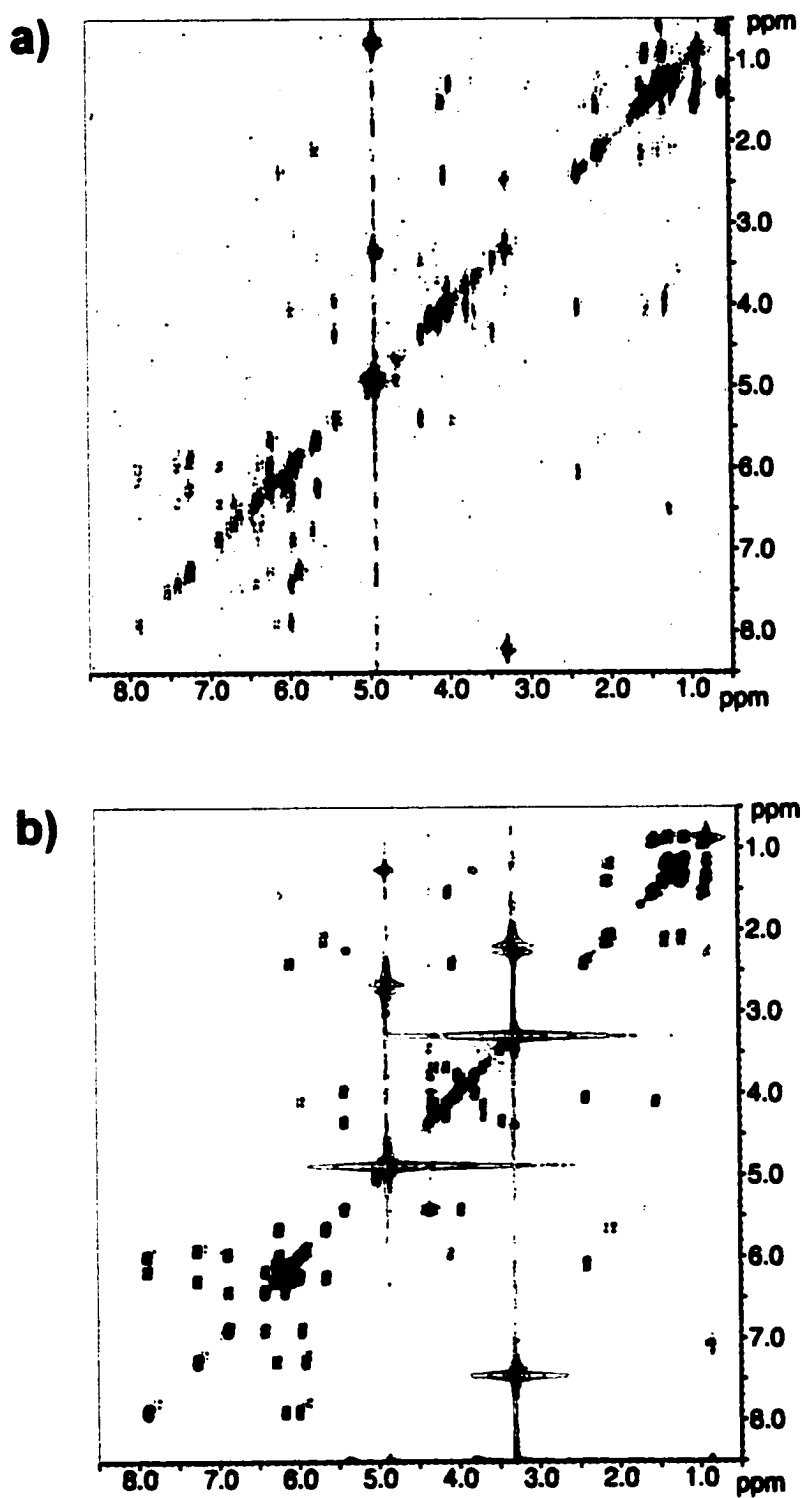
Fig. 26: ^{1}H COSY spectra of papulacandin B. a) ^{1}H COSY of [1,2-^{13}C$_2$] acetate-enriched fraction containing papB and related compounds. b) ^{1}H COSY of unlabeled pure papB.
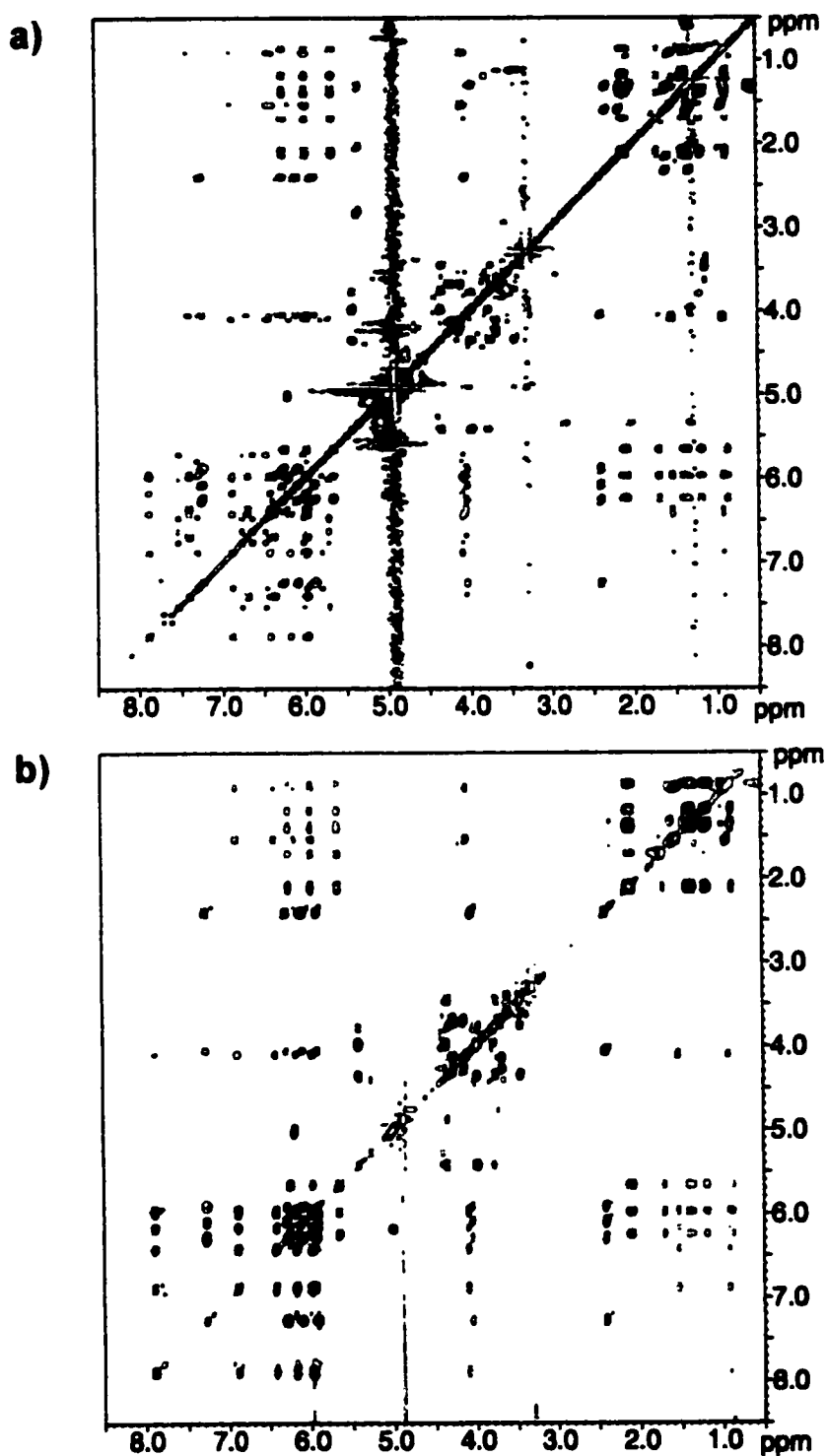
Fig. 27: ¹H TOCSY spectra (160ms mixing time) of papulacandin B. a) ¹H TOCSY of [1,2-¹³C₂] acetate-enriched fraction containing papB and related compounds. b) ¹H TOCSY of unlabeled, pure papB. Spin systems in the spectrum of the pure compound are present in the spectrum of the [1,2-¹³C₂] acetate-enriched fraction.
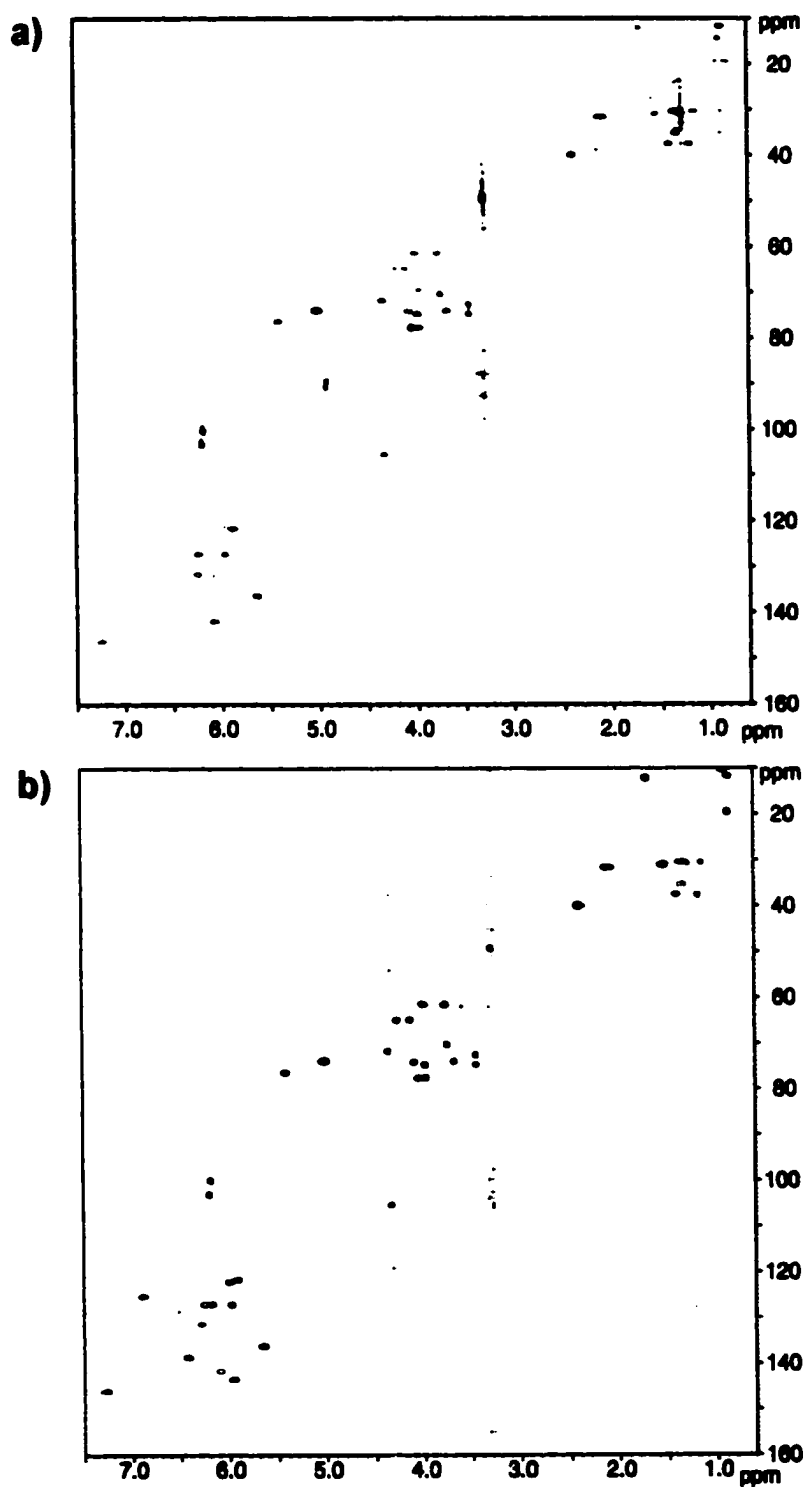
Fig. 28: ^{1}H-^{13}C HSQC/HMQC spectra of papulacandin B. a) ^{1}H-^{13}C HSQC spectrum of [1,2-^{13}C$_2$] acetate-enriched fraction containing papB and related compounds. b) ^{1}H-^{13}C HMQC of unlabeled, pure papB. ^{1}H-^{13}C resonance correllations in the spectrum of pure papB are present in that of the labeled fraction.

500 spectrometer and an unlabeled sample of PapB obtained from *A. montagnei* (C. Craft, P. Anacleto, and J.L. C. Wright unpublished results). In the labeled sample, the 2D and 1D spectra were used to verify or reassign the carbon resonances (Table 2) as well as determine the pattern of incorporation of ^{13}C derived from the $[1,2-^{13}C_2]$ acetate precursor.

3.2.5 Reassignment of papulacandin B carbon resonances

Analysis of the one-dimensional ^1H spectrum (Fig. 24) and ^{13}C spectrum (Fig. 25) further verified the identity of the labeled PapB when compared with the ^1H spectrum of the published structure [141] and by comparison with a standard prepared earlier at IMB. However, analysis of ^1H spin systems from 2D TOCSY spectra (Fig. 27) and of 1-bond $^{13}C-^1H$ connectivities from the 2D HSQC/HMQC spectra of PapB (Fig. 28), revealed inconsistencies between these observations and the tentative resonance assignments published in 1980 [149]. Corrections to the assignments were based on the TOCSY spectra (Fig. 27) that indicated 5 complete spin systems. The COSY data (Fig. 26) revealed the coupling sequence within each spin system, and the HSQC/HMQC (Fig. 28) and HMBC spectra (not shown) were used to identify the one- and three-bond couplings and $^{13}C-^1H$ connectivities respectively. With the exception of some carbons in the sugar moieties, where the assignments were ambiguous due to overlapping resonances of the associated protons, all PapB carbon resonances were accounted for in the corrected assignments (Table 2).

Table 2: Corrected papulacandin B carbon resonance assignments. J_{CC} coupling constants are shown for resonances of coupled carbons originating from intact [1,2-$^{13}C_2$] acetate.

C	δ ^{13}C	δ ^{1}H	J_{CC}	C	δ ^{13}C	δ ^{1}H	J_{CC}
1	111.96	x		6"	40.00	2.41	42.5
2	70.34	3.76		7"	77.63	4.05	47.1
3	72.54 a	3.45		8"	137.51	x	47.1
4	74.77 a	3.45		9"	127.12	5.97	u
5	73.97	3.68		10"	127.12	6.25	u
6	64.90	4.27 & 4.13		11"	136.18	5.65	43.3
7	73.88	5.03 & 4.99	42.7	12"	31.60	2.13 & 2.08	43.7
8	145.44	x	42.7	13"	37.54	1.42 & 1.18	34.6
9	116.40	x	67.3	14"	35.25	1.34	34.7
10	161.74	x	68.8	15"	30.45	1.37 & 1.16	34.9
11	99.90	6.17	69.1	16"	11.71	0.86	35.0
12	154.74	x	69.9	17"	12.19	1.72	
13	103.05	6.19	69.0	18"	19.47	0.88	
1'	105.32	4.34		1'''	168.38	x	
2'	76.40	5.42		2'''	122.13	5.99	
3'	74.66 b	3.97		3'''	140.97	7.88	
4'	77.5 b	3.98		4'''	126.99	6.17	
5'	71.77	4.32		5'''	138.68	6.41	
6'	61.50	3.99 & 3.77		6'''	125.27	6.89	
1"	169.10	x	75.2	7'''	143.51	5.96	
2"	121.63	5.91	75.3	8'''	74.11	4.10	
3"	146.08	7.26	55.2	9'''	30.96	1.54	
4"	131.52	6.28	55.6	10'''	10.24	0.91	
5"	141.67	6.08	42.2				

Footnotes: a: ^{13}C resonance assignments interchangeable. b: ^{1}H resonance assignments are interchangeable. x: Quaternary carbon. u: J_{CC} could not be determined due to overlapping carbon resonances. Chemical shift references: C^{1}HD$_2$OD = 3.30 ppm (^{1}H), ^{13}CD$_3$OD = 49.0ppm (^{13}C).

3.2.6 <u>Measurement of the isotope enrichment and labeling pattern in papulacandin B derived from [1,2-$^{13}C_2$] acetate</u>

The ^{13}C spectra of PapB labeled from [1,2-$^{13}C_2$] acetate were recorded under two different conditions: (a) A single-pulse spectrum with continuous {^{1}H} Waltz-decoupling in which signal/noise was maximized by the use of partially saturating conditions (acquisition time AQ = 2.2 s, 40° pulse, delay between end of acquisition and next pulse D1 = 0.1 s). (b) A similar single-pulse spectrum recorded under "quantitative" conditions [106, 107, 168], with decoupling only during acquisition (AQ=1.1 s, 55° pulse) and a long D1 delay (5 s), which reduces relative intensity distortions between different ^{13}C resonances that result from partial saturation and nuclear Overhauser enhancement in spectra of type (a).

To measure ^{13}C enrichments, a few μl of CH_2Cl_2 at natural ^{13}C abundance (assumed 1.108 % ^{13}C) was added to the solution as a natural abundance (NA) standard. The molar ratio R of PapB to CH_2Cl_2 was measured from integrals of the respective resonances in the ^{1}H spectrum, choosing only those PapB resonances that were clearly defined, and correcting for the number of protons contributing to each resonance. The % ^{13}C at position i of PapB was calculated from % ^{13}C = 1.108 I_i / R I_{CH2Cl2}, where I_i and I_{CH2Cl2} are the respective ^{13}C integrated resonance intensities (including all doublet and multiplet components) of position i and of the $^{13}CH_2Cl_2$ resonance. Patterns of intact acetate unit incorporation were determined from the intensities of ^{13}C singlet, doublet and

multiplet resonances, and from matching the $^1J_{CC}$ coupling constants. The isotope enrichment at the labeled positions is shown in Table 3.

3.3 Results

To determine the period in the *Apiospora montagnei* growth cycle in which PapB production rate is highest, a PapB production curve was constructed from the HPLC analytical data of *A. montagnei* methanol extracts that were sampled during the 8-day growing period (Fig. 22). These data were used to determine a suitable time in the growth cycle in which to administer the [1,2-$^{13}C_2$] acetate label so as to maximize the concentration of label available to the PapB biosynthetic enzyme(s) when the metabolite production rate is highest. Inspection of the production curve revealed a clear increase in PapB production on average between days two and five (Fig. 22). Therefore, it was determined that the label should be administered to the cultures in two pulses, the first on day three and the second on day four.

Analytical HPLC analysis of the flash C18 combined column fractions revealed the presence of PapB as well as other known papulacandins (Fig. 23). PapB was the most abundant compound in the sample followed by papulacandin C (PapC). The papulacandins were purified from this fraction by semi-preparative HPLC. The eluates corresponding to the papulacandin peaks on the chromatogram were collected following repeated injections, and some degradation from the "B" metabolite to the "C" metabolite and/or other compounds was observed during this chromatography.

Table 3: %^{13}C enrichment levels for carbon resonances of [1,2-^{13}C$_2$] acetate-labeled papulacandin B. Total %^{13}C and %^{13}C from intact [1,2-^{13}C$_2$] acetate are shown.

C	δ^{13}C	total %^{13}C	%^{13}C (intact label)	C	δ^{13}C	total %^{13}C	%^{13}C (intact label)
1	111.96	u	u	6"	40	18.3	12.0
2	70.34	4.8	0.1	7"	77.53	u	u
3	77.5	6.7	0.1	8"	137.51	15.6	11.1
4	74.77	9.4	0.1	9"	127.12	u	u
5	73.97	u	u	10"	127.12	u	u
6	64.9	8.1	0.1	11"	136.18	19.4	13.3
7	73.88	u	u	12"	31.6	18.3	15.6
8	145.44	u	u	13"	37.54	22.4	18.0
9	116.4	26.5	18.6	14"	35.25	21.7	17.3
10	161.74	31.7	25.4	15"	30.45	u	u
11	99.9	29.2	19.6	16"	11.71	21.7	14.6
12	154.74	28.0	24.4	17"	12.19	9.5	0.1
13	103.05	27.4	20.4	18"	19.47	7.1	0.1
1'	105.32	7.5	0.1	1'''	168.38	4.2	0.1
2'	76.4	5.7	0.1	2'''	122.13	2.8	0.1
3'	74.66	7.1	0.1	3'''	140.97	2.3	0.1
4'	77.5	u	u	4'''	126.99	u	u
5'	71.77	9.0	0.1	5'''	138.68	4.2	0.1
6'	61.5	6.4	0.1	6'''	125.27	5.1	0.1
1"	169.1	17.6	12.4	7'''	143.51	10.0	0.1
2"	121.63	19.3	10.6	8'''	74.11	u	u
3"	146.08	u	u	9'''	30.96	u	u
4"	131.52	29.3	17.8	10'''	10.24	6.3	0.1
5"	141.67	19.9	13.6				

Footnotes: u: enrichment not determined due to carbon resonance overlaps or impurities. Chemical shift references: C^{1}HD$_2$OD = 3.30ppm (^{1}H), ^{13}CD$_3$OD = 49.0ppm (^{13}C).

Though traces of other PapB-related compounds were detected in the NMR sample, the observed ^{1}H resonances (Fig. 24) are consistent with those of the ^{1}H spectrum obtained for a PapB sample isolated previously in our lab (C. Craft, P. Anacleto and J. L. C. Wright, unpublished result), and that reported in the literature [141]. This provided verification that the major compound isolated in this study is PapB. Further purification steps would likely have resulted in a lower yield of PapB, precluding quantitative determination of enrichment levels. Subsequent analyses of the ^{1}H (Fig. 24) and ^{13}C (Fig. 25) NMR spectra and the resulting 2D data of the unlabeled and ^{13}C-enriched PapB samples revealed some errors in the tentative carbon assignments reported earlier [149], and these data were used to re-assign those resonances (Table 2). This involved the identification of all long-range ^{1}H-^{1}H correlations of the various spin systems in the TOCSY (Fig. 27) with the short-range correlations between members of the spin system identified in the COSY (Fig. 26) starting from a known resonance and working along the carbon chain. Associated ^{13}C-^{1}H resonance correlations were subsequently identified in the HSQC (Fig. 28). This revealed that some published resonance assignments [149] for carbons of the C_{16} and C_{10} acyl chains had to be interchanged. Specifically, the published carbon resonance assignments for C4" and C9" were switched, the C5" resonance was reassigned to C8", the C8" resonance was reassigned to C11" and the C11" resonance was reassigned to C5". Also, the C17" and C18" resonance assignments were switched, as were those for C3'" and C7'" of the C_{10} acyl chain. With the exception of the sugar carbons C3 and C4 for which assignments were

interchangeable, all PapB ^{13}C resonances could be assigned (Table 2), permitting determination of the labeling pattern following incorporation of the [1,2-^{13}C$_2$] acetate precursor (Fig. 29).

The results of the ^{13}C NMR analysis of PapB labeled from [1,2-^{13}C$_2$] acetate are shown in Table 3. Matching of ^{1}J$_{CC}$ coupling constants (Table 2) identified the intact units originating from acetate (Fig. 29). Each ^{13}C resonance in the C1"-C16" side-chain of PapB was enriched through incorporation of 8 intact acetate units. The C7-C13 aromatic portion also contained 3 sets of ^{13}C-^{13}C doublets indicating incorporation of 3 intact acetate units, while the resonance for C9 appeared as an enriched singlet (Fig 30). Incorporation levels were so high that in some cases coupling between intact acetate units was observed (Fig 30).

Quantitative measurement of % ^{13}C at each position labeled from [1,2-^{13}C$_2$] acetate revealed a uniform enrichment of carbons 1"-16" and carbons 7-13 (aromatic system) above NA (average total % ^{13}C 16.5 ± 4.5 SD%). This included significant enrichment from scrambled precursor (5.6 ± 2.3 SD%). The contribution of scrambled label to the total enrichment was determined from the singlet intensity of ^{13}C resonances at positions where a proportion of intact double label had been incorporated, after subtraction of the singlet component due to NA ^{13}C. For resonances without doublets, enrichment above NA is assumed to originate from scrambled label, with the exception of C9" and C10" whose overlapping enriched resonances are assumed to have ^{13}C-^{13}C coupling satellites. As expected, carbons 1-6 and 1'-6' (sugar carbons) were not enriched
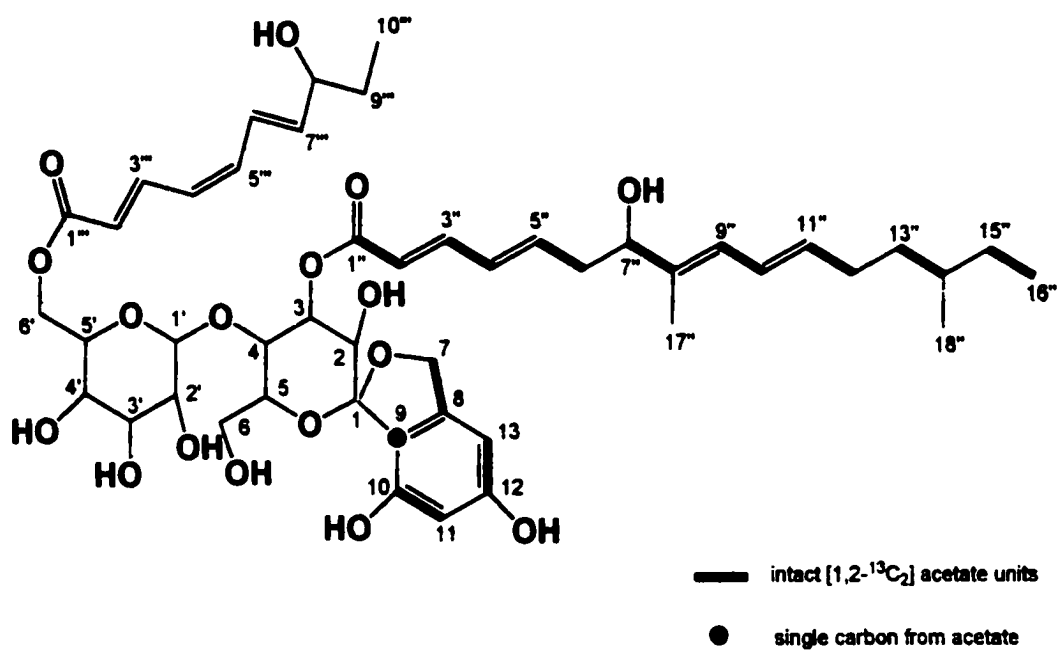
Fig. 29: Incorporation of [1,2-^{13}C$_2$] acetate into the structure of papulacandin B.
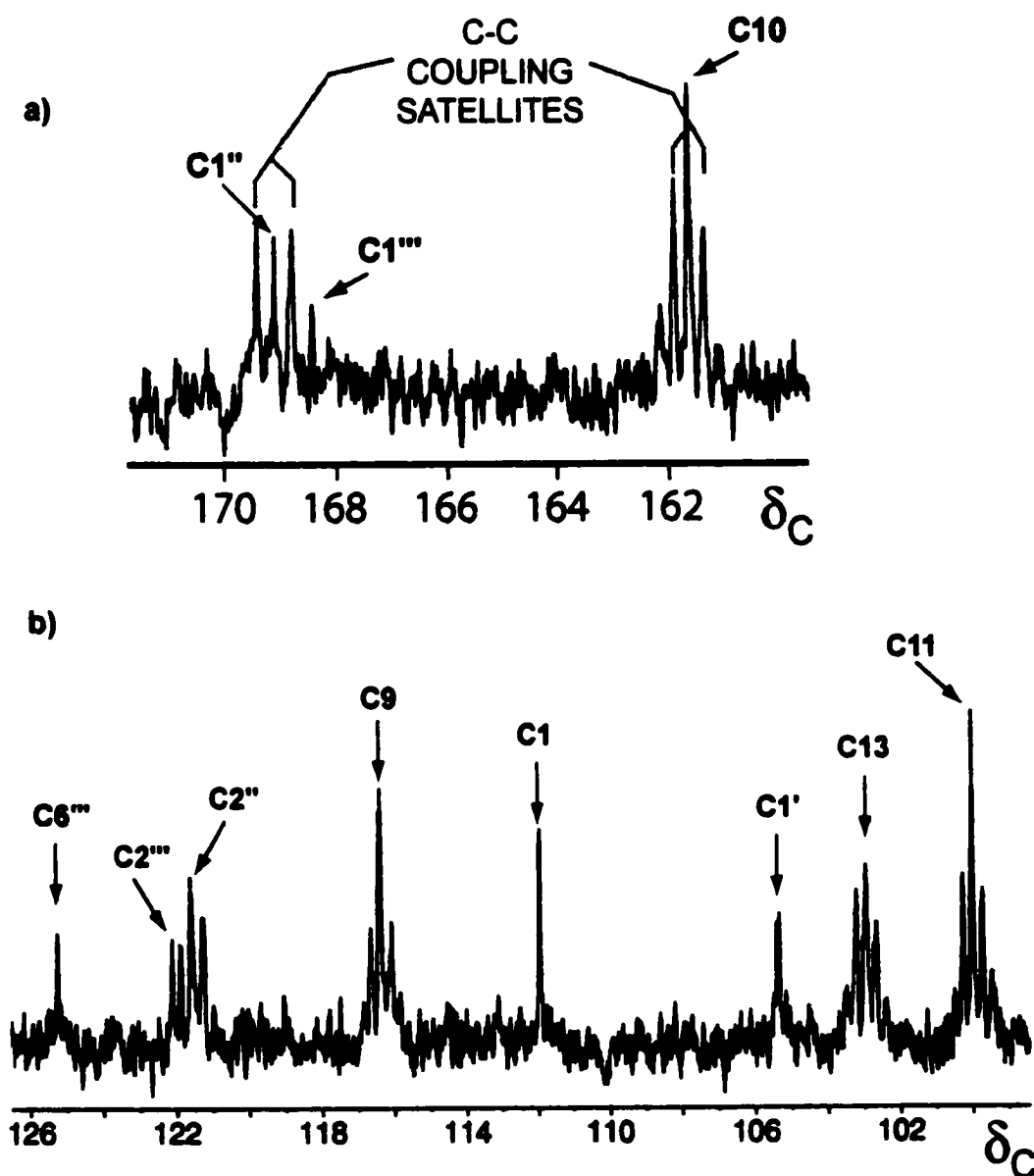
Fig. 30: Expanded regions of the ^{13}C spectrum of $[1,2-^{13}C_2]$ acetate-enriched papulacandin B. a) Doublets due to $^{13}C-^{13}C$ coupling between carbons of incorporated intact acetate units C1" (to C2") and C10 (to C11). The C1'" resonance is not enriched and shows no indication of $^{13}C-^{13}C$ coupling doublets. b) Doublets due to $^{13}C-^{13}C$ coupling between carbons of incorporated acetate units C2" (to C1"), C9 (to C8), C13 (to C12) and C11 (to C10). C6'", C2'", C1 and C1' are not enriched with intact $[1,2-^{13}C_2]$ acetate and show no indication of $^{13}C-^{13}C$ coupling doublets.

with intact label, though average enrichment from scrambled label for these carbon resonances was also significant (6.1 ± 1.5 SD%). Unexpectedly, carbons 1'''-10''' of PapB did not contain intact acetate units, and showed enrichment only from scrambled precursor (3.9 ± 2.6 SD%).

3.4 Discussion

Papulacandins are a unique class of fungal antibiotics with potential for drug development. As yet, however, studies on the biosynthesis of papulacandins have not been reported. The presence of modified acyl chains, and an aromatic moiety attached to a diglycoside in the structure of PapB (Fig. 21), indicates a complex assembly process involving PK and sugar biosynthetic steps.

To assess the anticipated role of acetate in the biosynthesis of PapB, [1,2-$^{13}C_2$] acetate was administered to PapB-producing cultures of *A. montagnei*. NMR analysis of labeled PapB isolated from these cultures revealed enrichment of specific moieties of the molecule following incorporation of intact acetate units (Fig. 29). The aromatic portion of the molecule (C7-C13), derived from a putative orsellinic acid intermediate, contained three intact acetate units in a predictable distribution. Position C9 was singly labeled and was part of a fourth intact unit that had undergone decarboxylation (Fig 29). A second moiety C1''-C16'', which describes the longer acyl side chain, was also labeled in a predictable fashion and contained eight intact acetate units (Fig 29). The additional methyl groups in the acyl side chain were not enriched, and are presumably derived from

methionine. In both these moieties there was measurable incorporation of scrambled acetate as well, but nevertheless the data confirmed the hypothesis that these portions of PapB were of PK origin.

Interestingly, and somewhat surprisingly, the C1'''-C10''' side chain, which was also expected to be of PK origin, did not contain any intact acetate units (Fig. 29), though it was labeled with scrambled acetate. There are several possibilities that might account for this. One is that the C_{10} side chain is not derived directly from the same acetate pool as the other PK portions of the molecule, but rather is assembled from an acetate pool obtained by recycling of previously formed fatty acids, perhaps originating from primary metabolism. This recycled acetate pool would account for the presence of scrambled label in the C_{10} side chain of PapB. If true, it might also suggest that the C1'''-C10''' chain is assembled at a different location within the cell where the necessary biosynthetic enzymes are prevented access to the enriched acetate pool. Another possibility is that the C_{10} acyl chain is attached as a means to export the metabolite from the producing fungal cell, and is assembled late in the biosynthetic process, from a scrambled fatty acid pool in the final biosynthetic step. Yet another even more intriguing explanation for the lack of intact acetate incorporation in the PapB C_{10} acyl chain is that it is produced by an as yet unknown non-PK pathway.

It is likely that papulacandins are produced within the fungal cell and then exported to the extracellular environment where they can inhibit the growth of competing microbes. Thus export of the papulacandins from the fungal cell may require attachment of the C_{10} acyl chain. Chemical modification of secondary

metabolites prior to export has been demonstrated for other microbes, usually as part of autoresistance mechanisms. Modifications to antibiotics prior to transport, and then removal of the modification upon export can confer autoresistance. *S. antibioticus*, for example, inactivates the antibiotic oleandomycin by glycosylation within the cell, and is reactivated by removal of the glucose moiety upon export [169, 170]. Likewise, the dinoflagellate *Prorocentrum lima* initially produces the phosphatase inhibitor okadaic acid as an inactive polysulfated ester derivative that is hydrolyzed to the active toxin upon export through the cell membrane [106]. Such examples lead to speculation that the C_{10} acyl chain of PapB is attached late in the biosynthetic pathway to facilitate export of the metabolite through the cell membrane. This is consistent with the apparent inability of PapD, which lacks a C_{10} acyl chain (Fig. 21), to penetrate yeast cells [165].

Of further interest is the fact that the $[1,2\text{-}^{13}C_2]$ acetate labeling pattern (Fig. 29) establishes that PapB is composed of at least two different types of PKs (aromatic and linear aliphatic) that differ in their degree of β-ketoreduction (Fig. 31). Presence of double bonds and hydroxyl groups in the linear aliphatic chains imply the programming of more complex reductive choices compared with the non-reductive reactions that result in the generation of aromatic PKs [119]. This indicates that these moieties of PapB are produced by separate PKS enzyme systems, the products of which are later assembled into PapB as illustrated in Figure 31. Thus PapB is a product of separate PKS systems that assemble the linear aliphatic and aromatic portions of the molecule respectively and hence the PapB biosynthetic gene cluster must contain at least two or more PKS genes.
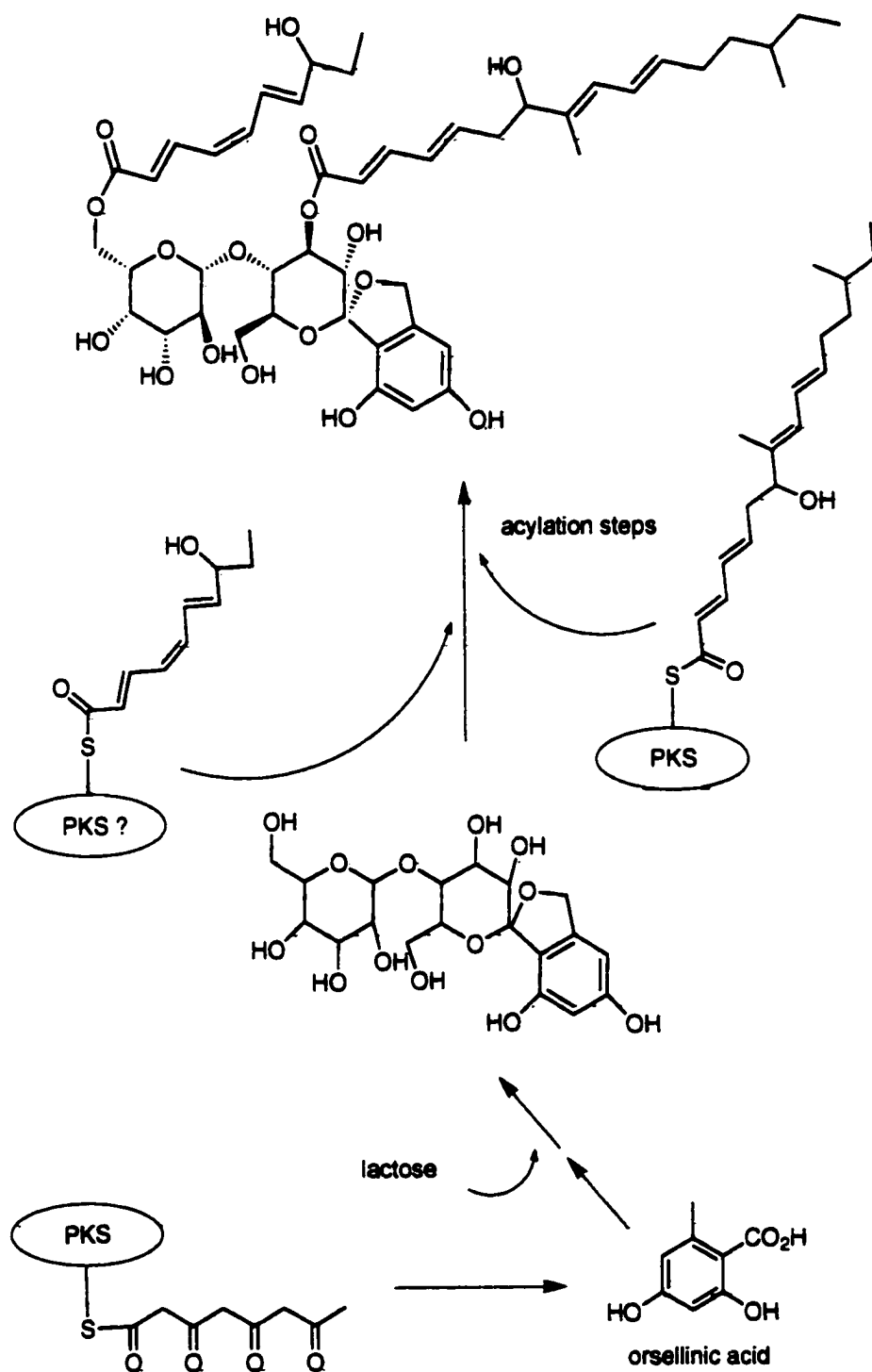
Fig. 31: Proposed scheme for the biosynthesis of papulacandin B. A PKS assembles orsellinic acid which then forms the papulacandin spiroketal diglycoside with a molecule of lactose. The long and short chain fatty acid moieties are assembled on individual PKSs and acylated to the spiroketal diglycoside to yield papulacandin B.

Fungal PKSs are known to differ with respect to the level of ketoreduction of the acetate units during the assembly of the PK chain [8]. This reductive organization of fungal PKs is determined by the amino acid sequence of the ketosynthase [120, 122]. Given the more complex reductive organization of the acyl side-chains, we would expect the PKS responsible for their assembly to be different and probably larger than the PKS for the aromatic portion. This is based on the assumption that the more complex reductive organization is due to the presence of specific ketoreductase, dehydrase and enoylreductase domains, which would be absent (or at least not utilized) in the PKS responsible for assembly of the aromatic portion. PKS gene size is generally proportional to the degree of ketoreduction required for biosynthesis, genes for more highly reduced PKs requiring additional ketoreductase sequence(s) [8]. Given the uniform enrichment of the aromatic and linear aliphatic portions of PapB from intact [1,2-$^{13}C_2$] acetate, it is reasonable to assume that the PKS enzymes function at the same time with access to enriched acetate from a common acetate pool. Separate PKS enzymes have also been shown to co-function in the production of the fungal metabolite lovastatin [124]. This metabolite is composed of two separate PK chains [171] and separate PKS genes code for the two PKS enzymes required in the biosynthesis [172].

It is reasonable to expect that the PapB biosynthetic gene cluster contains two distinct types of PKS genes for the production of aromatic and reduced PKs. Consistent with the occurrence of a non-reduced, 6MSAS-like aromatic structure within PapB (Fig. 21), we have isolated a ketosynthase gene fragment from the

same fungus, the deduced amino acid sequence of which is highly similar to the 6MSAS biosynthetic KS in Genbank (see section 2.0 of this thesis; manuscript in preparation). We postulate that this KS may be involved in the assembly of the aromatic portion of PapB. In addition, we have also isolated a KS gene fragment from *A. montagnei* that is highly similar to the aflatoxin PKS gene of *A. nidulans* (see section 2.0). It is not known whether this second PKS is involved in the assembly of the PapB sidechains, but it seems unlikely. On the other hand, a PK that resembles the aflatoxin precursor norsolorinic acid (Fig. 4) was recently isolated from the same *A. montagnei* isolate (J. Coleman, C. Craft and J. L. C. Wright pers. comm.) and yet another aromatic PK was reported from a terrestrial isolate of *Apiospora montagnei* [173]. It is possible that this second PKS gene is involved in the biosynthesis of either of these aromatic compounds. Future experiments will involve the use of these gene fragments as molecular probes to isolate the biosynthetic genes for these metabolites.

The proposed biosynthetic scheme for PapB (Fig 31) requires the participation of the disaccharide lactose. Not surprisingly this portion of the molecule was not labeled from acetate. In the biosynthesis of bacterial macrolides like erythromycin, the sugar moieties are attached by specific glycosyltransferases [7]. In the proposed biosynthesis of PapB (Fig 31), the lactose group is attached by a more complex and undefined mechanism to the tetraketide orsellinic acid group, resulting in the spirocyclic structure. Spirocyclic attachment of an aromatic ring to a sugar in this manner has not been reported for other non-papulacandin compounds.

4.0 Biosynthesis of DTX-5a and DTX-5b: Insertion of a Single Amino Acid in a Polyketide Chain.

4.1 Introduction

4.1.1 Structure and Biological Activity of DSP toxins

The Diarrhetic Shellfish Poisoning (DSP) toxins have been shown to be a complex family of compounds [92, 174]. The first member of the group to be identified was okadaic acid (Fig. 32), a cytotoxic compound isolated from the sponge *Halichondria okadaii* [65]. Shortly after, the same compound was isolated from the benthic marine dinoflagellate *Prorocentrum lima* [72]. Later, a toxin responsible for shellfish toxicity in Japanese mussels was characterized as the closely related compound DTX-1 [174] (Fig. 32). The only structural difference between OKA and DTX-1 was the additional methyl group in the terminal spiroketal ring system of DTX-1 [174] (Fig. 32). These compounds were found to be responsible for other shellfish toxin episodes around the world, and it was reported that they are produced by the dinoflagellate *Dinophysis acuminata* [174]. Since then, other groups have found that DSP toxins are produced by several temperate and sub-tropical benthic dinoflagellate species belonging to the genera *Dinophysis* and *Prorocentrum* [175-179]. Another closely related toxin DTX-2 (Fig. 32), was isolated from Irish mussels [180] reflecting a different methylation pattern in the terminal spiroketal ring system. Further research by various independent groups also uncovered a series of so-called diol esters (Fig.
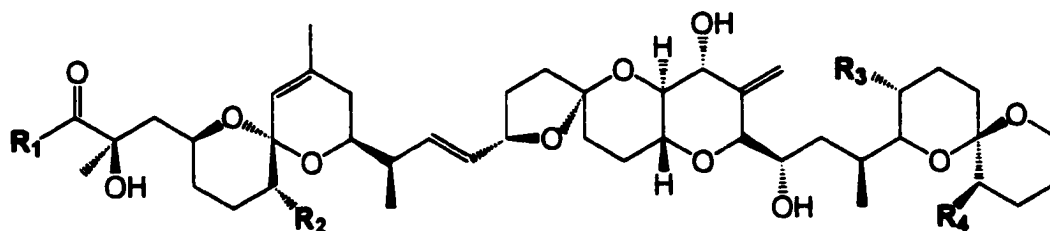
	R_1	R_2	R_3	R_4
1	OH	OH	CH_3	H
2	OH	OH	CH_3	CH_3
3	OH	OH	H	CH_3
4	OH	O-acyl	CH_3	CH_3
5		OH	CH_3	H
6		OH	CH_3	H
7		OH	CH_3	H

Fig. 32: Structures of the DSP toxins okadaic acid (1), DTX-1 (2), DTX-2 (3), DTX-1 acyl derivative (4), C_7 okadaic acid diol ester (5), C_8 okadaic acid diol ester (6), C_9 okadaic acid diol ester (7).

32) – usually okadaic acid derivatives that are esterified with a diol moiety ranging in size from $C_7 - C_9$ [105, 174, 177].

The DSP nucleus, okadaic acid (OKA) and DTX-1 (Fig. 32) are potent inhibitors of eukaryotic protein phosphatases PP1 and PP2A [181], resulting in various effects on biological systems that require protein phosphorylation and dephosphorylation. In mammals, OKA affects various biological systems including intestinal and vascular smooth muscle contraction [182] and macrophage mobility [183]. The inhibitory affect of OKA on protein phosphatases makes it both a useful agent for identifying biological processes involving protein phosphorylation/dephosphorylation [184], and a potent tumor-promoter in mammals [185]. Indeed, the effects of OKA on protein phosphorylation/dephosphorylation are profound and numerous and have recently led to its application in the study of neurodegenerative diseases such as Alzheimer's disease [186]. Inhibition of these protein phosphatases has been shown to require specific portions of the OKA molecule. Esterification of the carboxyl group or derivatization of the hydroxyl groups attached to the C1-C24 portion of OKA result in marked decrease in phosphatase inhibition [187]. Thus a free carboxyl group at least is essential for activity. Furthermore, the C1-C24 portion of OKA is known to adopt a circular conformation afforded by hydrogen bonding between C1 carboxyl, hydroxyl and ring oxygen constituents [65]. It has been suggested that this conformation of the C1-C24 portion of OKA is required for its inhibitory affect on protein phosphatases, and loss of critical H-bonds reduces activity [187].

The DSPs originally included the protein phosphatase inhibitors okadaic acid (OKA) and DTX-1 (Fig. 32) produced by the marine dinoflagellates *Prorocentrum* and *Dinophysis* spp. [174]. However, the picture has become more complicated since it was found that in toxin producing *Prorocentrum* sp., OKA and DTX-1 are actually generated by hydrolysis of larger sulfated esters such as dinophysistoxin 4 (DTX-4) [178] (Fig. 33). Despite earlier reports, these sulfated esters are essentially inactive towards PP1 and PP2A, and following this discovery, it has been proposed that these sulfates of the DSP toxins are the initial biosynthetic products [106]. Subsequent hydrolysis by a membrane-bound esterase upon extracellular transport yields the active toxins [106]. Since it has been shown that *Prorocentrum* species possess functional PP1 and PP2A phosphatases (Wright and MacKintosh unpublished results), storage of OKA as an inactive polar ester derivative within the cell and hydrolysis to the active toxin upon excretion would serve as an autoresistance mechanism to protect the dinoflagellate from its own toxin. Other microbes have adopted similar strategies. For example, antibiotics such the oleandomycin produced by *Streptomyces antibioticus*, are modified by glycosidation, protecting the cell from the antibiotic by increasing its rate of excretion through the cell membrane [188].

4.1.2 Biosynthesis of the DSP toxins

The unique chemical structure and bioactivity of the DSP toxins have inspired extensive biosynthetic study. Labeling studies with OKA and DTX-1 (referred to briefly in section 1.0) have revealed a complex biosynthetic pathway.
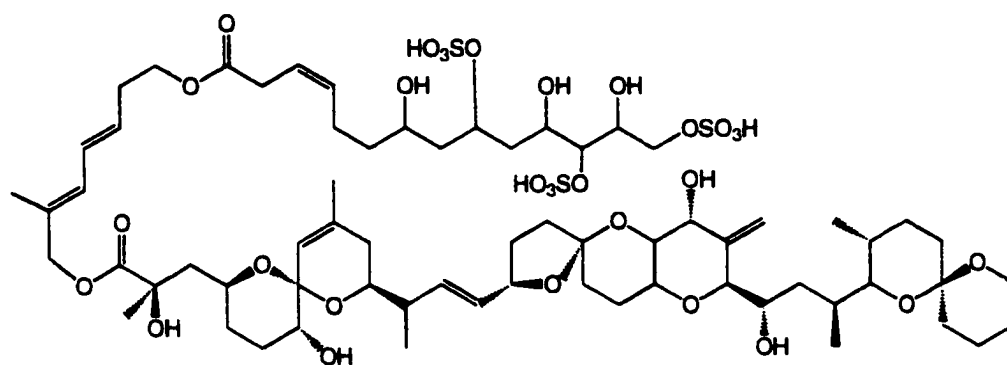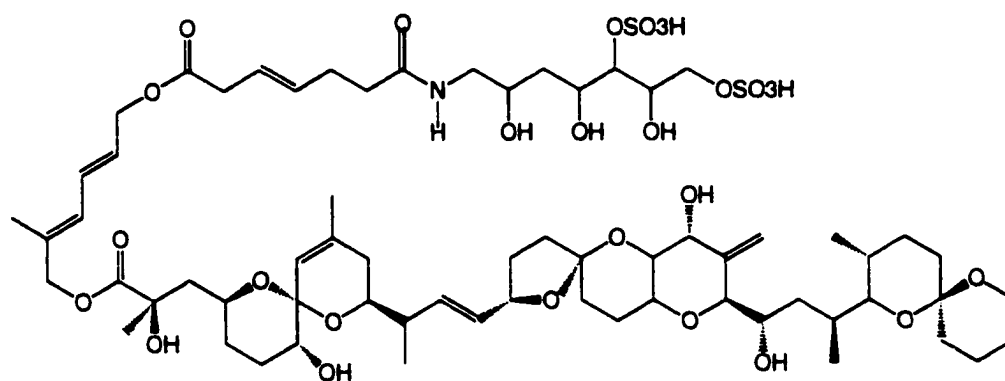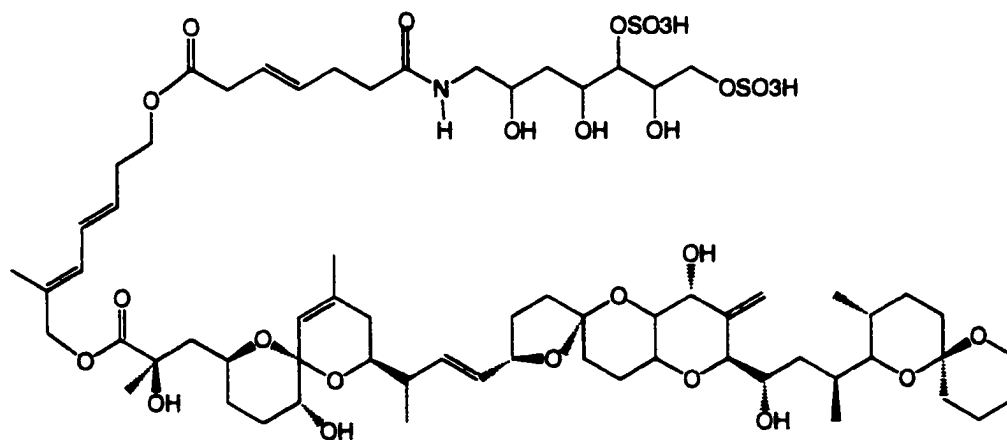
Fig. 33: Structures of the sulfated DSP toxins DTX-4, DTX-5a and DTX-5b.

It was originally observed that okadaic acid is labeled extensively from acetate, though some positions did not appear to be labeled and the labeling pattern was difficult to interpret [104, 105]. Later labeling studies of okadaic acid, the diol ester, and the large sulfated molecule were more conclusive [106, 107, 189], and revealed a series of unusual biosynthetic steps: It was found that DTX-4 is assembled from two PK chains (Fig. 34). Both of these PK chains require a glycolate starter unit, and are built up by a series of acetate additions, presumably in the usual PK manner [189]. However the nascent PK chain of the OKA portion of DTX-4 is heavily modified during this process. For example, a series of Favorski rearrangements are invoked to eject the carbonyl carbon of an intact PK acetate unit, resulting in a series of "isolated" backbone carbons derived from the methyl group of a cleaved acetate unit [106, 107]. Furthermore, all of the pendant methyl groups are derived from the methyl group of acetate (Fig. 34), an unusual feature in PK biosynthesis in which such pendant methyl groups are usually derived from methionine or by incorporation of a proprionate unit. It is postulated that these acetate-derived pendant methyl groups are attached to electrophilic carbons of the PK chain through an Aldol-like condensation involving acetate or malonate [107]. Further proof for this proposal came from the observed retention of two deuteriums at each of these methyl groups following the incorporation of [2-^{13}CD$_3$] sodium acetate [107] (Fig. 34).

Though rare, this methylation process was observed to occur during the biosynthesis of the marine bacterial product oncorhyncolide [87], and now seems to be a common feature in the biosynthesis of other dinoflagellate PKs [101]. For

1 R = OH

2 R =

3 R =

4 R =

⟶ intact [1,2-^{13}C$_2$] acetate units ■ [1-^{13}C] acetate ● [2-^{13}C] acetate

D or D$_2$ maximum number of D retained from [2-^{13}CD$_3$] acetate

[1,2-^{13}C$_2$] glycine and [2-^{13}C,^{15}N] glycine ✿ ✿ [1,2-^{13}C$_2$] glycolate

⟶O ^{18}O from [1-^{13}C,^{18}O] acetate or [2-^{13}C,^{18}O] glycolate
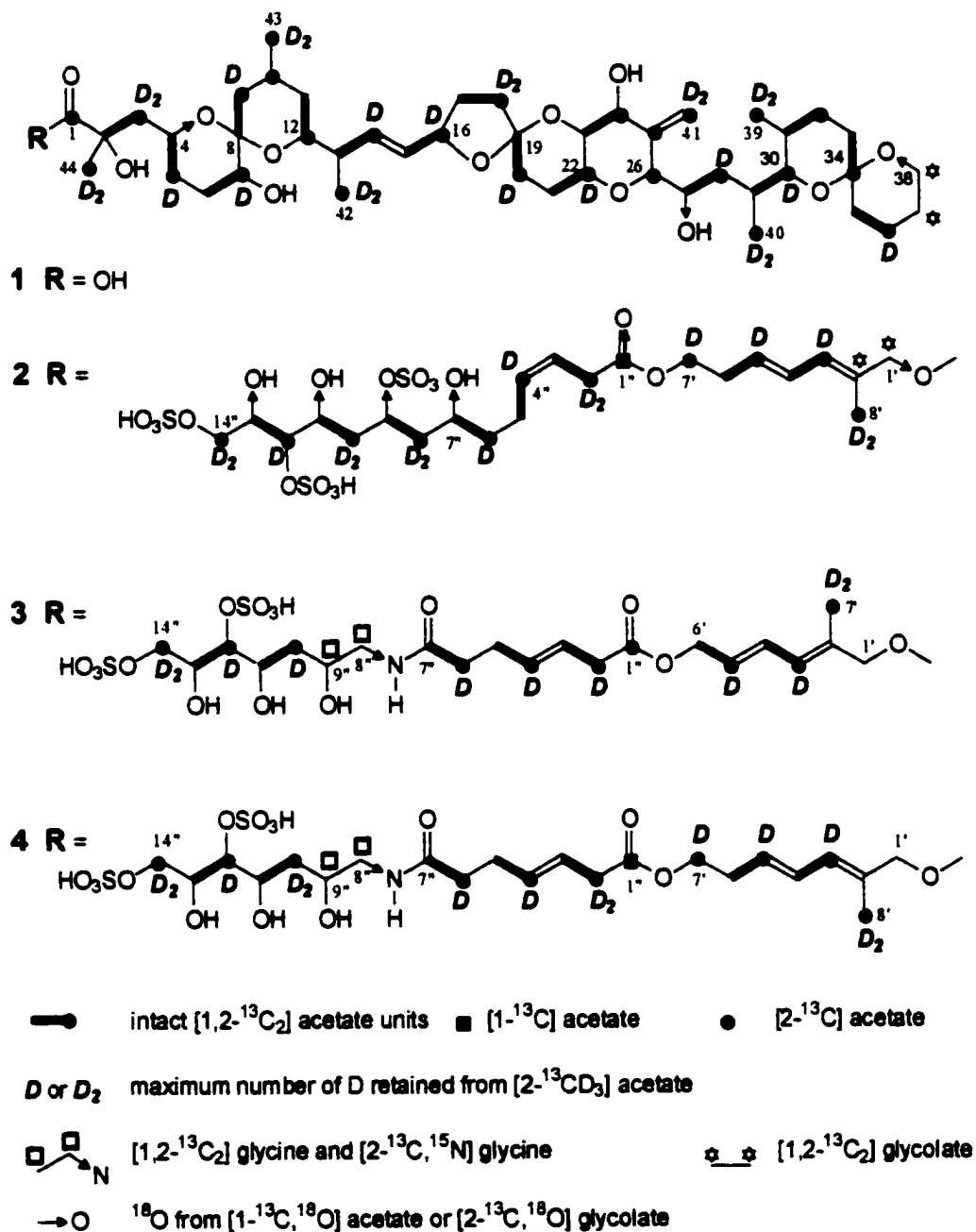
Fig. 34: Structures of okadaic acid 1, DTX-4 2, DTX-5a 3 and DTX-5b 4 showing incorporation of stable isotope labels determined from previous experiments (for 1 and 2), and from the experiments in this report (for 3 and 4).

example, these unusual PK biosynthetic processes could explain the labeling patterns observed in the brevetoxins [98-100] (Fig. 11) and amphidinolides [102, 103] (Fig. 12), neurotoxic and antitumor metabolites produced by *Amphidinium* and *Gymnodinium* sp. of dinoflagellates respectively. The carbon chains of the brevetoxins [99, 100] (Fig. 11) and amphidinolides [102, 103] (Fig. 12) both possess "isolated" backbone carbons derived from the methyl carbon of a cleaved acetate unit that interrupt the typical PK pattern of intact acetate condensations. In addition, the pendant methyl groups of the brevetoxins (Fig. 11) and the amphidinolides (Fig. 12) are also frequently derived from the methyl group of acetate.

The cyclization process that results in formation of the cyclic ether and spiroketal ring systems in okadaic acid is also the subject of considerable interest. Incorporation of $[1-^{13}C,^{18}O_2]$ acetate and $[2-^{13}C, ^{18}O]$ glycolate into OKA showed that two oxygen atoms (of C4 and C27) are derived from acetate and one oxygen atom (of C38) is derived from glycolate [107] (Fig. 34). Subsequent labeling experiments with $^{18}O_2$ showed that eight other oxygen atoms (of C1, C2, C7, C8, C19, C22, C24 and C30) were derived from this source [190], and mechanisms have been proposed that are consistent with these labeling results [190]. Incorporation of $H_2^{18}O$ water into OKA did not occur at the two acetate-derived oxygens (of C4 and C27) [191], indicating no exchange of acetate oxygen with the aqueous medium. This was interpreted to mean that an oxidative mechanism unlike that of actinomycete PKs is involved in OKA biosynthesis [191].

The biosynthesis of the sulfated side chain in DTX-4 (Fig. 34) reveals further intriguing complexity. As in the OKA portion of the molecule, the pendant methyl groups of the side chain are derived from the methyl group of acetate, and a Favorski-like elimination of backbone carbons is also observed. However, the oxygen of the ester bond in the side chain was not derived from ^{18}O-acetate [107]. Instead, it was found to arise by direct insertion of an oxygen atom between two carbons of an intact acetate unit by a Baeyer-Villiger-like mechanism, presumably catalyzed by flavin monooxygenase or a cytochrome P450 [107].

The discovery of two nitrogen-containing DSP derivatives, DTX-5a and 5b (Fig. 33), isolated from the sub-tropical dinoflagellate, *Prorocentrum maculosum* [179], poses some additional and fascinating biosynthetic questions. First, the generation of the two diol moieties is of interest. The diol portion of DTX-5a contains 7 carbons, whereas in DTX-5b it is composed of 8 carbons. Of further significance is the origin of the amide link in the side chain, and specifically how the nitrogen is incorporated.

A plausible hypothesis to account for the presence of nitrogen in DTX-5 would be the involvement of an amino acid in the construction of the side chain, and biosynthetic pathways involving a combination of amino acid and acetate precursors have been reported [3, 4, 29]. We therefore sought to establish the origins of the two diol side chains, and further examine the characteristics of the enzymatic reactions responsible for oxygen insertion in the side-chain, and determine the origin of the amide link in DTX-5a and DTX-5b. The experiments

reported here establish the biosynthetic origins of DTX-5a and DTX-5b via feeding experiments with $[1,2-^{13}C_2]$ sodium acetate, $[2-^{13}CD_3]$ sodium acetate, $[1,2-^{13}C_2]$ glycine and $[2-^{13}C, {}^{15}N]$ glycine.

4.2 Materials and Methods

4.2.1 Culturing of *Prorocentrum maculosum*

For each feeding experiment, *P. maculosum* cultures (48 L) were grown in acid-sterilized Fernbach flasks (2.8 L capacity) each containing 1 L of an enriched medium (1.0 mM $NaNO_3$; 50 µM NaH_2PO_4; 10 µM Fe.EDTA; 1 ml/L vitamins cyanocobalamin, biotin and thiamine.HCl; 0.5 g/L tris prepared in filtered (0.3 µm) seawater, pH 7.4). Prior to inoculation, the prepared medium was autoclaved (20 min, 121 °C) and allowed to cool overnight. Dinoflagellate cultures were inoculated by aliquoting portions (60 ml) of a *P. maculosum* stock culture (maintained by Pat Leblanc, IMB, Halifax) into each flask under sterile conditions. Cultures were incubated at 21 °C (16 h light, 8 h dark cycle, irradiance approximately 100 mole-photons/m^2/s) for 30 d and shaken twice daily to facilitate nutrient and light distribution throughout the cultures. The cultures were supplemented with $NaHCO_3$ 15 d following inoculation as follows: $NaHCO_3$ (10 g) was prepared as a stock solution (120 ml) and aliquots (2 ml) were added to each *P. maculosum* culture under sterile conditions. A typical yield of dinoflagellate biomass was 310 g (wet weight). Labeled precursors $[1,2-^{13}C_2]$ glycine (99 % ^{13}C), $[2-^{13}C, {}^{15}N]$ glycine (99 % ^{13}C, > 98 % ^{15}N) and $[1,2-^{13}C_2]$

sodium acetate (99 % ^{13}C) were prepared as stock solutions (1.0 g each in 53.5

ml sterile water) and autoclaved (121 ^{o}C, 15 min.). Following inoculation (28 d),

aliquots (2.0 ml) of each precursor solution were added to each Fernbach culture

under sterile conditions. All precursors were obtained from Cambridge Isotope

Laboratories except for [2-^{13}CD$_3$] acetate, which was prepared from [2-^{13}C]

acetate (99 % ^{13}C) as described below.

4.2.2 Preparation of [2-^{13}CD$_3$] acetate from [2-^{13}C] acetate

[2-^{13}CD$_3$] acetate was prepared from [2-^{13}C] acetate (3.0 g, 99 % ^{13}C) by

successive exchanges in D$_2$O (22 ml, 160 ^{o}C) in the presence of solid sodium

(approximately 130 mg). The mixture was evaporated to dryness following each

exchange period, dissolved in D$_2$O (22 ml) and the process repeated. The

reaction mixture following eight exchange reactions was collected and the pH

adjusted to 2.0 with HCl. The deuterated acetic acid was collected by distillation

and adjusted to pH 8.0 with NaOH. The mixture was evaporated to dryness and

the [2-^{13}CD$_3$] sodium acetate yield recorded. The [2-^{13}CD$_3$] acetate yield (99 %

^{13}C, > 99 % D as determined by NMR) obtained from two sets of eight exchange

reactions was 5.0 g.

4.2.3 Harvesting and extraction of Prorocentrum maculosum biomass

Cells of P. maculosum biomass were harvested by centrifugation 30 d

following inoculation and immersed in boiling water (10 min) to inactivate

esterases or lipases that hydrolyze either of the two ester linkages in DTX-5a and

5b. The dinoflagellate cells (weight not recorded) were extracted by sonication

(10 min) in methanol (approximately 3 L) and the extract evaporated to dryness

(Büchi RE III Rotovapor). The yield of methanol-extracted residue varied

between experiments, ranging from 8.78 g ([2-^{13}CD$_3$] acetate feeding

experiment) to 20.93 g ([1,2-^{13}C$_2$] glycine feeding experiment). For each

experiment, the methanol-soluble residue was dissolved in 70 % methanol: 30 %

water and partitioned successively against hexane (3 x 150 ml), diethyl ether (3 x

150 ml) and butanol (200 ml, 150 ml, 110 ml). The aqueous phase following

hexane extraction was adjusted to 75 % water prior to subsequent partitioning

steps.

4.2.4 Purification of DTX-5a and DTX-5b

After each feeding experiment, DTX-5a and 5b (Fig. 33) were purified from

the butanol-extracted residue obtained from the partitioning step. This began

with chromatography of the methanol-soluble residue using LH-20 (2 cm x 72

cm, 100 % methanol mobile phase). Fractions (76 x 100 drops) were collected

and analyzed by thin layer chromatography (Kieselgel 60 F-254 silica plates; 40

% butanol: 50 % water: 10 % acetic acid mobile phase, sprayed with vanillin).

Fractions containing DSPs appeared as pink spots on the vanillin-sprayed TLC

plates. DSP-containing fractions were combined, evaporated to dryness and

dissolved in a mixture of 60 % dichloromethane: 40 % methanol (1 ml) and

further purified by normal phase flash chromatography (silica gel (Sigma) column; 1.0 cm x 47.0 cm; 60 % dichloromethane: 40 % methanol mobile phase) under N_2 pressure. Fractions (72 x 50 drops) were collected and analyzed by TLC in the usual way. Once again, DSP-containing fractions were combined, evaporated to dryness and dissolved in methanol for LH-20 chromatography (0.9 cm x 53.4 cm; 100 % methanol mobile phase). Fractions (46 x 40 drops) were analyzed by TLC and those containing DSP toxins were once again combined and evaporated to dryness. The combined fractions were analyzed by analytical HPLC (Zorbax RX-C8, 4.6 mm x 2.5 cm column; 31 % acetonitrile: 69 % water, 1 mM ammonium acetate mobile phase; 1 ml/min. flow rate, U.V. detection at 235 nm) using DTX-5a and 5b standards (obtained from T. Hu, IMB, Halifax).

Final purification of DTX-5a and 5b was achieved by semi-preparative HPLC (Zorbax RX-C8, 4.6 mm x 2.5 cm column; 31 % acetonitrile: 69 % water, 1 mM ammonium acetate mobile phase; 1 ml/min. flow rate; U.V. detection at 235 nm). Peaks corresponding to DTX-5a and 5b were collected following multiple injections (50 μl) and fractions containing pure DTX-5a and 5b evaporated to dryness and stored at –20 °C.

4.2.5 NMR analysis of labeled DTX-5a and 5b

Samples (2-10 mg) of purified DTX-5a and 5b were dissolved in CD_3OD (0.6 ml in 5 mm Wilmad 535pp tubes) for NMR spectroscopy at 500.13 MHz (^{1}H) or 125.7 MHz (^{13}C), using Bruker AMX-500 and DRX-500 spectrometers, at 20

°C. Procedures for recording spectra under quantitative conditions and for measurement of absolute ^{13}C enrichment at each position, were similar to those previously described [106, 107, 168]. Quantitative ^{13}C spectra with {^{1}H}Waltz - or {^{1}H, D}Waltz/Garp – decoupling were recorded with 5 s delay and with no ^{1}H irradiation between acquisitions, to suppress NOE. A few μl of CH_2Cl_2 at natural ^{13}C abundance (assumed 1.108 % ^{13}C) was added to solution as a natural abundance (NA) "standard", the molar ratio r of DTX-5a (or 5b) to CH_2Cl_2 being measured from the ^{1}H spectrum. The % ^{13}C at position i of DTX-5a or 5b is given by % ^{13}C = 1.108 I_i / rI_{CH2Cl2}, where I_i and I_{CH2Cl2} are the respective ^{13}C integrated resonance intensities (including all doublet and multiplet components) of position i and of the $^{13}CH_2Cl_2$ resonance. Patterns of intact acetate unit incorporation were determined from the intensities of ^{13}C singlet, doublet and multiplet resonances, and from matching of $^{1}J_{CC}$ coupling constants. Two dimensional ^{13}C INADEQUATE spectra were also recorded from samples enriched from [1,2-$^{13}C_2$] acetate to confirm the positions of incorporation of intact ^{13}C-^{13}C units. Acquisition conditions were: f2 spectral width (SW2) 198.8 ppm, 1 K data points; f1 SW1 25 kHz, 512 increments; 320 scans / increment (DTX-5a); 192 scans/ increment (DTX-5b).

P. lima and the related dinoflagellate P. maculosum produce the structurally related PKs DTX-4 and DTX-5 respectively (Fig. 33). It was of interest, therefore, to determine the genetic organization of their PKS genes. The following section describes the isolation of DNA from P. lima and P.

maculosum and the construction of *P. lima* cDNA library as well as attempts to amplify PKS-related genes from these samples.

4.2.6 Isolation of DNA from *Prorocentrum maculosum* and *Prorocentrum lima*

To obtain DNA from *P. maculosum* and *P. lima* cells, a small portion of biomass was ground to a fine powder in liquid N_2. A small amount of frozen ground cells was suspended in cell lysis solution (600 µL, PureGene DNA Isolation Kit, Gentra Systems). The remainder of the Gentra DNA isolation protocol was followed using the plant DNA extraction protocol that involved an overnight cell digestion with proteinase K (16.6 U), an RNA degradation step with RNaseA (3.2 U) and selective precipitation of protein and carbohydrates. DNA samples were precipitated with isopropanol, resuspended in sterile water (50 µl) and stored at 5 ^{0}C.

4.2.7 Isolation of mRNA from *P. lima* for cDNA library construction

A cDNA library was prepared from *P. lima* mRNA and cloned into the bacteriophage lambda. This began with isolation of total RNA from freshly harvested *P. lima* cells (1.0 g to 4.0 g). Initial attempts to lyse the dinoflagellate cells by homogenization or grinding in liquid N_2 were unsuccessful. Subsequent purification steps by organic extraction in water-saturated phenol or TRIzol reagent (Life Technologies), or by CsCl gradient centrifugation resulted in low RNA yields. Higher RNA yields were obtained by rupturing the dinoflagellate

cells suspended in saline-EDTA (0.15 M NaCl, 0.1 M EDTA) at high pressure

(1000 psi) using a French press. The cell lysate was immediately transferred into

water-saturated phenol, 2 % sodium dodecyl sulfate (SDS) (20 ml), shaken

vigorously and centrifuged (6000 x g, 10 min). The aqueous phase was then

removed and extracted with an equal volume of water-saturated phenol and

centrifuged (6000 x g, 10 min). The aqueous phase from this extraction was

collected and extracted with an equal volume of 50 % water-saturated phenol:

chloroform. RNA was precipitated (-80 $^\circ$C) from the aqueous phase with $LiCl_2$ (2

M final concentration), and collected by centrifugation (12000 x g, 30 min),

washed with 70 % ethanol (10 ml) and resuspended in diethylpyrocarbonate

(DEPC)-treated water (200 μl). Aliquots (1, 3 and 5 μl) of the RNA sample were

electrophoresed (60 V, 1 h) through a 1 % agarose denaturing gel (0.2 M HOPS,

pH 7, 50 mM sodium acetate, 5 mM EDTA, 17 % formaldehyde running buffer) to

assess the RNA yield. Quality and yield of the total RNA was also assessed by

spectrophotometry ($A_{260/280}$ for RNA = 2.0 [126]). Spectrophotometric analysis of

the P. lima RNA determined that good quality ($A_{260/280}$ = 1.99) RNA (1.3 mg as

determined from the A_{260} reading = 1.69) was obtained. PolyA$^+$ mRNA was

purified from total P. lima RNA by affinity binding to oligo-dT cellulose (Invitrogen

FastTrack mRNA isolation kit) and spin chromatography with low salt buffer (250

mM NaCl, 10 mM Tris-Cl, pH 7.5 in DEPC-treated water) to remove rRNA and

low molecular weight RNAs. Pure mRNA was eluted from the oligo-dT by spin

chromatography in a low ionic strength buffer (10 mM Tris-Cl, pH 7.5 in DEPC-

treated water, 400 μl) and precipitated with ethanol. The mRNA was collected by

centrifugation (16000 x g, 30 min), resuspended in 50 µl elution buffer (10 mM Tris-Cl, pH 7.5 in DEPC-treated water) and quantitated by spectrophotometry (6.34 µg final yield from three purifications).

4.2.8 Preparation of a *P. lima* cDNA library from purified mRNA

A cDNA library was prepared from pure *P. lima* mRNA (ZAP-cDNA synthesis and Gigapak III Gold Cloning Kit, Stratagene) following the protocol recommended by the manufacturer. First strand cDNA synthesis reactions were performed separately on *P. lima* and control mRNA samples (5 µg each). To synthesise first strand cDNA, mRNA was primed with an oligo(dT) primer and transcribed by Moloney murine leukaemia virus reverse transcriptase (MMLV-RT). For both the *P. lima* and control first strand cDNA synthesis reactions, corresponding reactions were set up which included [α-^{32}P] dATP. Second strand cDNA synthesis reactions were performed on *P. lima* and control first strand cDNA reactions in the presence of [α-^{32}P] dATP. For second strand cDNA synthesis, RNaseH was used to degrade the RNA strand left over from the first strand synthesis reaction followed by DNA polymerase I to synthesize the second DNA strand. To visualize the first and second strand cDNAs, aliquots (1 µl) of reactions containing [α-^{32}P] dATP were electrophoresed (100 mA) through an alkaline agarose gel (1 %) that was subsequently dried, exposed to film overnight and the film developed. 1 kb DNA size markers (GibcoBRL) were [α-^{32}P] dATP-labeled at their 5' end using T4 polynucleotide kinase (GibcoBRL) and

co-electrophoresed with the first and second strand cDNA reactions. A size exclusion sepharose drip chromatography column was run on the radiolabeled cDNAs in order to isolate large cDNAs for the subsequent cloning reaction. Radioactive fractions were assumed to contain cDNAs and were subsequently analyzed by polyacrylamide gel electrophoresis (PAGE). Fractions containing the highest concentrations of large cDNAs were combined and purified by phenol: chloroform extraction. The quantity of cDNA in both the *P. lima* and control reactions was assessed by ethidium bromide plate assay. This involved comparison of cDNA samples to a serial dilution set of *Sty* I-digested lambda DNA of known concentration, both of which were stained with an equal concentration of ethidium bromide. The cDNAs of the *P. lima* and the control reactions were ligated into the Uni-Zap XR vector (Stratagene) and packaged into phage lambda using the protocol recommended by the manufacturer. cDNA library titer was established by infecting *E. coli* XL1-Blue MRF' cells with the packaged phage in the presence of IPTG (2.5 mM) and X-gal (4.2 mg/ml), plating the culture on NZY agarose (37 °C) and counting recombinant (white) plaques. The *P. lima* cDNA library was then amplified by infecting *E. coli* XL1-Blue MRF' cells in LB broth (recipe, 600 μl) and plating (150 mm plates) the culture on NZY top agarose (37 °C, 6 to 8 h). Phage were removed from the plates by suspension in SM buffer (0.2 M NaCl, 10 g/l tryptone, 5 g/l yeast extract pH 7; 10 ml per plate, rotation overnight at 4 °C). The amplified library was removed into 50 ml centrifuge tubes (Fisher Scientific) and supplemented with chloroform (5 % final concentration). Cell debris was removed by centrifugation, the supernatant

removed into fresh tubes (50 ml) and supplemented with 0.3 % chloroform. For long-term storage, cDNA library aliquots (1 ml) were incubated at –80 °C) in dimethylsulfoxide (DMSO) (7 %).

To determine the size of a representative sample of cDNAs in the *P. lima* library, 24 randomly selected plaques (from a previous titering step) were removed as agar plugs using a sterile glass pipet into SM buffer (100 μl) in separate microcentrifuge tubes. Phage were eluted from the agar plugs into the SM buffer by overnight incubation (4 °C). PCR reactions (50 μl) using M13 forward and reverse primers and aliquots (5 μl) of SM buffer containing eluted phage as template were performed. Aliquots (1 μl) of each PCR were electrophoresed (60 V, 1 h) through a 0.8 % agarose gel (1 x TBE running buffer).

4.2.9 Sequencing of randomly-selected *P. lima* cDNAs

Sequences of 36 randomly chosen *P. lima* cDNAs or expressed sequence tags (ESTs) were obtained. To isolate double-stranded circular cDNA subclones from recombinant lambda phage, a mass *in vivo* excision reaction was performed. This involved coinfection of *E. coli* (XL1-Blue MRF' strain) with recombinant lambda phage and a helper phage (ExAssist helper phage, Stratagene) expressing proteins required for excision of recombinant phagemid DNA. Recombinant phagemids were released from the *E. coli* XL1-Blue MRF' cells following cell rupture at 70 °C and used to infect *E. coli* (SOLR) cells (LB^amp

plates, overnight at 37 °C). 36 Colonies were randomly selected and cultured

separately overnight (LB broth, 3 ml). Aliquots (1.5 ml) of each overnight culture

were centrifuged (21000 x g, 5 min) and the medium decanted. Cells were

resuspended in proteinase K (200 µl, 1 U), incubated (37 °C, 2 h) and lysed by

incubation at 50 °C (30 min) followed by 90 °C (15 min). Cell debris was

removed by centrifugation and the supernatant stored (-20 °C). cDNA inserts in

lysate preparations were sequenced (Applied Biosystems 373 DNA sequencer)

via dye terminator cycle sequencing (sequencing protocol as in chapter 3).

P. lima DNA and cDNA library aliquots as well as P. maculosum DNA

aliquots were PCR screened for the presence of PKS genes using various

primers designed from alignments of known fungal PKS sequences.

4.3 Results

4.3.1 Incorporation of [1,2-^{13}C$_2$]- and [2-^{13}CD$_3$] acetate into DTX-5a and DTX-5b

^{13}C spectra from samples enriched from [1,2-^{13}C$_2$] acetate (Fig. 35)

showed that most ^{13}C resonances in both DTX-5a and DTX-5b contained ^{13}C-^{13}C

doublets indicating either intact incorporation from an acetate unit (doublets of

high intensity), or adjacent incorporation of labels originating from separate units

(doublets of lower intensity such as those found in the resonances of methyl

groups). Quantitative measurement of ^{13}C enrichment at each position, showed

that positions C1-C36, C39-C40, C3'-C7' (C3'-C8' in DTX-5b), C1"-C7" and C10"-

C14") were uniformly enriched (av. total % ^{13}C for these positions 4.8 ± 0.6 SD %
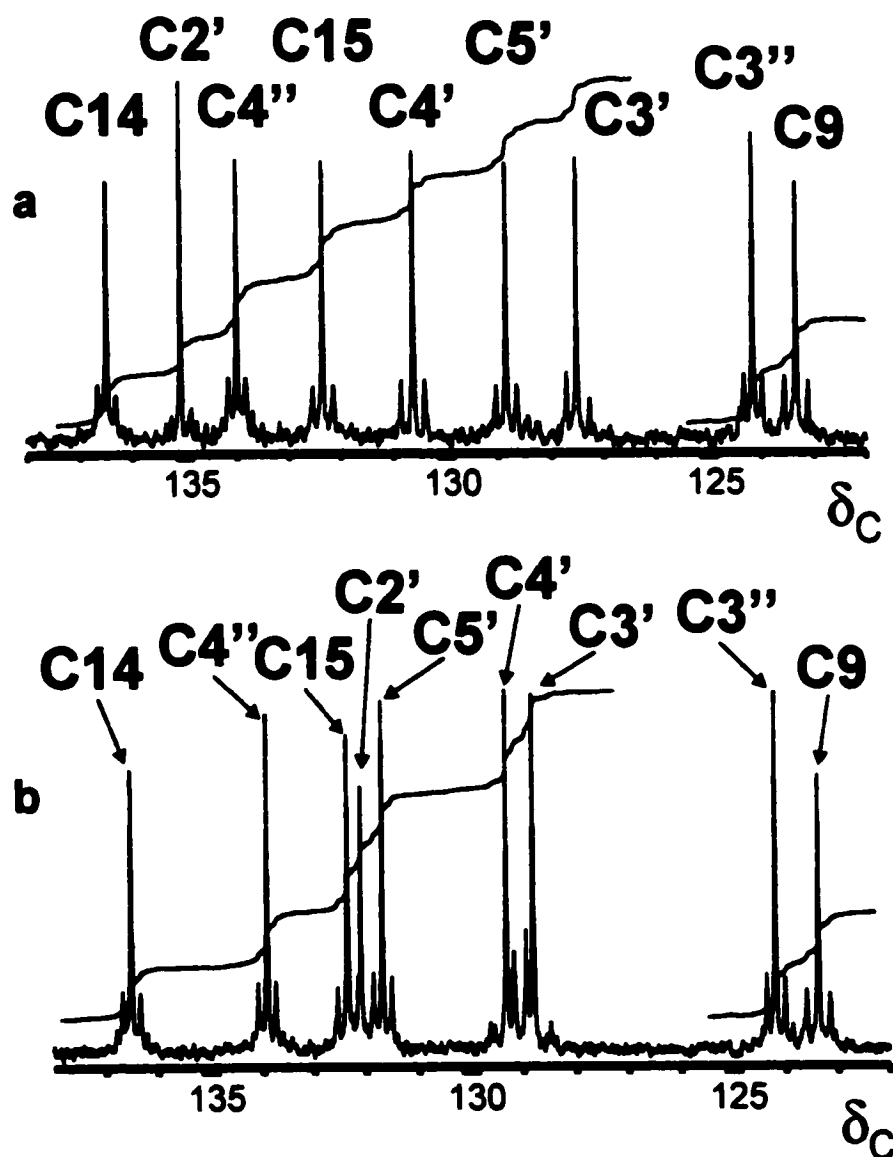
Fig. 35 Portions of the 125.7 MHz ¹³C NMR spectra of (a) 3 and (b) 4 enriched from [1,2-¹³C₂] acetate, and satellites due to incorporation of intact ¹³C-¹³C units, at C9, C14, C15, C2', C3', C4', C5', C3", C4". Integrals show uniform ¹³C enrichment at these carbons and a lower enrichment at C2' corresponding to incorporation of scrambled label only. In DTX-4, C2' was shown to originate from glycolate. Spectrum (a) was recorded under "quantitative" conditions with suppressed NOE whereas spectrum (b) was obtained without NOE suppression. The latter spectrum yielded relative enrichments of proton-bearing carbons close to those from a "quantitative" spectrum of the same compound, indicating that the latter in particular was yielding reliable enrichment values.

for DTX-5a, 3.7 ± 0.3 SD % for DTX-5b). Analysis of $^1J_{CC}$ coupling constants and 2D ^{13}C INADEQUATE spectra of DTX-5a and DTX-5b showed, in the OKA portion (C1-C44), a pattern of incorporation of intact acetate units, and single labels derived from acetate, identical to that previously found in DTX-4 (Fig. 34). The isotope labeling pattern for the diol portion C1'-C8' of DTX-5b was also identical to that in DTX-4. However, the labeling pattern for the diol moiety in DTX-5a was different and showed evidence that an acetate carboxyl-derived carbon (corresponding to C7' of DTX-4 and DTX-5b) which previously formed an intact acetate unit with C1" was deleted from the carbon backbone. Otherwise, the labeling pattern of DTX-5a was the same for the corresponding carbons C1'-C7' of DTX-4 and DTX-5b (note that the numbering system adopted for this report differs from that used originally for DTX-4 [179]). The remainder of the sidechain (C1"-C14") was labeled in the same manner in both DTX-5a and DTX-5b, showing intact ^{13}C-^{13}C pairs from C2" to C7" and from C10" to C13", and single carbons derived from acetate at C1" and C14" (Fig. 34).

Positions C37, C38, C1', and C2' showed lower levels of incorporation of ^{13}C from [1,2-^{13}C$_2$] acetate (av. 3.3 ± 1.0 % SD for DTX-5a, 3.0 ± 0.1 SD % for DTX-5b), and no doublet components corresponding to coupling within these pairs, consistent with the finding for DTX-4 that these positions are only indirectly labeled from scrambled acetate via glycolate, without retention of an intact ^{13}C-^{13}C unit. Positions C8" and C9" similarly showed low incorporation (av. 3.4 ± 0.6 SD % for DTX-5a, 2.0 ± 0.3 SD % for DTX-5b) and lack of ^{13}C-^{13}C coupling between them. Compared with DTX-4, total ^{13}C enrichments were lower and the

proportion of enrichment due to scrambling of the $[1,2\text{-}^{13}C_2]$ acetate label was higher, amounting to 2.0 ± 0.4 SD % ^{13}C in DTX-5a and 1.7 ± 0.2 SD % ^{13}C in DTX-5b. This was determined from the singlet intensity of ^{13}C resonances at positions where a proportion of intact double label had been incorporated, after subtraction of the singlet component from the calculable fraction of NA acetate. Thus all the acetate-derived ^{13}C at positions C37, C38, C1', C2', C8" and C9" can be attributed to scrambled label. The average relative intensity $I_d/(I_s+I_d)$ of doublet to total (singlet + doublet) intensity, after subtraction of the NA contribution to the singlet resonances but including the scrambled component, was 0.45 ± 0.06 SD (DTX-5a) or 0.37 ± 0.06 SD (DTX-5b) for carbons that were members of intact $^{13}C\text{-}^{13}C$ units, and 0.23 ± 0.05 SD (DTX-5a) or 0.16 ± 0.03 SD (DTX-5b) for pendant methyl and vinyl carbons. This is consistent with synthesis of a proportion of the compounds from a highly ^{13}C-enriched pool (> 23 % ^{13}C in DTX-5a, > 16 % ^{13}C in DTX-5b), with subsequent (or prior) dilution by material containing lower levels of label, down to and including NA. Other non-methyl carbons bearing single acetate-derived labels (C1, C10, C25, C26, C7' (in DTX-5b), C1" and C14") had resonances with satellites indicating probabilities of adjacent incorporation similar to the methyl carbons. As amounts of compound were smaller, enrichments lower, and the extent of scrambling greater than for DTX-4, multiplets (doublets of doublets) due to adjacent incorporation of three or more ^{13}C were not observed in spectra of DTX-5a and DTX-5b.

The pattern of $[1,2\text{-}^{13}C_2]$ acetate incorporation along the side-chains of DTX-5a and DTX-5b (Fig. 34) suggests some interesting parallels to DTX-4 [106,

107]. In particular, the differing lengths of the C1'-C6' moiety in DTX-5a and the C1' –C7' moiety in DTX-5b prompted an examination of the spectra for evidence of Baeyer-Villiger (BV) insertion of oxygen between C6' and C1" of DTX-5a, or between C7' and C1" of DTX-5b [107]. In the latter case, the labeling pattern suggested that the oxygen would be inserted between two carbons of an intact acetate unit as in DTX-4. This would result in doublet satellite peaks ($^2J_{COC}$ ca 2.6 Hz) of the C7' and C1" resonances having the same relative intensity to the singlet resonances as other $^1J_{CC}$ doublets arising from incorporation of intact acetate units. Such satellites were found for DTX-5b, supporting the hypothesis that oxygen is inserted between two carbons of an intact acetate unit. This was not observed with the C6' and C1" resonances of DTX-5a (Fig. 36) since these carbons arise from separate acetate units.

The quantitative ^{13}C spectra of DTX-5a and DTX-5b labeled from [2-$^{13}CD_3$] acetate showed that C1" in DTX-5a is derived from the methyl, and in DTX-5b from the carboxyl carbon of acetate (Fig. 34). These results suggest that the enzyme complex responsible for the Baeyer-Villiger reaction in DTX-5a and DTX-5b inserts oxygen at a specific distance (14 carbons and 1 nitrogen) from the C14" end of the PK chain. This can be compared with the distance of 14 carbons in DTX-4.

Further comparisons of acetate incorporation between DTX-4, DTX-5a and DTX-5b were possible, following the [2-$^{13}CD_3$] acetate feeding experiments. Examination of the spectra of labeled DTX-5a and DTX-5b provided evidence of D-retention (and hence the fate of acetate hydrogen) as indicated by isotopically-
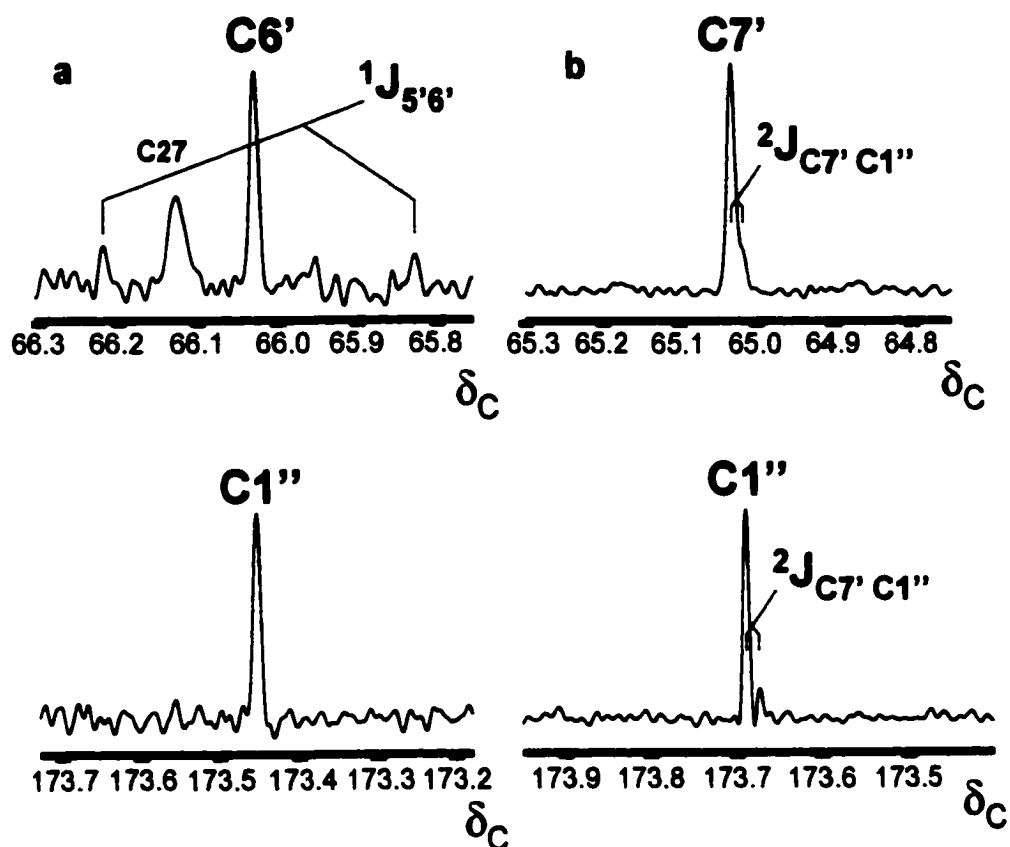
Fig. 36 Lorentz-Gauss resolution-enhanced portions of the 125.7 MHz ^{13}C NMR spectra of (a) DTX-5a and (b) DTX-5b enriched from [1,2-^{13}C$_2$] acetate, showing resonances for C6' and C1" of DTX-5a and for C7' and C1" of DTX-5b. The latter peaks show isotopically-shifted ^{13}C-^{13}C doublets ($^2J_{COC}$ ca 2.5 Hz) indicating that, in DTX-5b, O has been inserted between two carbons of a previously intact unit derived from acetate. The relative intensity of these doublets is the same as for $^1J_{CC}$ doublets at other positions. No such small couplings are seen in the resonances of DTX-5b.

shifted peaks in the ^{13}C spectra recorded with {^1H, D}-decoupling (Fig. 37). Despite lower enrichments than were obtained previously with DTX-4, and a greater degree of scrambling of the label, the pattern of D-retention in the OA moiety of DTX-5b was found to be identical with that for DTX-4 (Fig. 34). All methyl groups retained up to two D. The sidechain of DTX-5b retained up to two D at each of C8', C2", C10" and C14" showing that, as in corresponding positions in DTX-4, dehydration does not occur at these positions following β-keto reduction. Other acetate methyl-derived positions on the sidechain retained one D as in DTX-4. The results for DTX-5a were similar although it was not possible to detect peaks indicating D_2-retention at C18, C2" or C10", probably owing to insufficient signal/noise (average enrichments were higher for DTX-5a than for DTX-5b, but the quantity of material was smaller). Nevertheless, apart from these differences, the pattern of D-retention was fully consistent with DTX-4 and DTX-5b.

The quantitative ^{13}C NMR data for DTX-5a and DTX-5b, labeled from [2-$^{13}CD_3$] acetate, showed an average ^{13}C enrichment of 4.6 ± 0.5 % SD (DTX-5a) or 2.5 ± 0.3 % (DTX-5b) for all carbons originating from the methyl group of acetate (Fig 34). Other positions had a ^{13}C enrichment of 3.5 ± 0.5 % SD (DTX-5a) and 2.0 ± 0.3 % (DTX-5b). The difference, 1.1 % ^{13}C (for DTX-5a) or 0.5 % ^{13}C (for DTX-5b), is the enrichment due to incorporation of unscrambled label. Given that the [2-^{13}C] acetate label is 95 % ^{13}C, another 1.108 (1.0 - 0.05) % = 1.1 % ^{13}C at all positions was determined to originate from endogenous acetate at natural isotopic abundance. The remaining ^{13}C enrichment (av. 2.4 % ^{13}C for
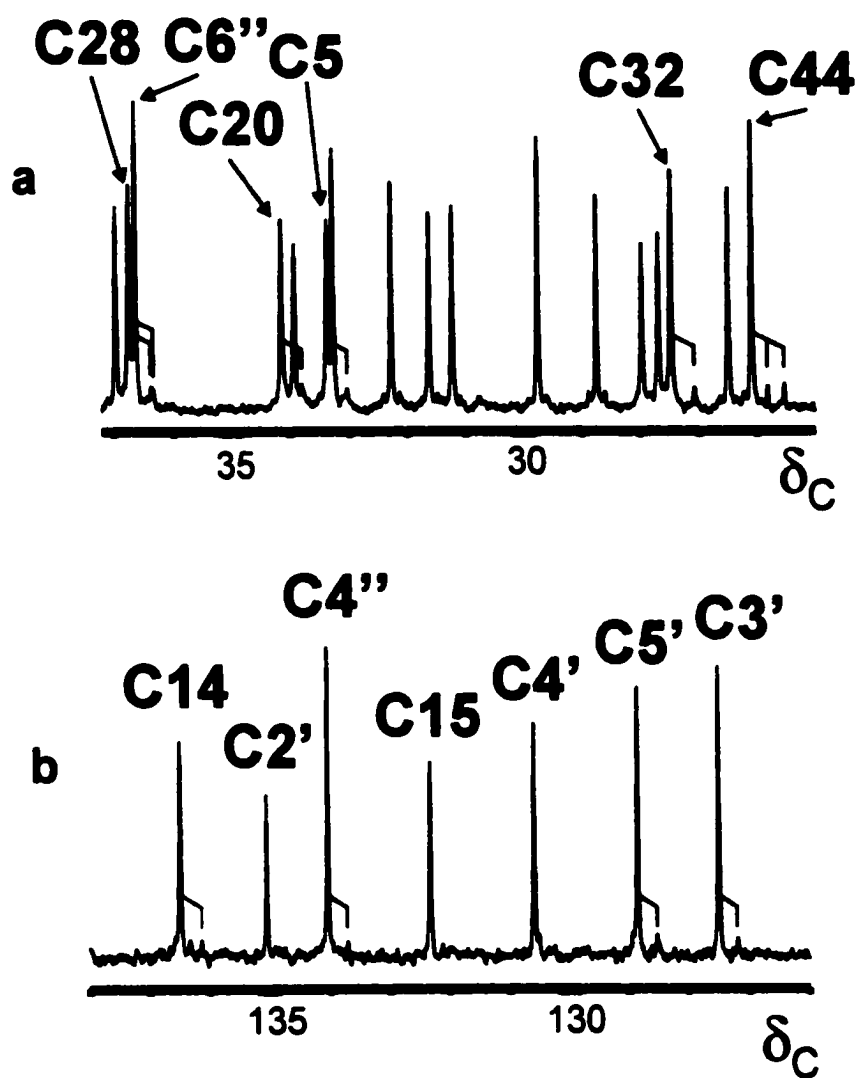
Fig. 37 Portions of the 125.7 MHz ^{13}C NMR spectra of (a) DTX-5a and (b) DTX-5b enriched from [2-^{13}CD$_3$] acetate. Isotopically shifted peaks indicate D-retention.

DTX-5a and 0.9 % ^{13}C for DTX-5b) represents a high degree of scrambling of the [2-^{13}CD$_3$] acetate label.

After subtraction of the average scrambled label and NA contributions to the non-isotopically-shifted component of each resonance, the retention R % of D from unscrambled [2-^{13}CD$_3$] acetate label was calculated approximately from the relative peak heights of the isotopically shifted (intensity I_{D1}, I_{D2}) and the remaining unshifted (residual intensity I_0) components. Thus for a CH group, R % = $100 I_{D1}/(I_{D1} + I_0)$; for a CH$_2$, R % = $100 (I_{D1} + 2I_{D2}) / (2 (I_0 + I_{D1} + I_{D2}))$; and for a CH$_3$ group, R % = $100 (I_{D1} + 2I_{D2} + 3I_{D3}) / (3 (I_0 + I_{D1} + I_{D2} + I_{D3}))$. Average D-retention R_{av}. was similar for both compounds and for different moieties within them: for labeled positions in the OA moiety of DTX-5a and DTX-5b respectively, R_{av} was 31 ± 10 % SD and 32 ± 11 %; for all Me groups R_{av} was 39 ± 6 SD and 34 ± 3 %, and for labeled positions in the side-chains 34 ± 6 % SD and 32 ± 10%. These results strongly suggest assembly of the entire molecule from a uniform acetate pool containing both intact and scrambled labels, and a much larger mole fraction of NA acetate. Owing to the difficulties in performing quantitative measurements with small quantities of material at low enrichment, in the presence of a high degree of scrambling, the errors for D-retention at individual positions are large (ca ± 15 % D). Nevertheless the assumption of uniform ^{13}C enrichment from acetate across the molecule is justified by the results obtained from the [1,2-^{13}C$_2$] acetate precursor experiments.

4.3.2 Incorporation of [1,2-^{13}C$_2$]- and [2-^{13}C,^{15}N] glycine precursors into DTX-5a and DTX-5b

In DTX-5a and 5b (Fig. 34), neither C-8" nor C-9" incorporated unscrambled acetate directly, indicating that they originated from another biosynthetic source. Inspection suggested that C-8", C-9" and the adjacent N might be formed from a glycine unit and so cultures of *P. maculosum* cultures were supplemented with [1,2-^{13}C$_2$] glycine and [2-^{13}C,^{15}N] glycine in separate experiments. In both DTX-5a and 5b, incorporation of [1,2-^{13}C$_2$] glycine resulted in exclusive labeling at C8", C9" as indicated by satellite doublets at the C8" and C9" resonances ($^1J_{CC}$ 40.2 Hz, enrichment to 1.6 ± 0.1 % ^{13}C for 3, 1.6 ± 0.1 % ^{13}C for 4) (Fig. 38). Following incorporation of [2-^{13}C,^{15}N] glycine only at the C8" resonance in each compound displayed an additional doublet ($^1J_{CN}$ 10.4 Hz, enrichment to 1.9 ± 0.1 % ^{13}C for 3, 1.8 ± 0.1 % ^{13}C for 4) (Fig. 39). No other carbons were enriched from these precursors, and there was no measurable scrambling of label, the measured % ^{13}C for all other carbons corresponding to NA (1.1 ± 0.2 %).

4.3.3 Screening of *P. lima* and *P. maculosum* DNA and *P. lima* cDNA for PKS genes

Attempts to amplify PKS-related DNA fragments from *P. lima* and *P. maculosum* DNA and *P. lima* cDNA using primers designed from alignments of
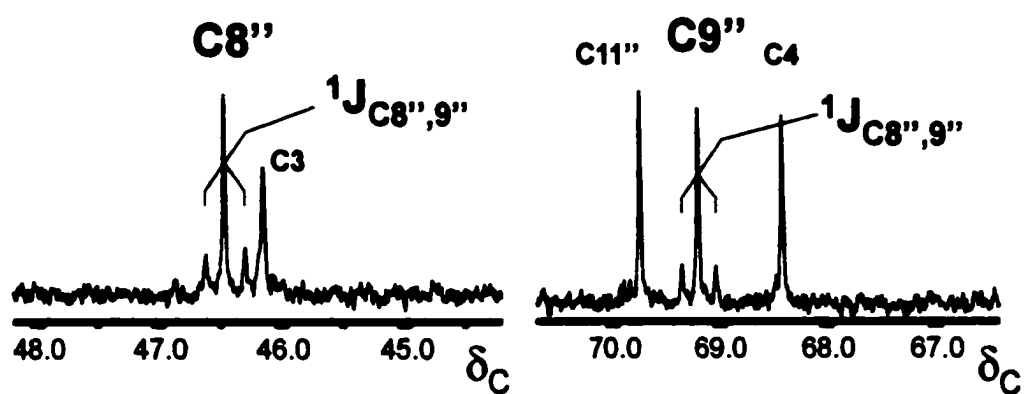
Fig. 38: Portions of the 125.7 MHz ^{13}C NMR spectrum of DTX-5b enriched from [1,2-^{13}C$_2$] glycine. Arrows indicate ^{13}C-^{13}C coupling satellites due to incorporation of the intact C2 unit of glycine into the C8" and C9" positions of DTX-5b.

fungal PKS sequences were unsuccessful. These reactions usually did not amplify any product, though in some cases several products were evident upon electrophoresis (not shown) with significant smearing between bands. Such products were usually amplified using a reduced annealing temperature (below the calculated Tm for the lowest % G+C primer) and were assumed to originate from non-specific primer annealing. Random sequencing of *P. lima* ESTs derived from the cDNA library did not result in isolation of a PKS-related cDNA fragment. Most of the cDNAs sequenced were less than 500 bp in length, were comprised of highly repetitive 2-3 nucleotide sequence and had no positive match when queried against the Genbank database. Two of the 36 ESTs had a significant match to sequences in Genbank. These were EST 8, which was similar to *Plasmodium vivax* cytochrome oxidase genes (BLASTn score = 1e-14) and EST28, which was similar to *Vitis vinifera* (grape) alcohol dehydrogenase (BLASTn score = 1e-10). However, the small cDNA sizes and highly repetitive sequences made pursuit of a larger-scale *P. lima* EST survey unrealistic.

4.4 Discussion

The incorporation of $[1,2-^{13}C_2]$ acetate into DTX-5a and DTX-5b, establishes the PK mechanism of their biosynthesis (Fig. 34). Thus assembly of DTX-5a and 5b by the subtropical species *P. maculosum*, is entirely consistent with the biosynthesis of DTX-4 produced by the temperate-water dinoflagellate *P. lima* (Fig. 35)[106]. In both types of compounds, the OKA moiety is assembled by an identical process involving a Favorski-like elimination of carboxyl acetate

carbons from the nascent polyketide chain and addition of pendant methyl groups from the methyl carbons of acetate. The combination of these processes is rare in nature, yet it occurs fairly frequently in dinoflagellate biosynthesis.

The most significant difference between DTX-4 and the DTX-5a and 5b pair, resides in the structure of the sulfated side chain of the molecules (Fig. 33): The earlier labeling work with DTX-4 clearly established that this portion of the molecule is a PK chain incorporating a glycolate starter unit, into which an oxygen atom is inserted to create an ester link. A similar pathway is followed in the biosynthesis of the DTX-5 molecules, and the ester link is also present in the side chain of both compounds. However, the length of the so-called diol ester moiety in DTX-5a is one carbon shorter compared with DTX-5b and DTX-4. The labeling data reveal that this is accounted for by the deletion of a carboxyl acetate carbon – presumably by a Favorski-like mechanism – to yield a shorter chain (by one carbon) in DTX-5a. This result underscores a precise substrate specificity in which oxygen is inserted in the chain at a predetermined length (14 carbons and a nitrogen atom) from the terminus. Thus, the enzymatic system that catalyzes the insertion reaction (a putative Baeyer-Villigerase) uses this end of the molecule to determine the point of oxygen insertion. Furthermore, in DTX-5a, oxygen insertion must occur after elimination of a carbon that previously formed a two-carbon unit with C1". This suggests that this step is post-PKS synthesis, and occurs as a tailoring step after the PK chain has been formed. It could also be interpreted to mean that the Favorski rearrangement occurs on the PKS during synthesis of the nascent PK chain. Decarboxylation of the terminal

acetate group may result in the release of the nascent PK chain from the PKS and the sulfation reactions probably occur after this event.

A significant difference between DTX-4 and the DTX-5 compounds (Fig. 33) is the presence of an amide link in the side chain of both DTX-5a and DTX-5b. The failure of [1,2-$^{13}C_2$] acetate to label either C-8" or C-9" in either of the DTX-5 molecules clearly indicated the participation of another precursor. This two-carbon unit with contiguous nitrogen suggested that the amino acid glycine might be incorporated directly into the nascent PK chain. This was confirmed in two separate feeding experiments in which cultures of *P. maculosum* were supplemented with [1,2-$^{13}C_2$]- and [2-$^{13}C,^{15}N$] glycine. The presence of a nitrogen atom and adjacent C8" and C9" in the sulfated side-chain of DTX-5a and 5b, which were not derived from acetate (Fig. 34), indicated that an amino acid is used to assemble this portion of the molecule. Hybrid PK/amino acid metabolites have been isolated previously [29]. The suspected amino acid derived portion of DTX-5 is structurally similar to glycine. Therefore, we supplemented DTX-5-producing cultures of *P. maculosum* with [1,2-$^{13}C_2$]- and [2-$^{13}C,^{15}N$] glycine in separate feeding experiments. In both compounds, incorporation of [1,2-$^{13}C_2$]-glycine resulted in labeling of C8"and C9" only, and the ^{13}C NMR data (Fig. 38) indicated that the carbon skeleton of glycine was incorporated intact. In the second feeding experiment, incorporation of [2-$^{13}C,^{15}N$] glycine revealed that the glycine nitrogen was also retained during uptake and biosynthesis (Fig. 39).
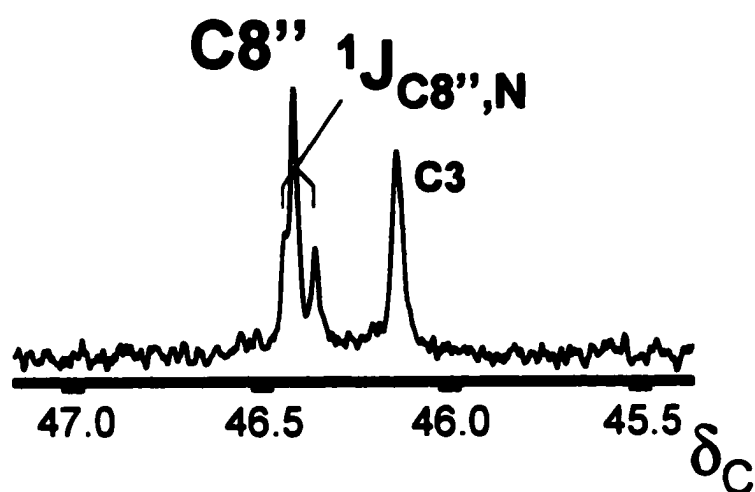
Fig. 39: Portion of the 125.7 MHz ^{13}C NMR spectrum of DTX-5b enriched from [2-^{13}C, ^{15}N] glycine. Arrows indicate ^{13}C-^{15}N coupling satellites due to incorporation of the intact ^{13}C-^{15}N unit of glycine into the N and C8" positions of DTX-5b.

The manner in which glycine is incorporated into the DTX-5a and 5b sulfated side-chain suggests that it may be used as an extender unit in the growing PK rather than as a starter unit. This is a rare example of a metabolite in which an amino acid is used as an extender unit in the middle of a growing PK chain. Since no ^{13}C-^{13}C coupling occurred between C-8" and C-9" of [1,2-$^{13}C_2$] acetate–labeled DTX-5, we conclude that the incorporation of glycine into DTX-5 is not the result of relaxed substrate specificity of the PKS. An intriguing possibility is that DTX-5a and 5b are assembled on a modular PKS enzyme that contains a module dedicated to the insertion of glycine into the growing PK. It is likely that the DTX-5 synthase is a hybrid of PKS and non-ribosomal peptide synthase (NRPS). Hybrid PKS/NRPS genes have been isolated from terrestrial cyanobacteria [90, 192] and actinomycetes [3]. Likewise, PKS and NRPS genes were isolated from a marine cyanobacterium known to produce the hybrid PK-peptide metabolite nodularin [109], though the entire biosynthetic gene has not been cloned and it is as yet unknown if it encodes a hybrid PKS/NRPS.

An assembly scheme for the side chain of the DTX-5 compounds is proposed (Fig. 40) that involves extension of a glycolate starter unit with 6 molecules of acetate followed by incorporation of a glycine molecule that is subsequently extended with another 3 acetate units. The assembly is proposed to occur on a modular hybrid PKS/NRPS/PKS, though involvement of separate enzymes cannot be ruled out. At the time of writing, however, all hybrid PKS/NRPS systems characterized at the molecular level are modular [30].
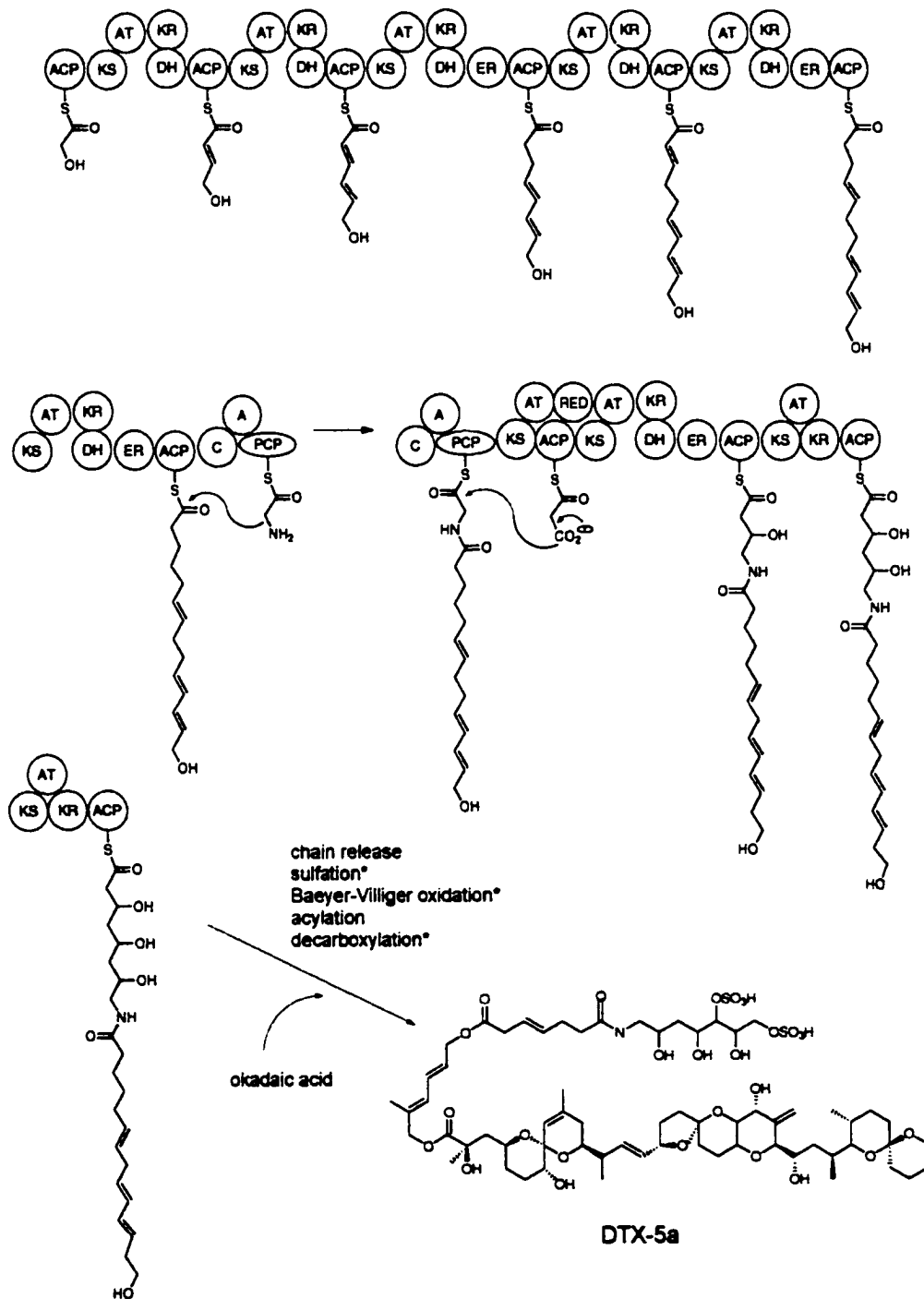
Fig. 40: Proposed scheme for assembly of the DTX-5a sulfated side-chain on a hybrid modular PKS/NRPS/PKS. ACP, acyl carrier protein; AT, acyl transferase; KS, ketosynthase; KR, ketoreductase; DH, dehydratase; ER, enoyl reductase; A, adenylation; C, condensation; PCP, peptidyl carrier protein; RED, reduction domain. * denotes reactions which may or may not occur while the molecule is attached to the enzyme, prior to esterification with okadaic acid.

The presence of an amino acid in the sulfated side-chains of both DTX-5a and DTX-5b may indicate different structural requirements for production of OKA as sulfated ester derivatives in different dinoflagellate species. It has been suggested that OKA is initially synthesized within dinoflagellate cells as non-toxic sulfated ester derivatives to assure autoresistance [106]. Hydrolysis to the active toxin would occur upon excretion to the extracellular environment, likely catalyzed by an inter-membrane esterase [106]. Consistent with this hypothesis is the observation that the sulfated ester derivatives of OKA are markedly less toxic than OKA in mouse bioassays [178, 179], and modification of the OKA C1 carboxyl reduces its inhibitory affect on protein phosphatases [187]. Furthermore, incubation of boiled *P. lima* cells with non-boiled *P. lima* culture resulted in complete hydrolysis of DTX-4 to OKA, presumably due to the presence of active esterase in the non-boiled culture (unpublished results). The chemical significance of the structural differences between the sulfated side-chains of DTX-4 and DTX-5a and 5b is unknown. The different structures of DTX-4, DTX-5a and 5b (Fig. 33), all of which involve the sulfated side-chain, may reflect specific requirements for their proper function in the environments in which *P. lima* and *P. maculosum* occur. Water temperature, salinity, pH and/or variety of competing microbes may have contributed to the selective pressure that determined the evolution of DSP synthases responsible for the assembly of DTX-4, DTX-5a and DTX-5b.

The labeling data clearly show that DTX-4 and DTX-5 compounds are PK derived. In both cases, the PK chain is extensively modified, yet the role of a

PKS in the biosynthesis of these compounds seems clear. It was of interest therefore, to isolate and sequence *P. lima* and *P. maculosum* PKS genes so as to 1) assess the level of similarity between dinoflagellate and known PKS genes from bacteria and fungi and 2) determine the relationship between dinoflagellate PKS gene sequence and biosynthesis of PK compounds they produce. To this end we examined *P. lima* DNA and cDNA and *P. maculosum* DNA for PKS genes. PCR screening of *P. lima* DNA and cDNA or *P. maculosum* DNA with degenerate primers designed using known fungal PKS sequences did not result in the amplification of PKS genes. This is likely due to sequence divergence between fungal and dinoflagellate PKS sequences. Given the unique chemistry that is a hallmark of dinoflagellate PK biosynthesis [101], their PKSs are likely to be significantly different from those of bacteria and fungi. Thus, PCR primers that bind PKS genes in the DNA of fungi or bacteria would not bind corresponding sequences in dinoflagellate DNA. It is therefore unlikely that dinoflagellate PKS genes can be isolated by way of PCR or molecular hybridization using PCR primers or probe DNAs derived from bacterial or fungal PKSs. The observation that PCR primers designed to amplify certain fungal ketosynthase (KS) genes do not amplify such genes in other fungi [120, 122] (also see section 2.0 of this thesis) is also an indication that they might not amplify dinoflagellate PKS genes. These results indicate that isolation of dinoflagellate PKS genes will require strategies not involving hybridization with DNAs derived from non-dinoflagellate genes. Potential experiments that could result in the isolation of dinoflagellate PKS genes are discussed in section 1.5 of

this thesis. Despite these challenges, genetic determinants of PK synthesis in dinoflagellates remain unknown. Therefore, the goal of identifying dinoflagellate PKS genes and harnessing their biosynthetic potential will continue to spur efforts of many scientists.

5.0 References

1. Simpson, T. J. (1995) Polyketide Biosynthesis, *Chem. Indust.*, 407-411.

2. Vining, L. C. (1992) Secondary metabolism, inventive evolution and biochemical diversity--a review, *Gene. 115*, 135-40.

3. Du, L. & Shen, B. (2001) Biosynthesis of hybrid peptide-polyketide natural products., *Curr. Opin. Drug Discov. Devel. 4*, 215-28.

4. Du, L., Sanchez, C. & Shen, B. (2001) Hybrid peptide-polyketide natural products: biosynthesis and prospects toward engineering novel molecules., *Metab. Eng. 3*, 78-95.

5. Mendez, C., Weitnauer, G., Bechthold, A. & Salas, J. A. (2000) Structure alteration of polyketides by recombinant DNA technology in producer organisms--prospects for the generation of novel pharmaceutical drugs., *Curr. Pharm. Biotechnol. 1*, 355-95.

6. Wright, L. F. & Hopwood, D. A. (1976) Actinorhodin is a chromosomally-determined antibiotic in *Streptomyces coelicolor* A3(2), *J. Gen. Microbiol. 96*, 289-97.

7. Rawlings, B. J. (2001) Type I polyketide biosynthesis in bacteria (Part A-erythromycin biosynthesis), *Nat. Prod. Rep. 18*, 190-227.

8. Fujii, I. (1999) Polyketide biosynthesis in filamentous fungi, in *Comrehensive Natural Products Chemistry* (Sankawa, U., ed pp. 409-441, Elsevier Science, Amsterdam.

9. Jez, J. M. & Noel, J. P. (2000) Mechanism of chalcone synthase. pKa of the catalytic cysteine and the role of the conserved histidine in a plant polyketide synthase., *J. Biol. Chem. 275*, 39640-6.

10. Wright, J. L., Vining, L. C., McInnes, A. G., Smith, D. G. & Walter, J. A. (1977) Use of ^{13}C in biosynthetic studies. The labelling pattern in tenellin enriched from isotope-labelled acetate, methionine, and phenylalanine, *Can. J. Biochem. 55*, 678-85.

11. Vederas, J. C. (1987) The use of stable isotopes in biosynthetic studies., *Nat. Prod. Rep. 4*, 277-337.

12. Dimroth, P., Walter, H. & Lynen, F. (1970) Biosynthesis of 6-methylsalicylic acid, *Eur. J. Biochem. 13*, 98-110.

13. Piel, J., Hertweck, C., Shipley, P. R., Hunt, D. M., Newman, M. S. & Moore, B. S. (2000) Cloning, sequencing and analysis of the enterocin biosynthesis gene cluster from the marine isolate '*Streptomyces maritimus*': evidence for the derailment of an aromatic polyketide synthase., *Chem. Biol. 7*, 943-55.

14. Molnar, I., Schupp, T., Ono, M., Zirkle, R., Milnamow, M., Nowak_Thompson, B., Engel, N., Toupet, C., Stratmann, A., Cyr, D. D., Gorlach, J., Mayo, J. M., Hu, A., Goff, S., Schmid, J. & Ligon, J. M. (2000) The biosynthetic gene cluster for the microtubule-stabilizing agents epothilones A and B from *Sorangium cellulosum* So ce90., *Chem. Biol. 7*, 97-109.

15. Suwa, M., Sugino, H., Sasaoka, A., Mori, E., Fujii, S., Shinkawa, H., Nimi, O. & Kinashi, H. (2000) Identification of two polyketide synthase gene clusters on the linear plasmid pSLA2-L in Streptomyces rochei., *Gene. 246*, 123-31.

16. Petkovic, H., Hrauneli, D., Raspor, P. & Hunter, I. (2000) The use of molecular biology to reprogram Streptomyces to make polyketide antibiotics more efficiently, and create novel secondary metabolites., *Pflugers Archiv. Eur. J. Physiol. 439*, R87-9.

17. Lal, R., Kumari, R., Kaur, H., Khanna, R., Dhingra, N. & Tuteja, D. (2000) Regulation and manipulation of the gene clusters encoding type-I PKSs., *Trends in Biotechnol. 18*, 264-74.

18. Gaisser, S., Reather, J., Wirtz, G., Kellenberger, L., Staunton, J. & Leadlay, P. F. (2000) A defined system for hybrid macrolide biosynthesis in *Saccharopolyspora erythraea.*, *Mol. Microbiol. 36*, 391-401.

19. Carreras, C. W. & Ashley, G. W. (2000) Manipulation of polyketide biosynthesis for new drug discovery., *EXS. 89*, 89-108.

20. Khosla, C. & Harbury, P. B. (2001) Modular enzymes, *Nature. 409*, 247-252.

21. Moore, B. S. & Piel, J. (2000) Engineering biodiversity with type II polyketide synthase genes., *Antonie Van Leeuwenhoek. 78*, 391-8.

22. Collie, J. N. (1907) Derivatives of the multiple ketene group, *Proc. Chem. Soc. 23*, 230-231.

23. Birch, A. J. & Donovan, F. W. (1953) Studies in relation to biosynthesis. I. Some possible routes to derivatives of orcinol and phloroglucinol., *Aust. J. Chem. 6*, 360-368.

24. Hopwood, D. A. & Sherman, D. H. (1990) Molecular genetics of polyketides and its comparison to fatty acid biosynthesis, *Annu. Rev. Genet. 24*, 37-66.

25. Bentley, R. & Bennett, J. W. (1999) Constructing Polyketides: From Collie to Combinatorial Biosynthesis, *Annu. Rev. Microbiol. 53*, 411-46.

26. Wright, L. F. & Hopwood, D. A. (1976) Identification of the antibiotic determined by the SCP1 plasmid of *Streptomyces coelicolor* A3(2), *J. Gen. Microbiol. 95*, 96-106.

27. Rudd, B. A. & Hopwood, D. A. (1979) Genetics of actinorhodin biosynthesis by *Streptomyces coelicolor* A3(2), *J. Gen. Microbiol. 114*, 35-43.

28. Brown, D. W., Yu, J. H., Kelkar, H. S., Fernandes, M., Nesbitt, T. C., Keller, N. P., Adams, T. H. & Leonard, T. J. (1996) Twenty-five coregulated transcripts define a sterigmatocystin gene cluster in *Aspergillus nidulans*, *Proc. Natl. Acad. Sci. U.S.A. 93*, 1418-22.

29. Silakowski, B., Nordsiek, G., Kunze, B., Blocker, H. & Muller, R. (2001) Novel features in a combined polyketide synthase/non-ribosomal peptide synthetase: the myxalamid biosynthetic gene cluster of the myxobacterium *Stigmatella aurantiaca* Sga15., *Chem. Biol. 8*, 59-69.

30. Doekel, S. & Marahiel, M. A. (2001) Biosynthesis of natural products on modular peptide synthetases., *Metab. Eng. 3*, 64-77.

31. Strohl, W. R. (2001) Biochemical engineering of natural product biosynthesis pathways., . *3*, 4-14.

32. Forrester, P. I. & Gaucher, G. M. (1972) Conversion of 6-methylsalicylic acid into patulin by *Penicillium urticae*, *Biochemistry. 11*, 1102-7.

33. Wang, I. K., Reeves, C. & Gaucher, G. M. (1991) Isolation and sequencing of a genomic DNA clone containing the 3' terminus of the 6-methylsalicylic acid polyketide synthetase gene of *Penicillium urticae*, *Can. J. Microbiol. 37*, 86-95.

34. Cortes, J., Haydock, S. F., Roberts, G. A., Bevitt, D. J. & Leadlay, P. F. (1990) An unusually large multifunctional polypeptide in the erythromycin-producing polyketide synthase of *Saccharopolyspora erythraea*, *Nature*. *348*, 176-8.

35. Beck, J., Ripka, S., Siegner, A., Schiltz, E. & Schweizer, E. (1990) The multifunctional 6-methylsalicylic acid synthase gene of *Penicillium patulum*. Its gene structure relative to that of other polyketide synthases, *Eur. J. Biochem. 192*, 487-98.

36. Bedford, D. J., Schweizer, E., Hopwood, D. A. & Khosla, C. (1995) Expression of a functional fungal polyketide synthase in the bacterium *Streptomyces coelicolor* A3(2), *J. Bacteriol. 177*, 4544-8.

37. Fujii, I., Mori, Y., Watanabe, A., Kubo, Y., Tsuji, G. & Ebizuka, Y. (2000) Enzymatic synthesis of 1,3,6,8-tetrahydroxynaphthalene solely from malonyl coenzyme A by a fungal iterative type I polyketide synthase PKS1., *Biochemistry. 39*, 8853-8.

38. Applebaum, R. S. & Marth, E. H. (1981) Biogenesis of the C20 polyketide, aflatoxin. A review, *Mycopathologia. 76*, 103-14.

39. Bhatnagar, D., Erhlich, K. C. & Cleveland, T. E. (1991) Oxidation-reduction reactions in biosynthesis of secondary metabolites., in *Handbook of Applied Mycology: Mycotoxins in Ecological Systems*. (Bhatnagar, D., Lillehoj, E. B. & Arora, D. K., eds) pp. 285-266, Marcel Dekker, Inc., New York.

40. Bennett, J. W. & Christensen, S. B. (1983) New perspectives on aflatoxin biosynthesis, *Adv. Appl. Microbiol. 29*, 53-92.

41. Yu, J., Cary, J. W., Bhatnagar, D., Cleveland, T. E., Keller, N. P. & Chu, F. S. (1993) Cloning and characterization of a cDNA from *Aspergillus parasiticus* encoding an O-methyltransferase involved in aflatoxin biosynthesis, *Appl. Environ. Microbiol. 59*, 3564-71.

42. Trail, F., Chang, P. K., Cary, J. & Linz, J. E. (1994) Structural and functional analysis of the nor-1 gene involved in the biosynthesis of aflatoxins by *Aspergillus parasiticus*, *Appl. Environ. Microbiol. 60*, 4078-85.

43. Trail, F., Mahanti, N., Rarick, M., Mehigh, R., Liang, S. H., Zhou, R. & Linz, J. E. (1995) Physical and transcriptional map of an aflatoxin gene cluster in *Aspergillus parasiticus* and functional disruption of a gene involved early in the aflatoxin pathway, *Appl. and Environ. Microbiol. 61*, 2665-73.

44. Yu, J. H. & Leonard, T. J. (1995) Sterigmatocystin biosynthesis in *Aspergillus nidulans* requires a novel type I polyketide synthase, *J. Bacteriol.* 177, 4792-800.

45. Feng, G. H. & Leonard, T. J. (1995) Characterization of the polyketide synthase gene (pksL1) required for aflatoxin biosynthesis in *Aspergillus parasiticus, J. Bacteriol.* 177, 6246-54.

46. Chang, P. K., Cary, J. W., Yu, J., Bhatnagar, D. & Cleveland, T. E. (1995) The *Aspergillus parasiticus* polyketide synthase gene pksA, a homolog of *Aspergillus nidulans* wA, is required for aflatoxin B1 biosynthesis, *Mol. Gen. Genet.* 248, 270-7.

47. Mahanti, N., Bhatnagar, D., Cary, J. W., Joubran, J. & Linz, J. E. (1996) Structure and function of fas-1A, a gene encoding a putative fatty acid synthetase directly involved in aflatoxin biosynthesis in *Aspergillus parasiticus, Appl. Environ. Microbiol.* 62, 191-5.

48. Brown, D. W., Adams, T. H. & Keller, N. P. (1996) *Aspergillus* has distinct fatty acid synthases for primary and secondary metabolism, *Proc. Natl. Acad. Sci. U.S.A.* 93, 14873-7.

49. Keller N.P., Watanabe C.M., Kelkar H.S., Adams T.H. & C.A., T. (2000) Requirement of monooxygenase-mediated steps for sterigmatocystin biosynthesis by Aspergillus nidulans., *Applied and Environmental Microbiology.* 66, 359-62.

50. Yu, J., Chang, P. K., Cary, J. W., Wright, M., Bhatnagar, D., Cleveland, T. E., Payne, G. A. & Linz, J. E. (1995) Comparative mapping of aflatoxin pathway gene clusters in *Aspergillus parasiticus* and *Aspergillus flavus, Appl. Environ. Microbiol.* 61, 2365-71.

51. Donadio, S., Staver, M. J., McAlpine, J. B., Swanson, S. J. & Katz, L. (1991) Modular organization of genes required for complex polyketide biosynthesis, *Science.* 252, 675-9.

52. Donadio, S., Staver, M. J., McAlpine, J. B., Swanson, S. J. & Katz, L. (1992) Biosynthesis of the erythromycin macrolactone and a rational approach for producing hybrid macrolides, *Gene.* 115, 97-103.

53. Bevitt, D. J., Cortes, J., Haydock, S. F. & Leadlay, P. F. (1992) 6-Deoxyerythronolide-B synthase 2 from *Saccharopolyspora erythraea.* Cloning of the structural gene, sequence analysis and inferred domain structure of the multifunctional enzyme, *Eur. J. Biochem.* 204, 39-49.

54.   Donadio, S., McAlpine, J. B., Sheldon, P. J., Jackson, M. & Katz, L. (1993) An erythromycin analog produced by reprogramming of polyketide synthesis, *Proc. Natl. Acad. Sci. U. S. A. 90*, 7119-23.

55.   Aggarwal, R., Caffrey, P., Leadlay, P. F., Smith, C. J. & Staunton, J. S. (1995) The Thioesterase of the Erythromycin-producing Polyketide Synthase: Mechanistic Studies *in vitro* to Investigate its Mode of Action and Substrate Specificity, *J. Chem. Soc. Chem. Commun.*, 1519-20.

56.   Kao, C. M., Luo, G., Katz, L., Cane, D. E. & Khosla, C. (1995) Manipulation of Macrolide Ring size by Directed Mutagenesis of a Modular Polyketide Synthase, *J. Am. Chem. Soc. 117*, 9105-6.

57.   McDaniel, R., Thamchaipenet, A., Gustafsson, C., Fu, H., Betlach, M. & Ashley, G. (1999) Multiple genetic modifications of the erythromycin polyketide synthase to produce a library of novel unnatural natural products, *Proc. Natl. Acad. Sci. U. S. A. 96*, 1846-51.

58.   Xue, Q., Ashley, G., Hutchinson, C. R. & Santi, D. V. (1999) A multiplasmid approach to preparing large libraries of polyketides, *Proc. Natl. Acad. Sci. U. S. A. 96*, 11740-5.

59.   Roberts, G. A., Staunton, J. & Leadlay, P. F. (1993) Heterologous expression in *Escherichia coli* of an intact multienzyme component of the erythromycin-producing polyketide synthase, *Eur. J. Biochem. 214*, 305-11.

60.   Lombo, F., Pfeifer, B., Leaf, T., Ou, S., Kim, Y. S., Cane, D. E., Licari, P. & Khosla, C. (2001) Enhancing the atom economy of polyketide Biosynthetic processes through metabolic engineering, *Biotechnol. Prog. 17*, 612-617.

61.   Tsuji, S. Y., Cane, D. E. & Khosla, C. (2001) Selective protein-protein interactions direct channeling of intermediates between polyketide synthase modules., *Biochemistry. 40*, 2326-31.

62.   Liberra, K. & Lindequist, U. (1995) Marine fungi--a prolific resource of biologically active natural products?, *Pharmazie. 50*, 583-8.

63.   Smith, C. J., Abbanat, D., Bernan, V. S., Maiese, W. M., Greenstein, M., Jompa, J., Tahir, A. & Ireland, C. M. (2000) Novel polyketide metabolites from a species of marine fungi., *J. Nat. Prod. 63*, 142-5.

64.   Faulkner, D. J. (2000) Marine natural products, *Nat. Prod. Rep. 17*, 7-55.

65. Tachibana, K., Scheuer, P. J., Tsukitani, Y., Kikuchi, H., Van Engen, D., Clardy, J., Gopichaud, Y. & Schmitz, F. J. (1981) Okadaic acid, a Cytotoxic Polyether from Two Marine Sponges of the Genus Halichondria., J. Am. Chem. Soc. 103, 2469-2471.

66. Kobayashi, M., Aoki, S., Gato, K. & Kitagawa, I. (1996) Marine natural products XXXVIII. Absolute stereostructures of altohyrtins A, B and C and 5-desacetylaltohyrtin A, potent cytotoxic macrolides, from the Okinawan marine sponge Hyrtios altum, Chem. Pharm. Bull. 44, 2142-2149.

67. Kobayashi, M. & Kitagawa, I. (1999) Marine spongean cytotoxins., J. Nat. Toxins. 8, 249-58.

68. Manker, D. C., Faulkner, D. J., Stout, T. J. & Clardy, J. (1989) The Baconipyrones: Novel polypropionates from the pulmonate Siphonaria baconi, J. Org. Chem. 54, 5371-5374.

69. Petit, G. R., Herald, C. L., Kamano, Y., Gust, D. & Aoyagi, R. (1983) The structure of bryostatin 2 from the marine bryozoan Bugula neritina, J. Nat. Prod. 46, 528-531.

70. Gustafson, K. & Andersen, R. J. (1982) Triophamine, a unique diacylguanidine from the dorid nudibranch Triopha catalinae (Cooper), J. Org. Chem. 47, 2167-2169.

71. Williams, D. E., Ayer, S. W. & Andersen, R. J. (1986) Diaulusterols A and B from the skin extracts of the dorid nudibranch Diaulula sandiegensis, Can. J. Chem. 64, 1527.

72. Murakami, Y., Oshima, Y. & Yasumoto, T. (1982) Identification of Okadaic Acid as a toxic component of a marine dinoflagellate Prorocentrum lima., Bull. Jap. Soc. Sci. Fish. 48, 69-72.

73. Wright, J. L. C. (1995) Dealing with seafood toxins: present approaches and future options, Food Res. Internat. 28, 347-358.

74. König, G. M. & Wright, A. D. (1996) Marine natural products research: current directions and future potential, Planta Med. 62, 193-211.

75. Moore, B. S. (1999) Biosynthesis of marine natural products: microorganisms and macroalgae, Nat. Prod. Rep. 16, 653-674.

76. Ford, P. W., Gadepalli, M. & Davidson, B. S. (1998) Halawanones A-D, new polycyclic quinones from a marine-derived streptomycete, J. Nat. Prod. 61, 1232-1236.

77.   Gustafson, K., Roman, M. & Fenical, W. (1989) The macrolactins, a novel class of antiviral and cytotoxic macrolides from a deep-sea marine bacterium, *J. Am. Chem. Soc. 111*, 7519-7524.

78.   Rychnovsky, S. D., Skalitzky, D. J., Pathirana, C., Jensen, P. R. & Fenical, W. (1992) Stereochemistry of the macrolactins, *J. Am. Chem. Soc. 114*, 671-677.

79.   Poch, G. K. & Gloer, J. B. (1989) Obionin A: a new polyketide metabolite from the marine fungus *Lyptoshpaeria obiones, Tetrahedron Lett. 30*, 3483-3486.

80.   Breinholt, J., Jensen, G. W., Nielsen, R. I., Olsen, C. E. & Frisvad, J. C. (1993) Antifungal macrocyclic polyactones from *Penicillium verruculosum*, *J. Antibiot. 46*, 1101-1108.

81.   Graber, M. A. & Gerwick, W. H. (1998) Kalkipyrone, a toxic g-pyrone from an assemblage of the marine cyanobacteria *Lyngbya majuscula* and *Tolypothrix* sp., *J. Nat. Prod. 61*, 677-680.

82.   Carmeli, S., Moore, R. E., Patterson, G. M. I. & Yoshida, W. Y. (1993) Biosynthesis of tolytoxin. Origin of the carbons and heteroatoms, *Tetrahedron. Lett. 34*, 5571-5574.

83.   Needham, J., Andersen, R. J. & Kelly, M. T. (1991) Oncorhyncolide, a novel metabolite of a bacterium isolated from seawater, *Tetrahedron Lett. 32*, 315-318.

84.   Carmichael, W. W., Beasley, V., Bunner, D. L., Eloff, J. N., Falconer, I., Gorham, P., Harada, K., Krishnamurthy, T., Yu, M. J. & Moore, R. E. (1988) Naming of cyclic heptapeptide toxins of cyanobacteria (blue-green algae), *Toxicon. 26*, 971-973.

85.   de Silva, E. D., Williams, D. E., Andersen, R. J., Klix, H., Holmes, C. F. B. & Allen, T. M. (1992) Motuporin, a potent protein phosphatase inhibitor isolated from the Papua New Guinea sponge *Theonella swinhoei* Gray., *Terahedron Lett. 33*, 1561-1564.

86.   Jensen, P. R. & Fenical, W. (1994) Strategies for the discovery of secondary metabolites from marine bacteria: ecological perspectives, *Annu. Rev. Microbiol. 48*, 559-84.

87.   Needham, J., Andersen, R. J. & Kelly, M. T. (1992) Biosynthesis of Oncorhyncolide, a Metabolite of the Seawater Bacterial Isolate MK157, *J. Chem. Soc., Chem. Commun.*, 1367-1369.

88. Biabani, M. A. F. & Laatsch, H. (1998) Advances in Chemical Studies on Low-Molecular Weight Metabolites of Marine Fungi, *J. Prakt. Chem. 340*, 589-607.

89. Moore, R. E., Chen, J. L., Moore, B. S. & Patterson, G. M. L. (1991) Biosynthesis of Microcystin-LR. Origin of the Carbons in the Adda and Masp Units., *J. am. Chem. Soc. 113*, 5083-5084.

90. Nishizawa, T., Ueda, A., Asayama, M., Fujii, K., Harada, K., Ochi, K. & Shirai, M. (2000) Polyketide synthase gene coupled to the peptide synthetase module involved in the biosynthesis of the cyclic heptapeptide microcystin, *J. Biochem. (Tokyo). 127*, 779-89.

91. Taylor, F. J. R. (1987) General group characteristics; special features of interest; short history of dinoflagellate study, in *The Biology of Dinoflagellates* (Taylor, F. J. R., ed pp. 1-23, Blackwell Scientific Publications, London.

92. Wright, J. L. C. & Cembella, A. D. (1998) Ecophysiology and Biosynthesis of Polyether Marine Biotoxins, in *Physiological Ecology of Harmful Algal Bloms* (Andersen, D. M., Cembella, A. D. & Hallegraeff, G. M., eds) pp. 427-451, Springer, New York.

93. Murakami, M., Makabe, K., Yamaguchi, K. & Konosu, S. (1988) Goniodomin A, a novel polyether macrolide from the dinoflagellate *Goniodoma pseudogoniaulax*, *Tetrahedron Lett. 29*, 1149-1152.

94. Hu, T., Curtis, J. M., Oshima, Y., Quilliam, M. A., Walter, J. A., Watson-Wright, W. M. & Wright, J. L. C. (1995) Spirolides B and D, Two Novel Macrocycles Isolated from the Digestive Glands of Shellfish, *J. Chem. Soc. Chem. Commun.*, 2159-2161.

95. Torigoe, K., Murata, M. & Yasumoto, T. (1988) Prorocentrolide, a Toxic Nitrogenous Macrocycle from a Marine Dinoflagellate, *Prorocentrum lima*, *J. Am. Chem. Soc. 110*, 7876-7877.

96. Kobayashi, M., Sato, M. & Ishibashi, M. (1993) Amphidinolide J: A cytotoxic macrolide from the marine dinoflagellate *Amphidinium* sp. Determination of the absolute stereochemistry, *J. Org. Chem. 58*, 2645-2646.

97. Lin, Y.-Y. & Risk, M. (1981) Isolation and Structure of Brevetoxin B from the "Red Tide" Dinoflagellate *Ptychodiscus brevis*, *J. Am. Chem. Soc. 103*, 6773-6775.

98. Lee, M. S., Repeta, D. J. & Nakanishi, K. (1986) Biosynthetic Origins and Assignments of ^{13}C NMR Peaks of Brevetoxin B, *J. Am. Chem. Soc. 108*, 7855-7856.

99. Chou, H. & Shimuzu, Y. (1987) Biosynthesis of Brevetoxins. Evidence for the Mixed Origin of the Backbone Carbon Chain and the Possible Involvement of Dicarboxylic Acids, *J. Am. Chem. Soc. 109*, 2184-2185.

100. Lee, M. S., Qin, G., Nakanishi, K. & Zagorski, G. (1989) Biosynthetic Studies of Brevetoxins, Potent Neurotoxins Produced by the Dinoflagellate *Gymnodinium breve*, *J. Am. Chem. Soc. 111*, 6234-6241.

101. Rein, K. S. & Borrone, J. (1999) Polyketides from dinoflagellates: origins, pharmacology and biosynthesis, *Comp. Biochem. Physiol. B. Biochem. Mol. Biol. 124*, 117-131.

102. Kobayashi, J., Takahashi, M. & Ishibashi, M. (1995) Biosynthetic Studies of Amphidinolide J: Explanation of the Generation of the Unusual Odd-numbered Macrocyclic Lactone, *J. Chem. Soc., Chem. Commun.*, 1639-1640.

103. Kobayashi, J., Kubota, T., Endo, T. & Tsuda, M. (2001) Amphidinolides T2, T3, and T4, new 19-membered macrolides from the dinoflagellate *Amphidinium* sp. and the biosynthesis of amphidinolide T1., *J. Org. Chem. 66*, 134-42.

104. Norte, M., Padilla, A. & Fernandez, J. J. (1994) Studies on the Biosynthesis of the Polyether Marine Toxin Dinophysistoxin-1 (DTX-1), *Tetrahedron Lett. 35*, 1441-1444.

105. Norte, M., Padilla, A., Fernandez, J. J. & Souto, M. L. (1994) Structural Determination and Biosynthetic Origin of Two Ester Derivatives of Okadaic Acid Isolated From *Prorocentrum lima, Tetrahedron. 50*, 9175-9180.

106. Needham, J., Hu, T., McLachlan, J. L., Walter, J. A. & Wright, J. L. C. (1995) Biosynthetic Studies of the DSP Toxin DTX-4 and an Okadaic Acid Diol Ester, *J. Chem. Soc., Chem. Commun.*, 1623-1624.

107. Wright, J. L. C., Hu, T., McLachlan, J. L., Needham, J. & Walter, J. A. (1996) Biosynthesis of DTX-4: Confirmation of a Polyketide Pathway, Proof of a Baeyer-Villiger Oxidation Step, and Evidence for an Unusual Carbon Deletion Process, *J. Am. Chem. Soc. 118*, 8757-8758.

108. Metz, J. G., Roessler, P., Facciotti, D., Levering, C., Dittrich, F., Lassner, M., Valentine, R., Lardizabal, K., Domergue, F., Yamada, A., Yazawa, K., Knauf, V. & Browse, J. (2001) Production of polyunsaturated fatty acids by polyketide synthases in both prokaryotes and eukaryotes., *Science. 293,* 290-3.

109. Moffitt, M. C. & Neilan, B. A. (2001) On the presence of peptide synthetase and polyketide synthase genes in the cyanobacterial genus *Nodularia., Fems Microbiol. Lett. 196,* 207-14.

110. Rizzo, P. J. (1987) Biochemistry of the dinoflagellate nucleus., in *The Biology of Dinoflagellates* (Taylor, F. J. R., ed pp. 143-173, Blackwell Scientific Publications, London.

111. Plumley, F. G. (1997) Marine algal toxins: Biochemistry, genetics and molecular biology, *Limnol. Oceanogr. 42,* 1252-1264.

112. ten Lohuis, M. R. & Miller, D. J. (1998) Genetic transformation of Dinoflagellates (*Amphidinium* and *Symbiodinium*): expression of GUS in microalgae using heterologous promoter constructs, *Plant J. 13,* 427-435.

113. Strong, W. B. & Nelson, R. G. (2000) Preliminary profile of the *Cryptosporidium parvum* genome: an expressed sequence tag and genome survey sequence analysis, *Mol. Biochem. Parasitol. 107,* 1-32.

114. Fujii, I., Ono, Y., Tada, H., Gomi, K., Ebizuka, Y. & Sankawa, U. (1996) Cloning of the polyketide synthase gene atX from *Aspergillus terreus* and its identification as the 6-methylsalicylic acid synthase gene by heterologous expression, *Mol. Gen. Genet. 253,* 1-10.

115. Sweeney, M. J. & Dobson, A. D. (1999) Molecular biology of mycotoxin biosynthesis, *Fems Microbiol. Lett. 175,* 149-63.

116. Hajjaj, H., Klaebe, A., Loret, M. O., Goma, G., Blanc, P. J. & Francois, J. (1999) Biosynthetic Pathway of Citrinin in the Filamentous Fungus *Monoascus ruber* as Revealed by [13]C Nuclear Magnetic Resonance, *Appl. Environ. Microbiol.,* 311-314.

117. Doolittle, W. F. (1999) Lateral genomics., *Trends Cell. Biol. 9,* M5-8.

118. Walton, J. D. (2000) Horizontal gene transfer and the evolution of secondary metabolite gene clusters in fungi: an hypothesis., *Fungal Genet. Biol. 30,* 167-71.

119. Hopwood, D. A. (1997) Genetic contributions to understanding polyketide synthases., *Chem. Rev. 97,* 2465-2497.

120. Bingle, L. E., Simpson, T. J. & Lazarus, C. M. (1999) Ketosynthase domain probes identify two subclasses of fungal polyketide synthase genes, *Fungal Genet. Biol. 26*, 209-23.

121. Bell, A. A. & Wheeler, M. H. (1986) Biosynthesis and function of fungal melanins, *Ann. Rev. Phytopathol. 24*, 411-451.

122. Nicholson, T. P., Rudd, B. A., Dawson, M., Lazarus, C. M., Simpson, T. J. & Cox, R. J. (2001) Design and utility of oligonucleotide gene probes for fungal polyketide synthases, *Chem. Biol. 8*, 157-78.

123. Jones, C. A., Sidebottom, P. J., Cannell, R. J., Noble, D. & Rudd, B. A. (1992) The squalestatins, novel inhibitors of squalene synthase produced by a species of *Phoma*. III. Biosynthesis, *J. Antibiot. (Tokyo). 45*, 1492-8.

124. Hutchinson, C. R., Kennedy, J., Park, C., Kendrew, S., Auclair, K. & Vederas, J. (2000) Aspects of the biosynthesis of non-aromatic fungal polyketides by iterative polyketide synthases., *Antonie Van Leeuwenhoek. 78*, 287-95.

125. Yang, G., Rose, M. S., Turgeon, B. G. & Yoder, O. C. (1996) A polyketide synthase is required for fungal virulence and production of the polyketide T-toxin, *Plant Cell. 8*, 2139-50.

126. Sambrook, J., Fritsh, E. F. & Maniatis, T. (1989) *Molecular Cloning: A Laboratory Manual*, 2 edn, Cold Spring Harbor Laboratory Press, New York.

127. Altschul, S. F., Gish, W., Miller, W., Myers, E. W. & Lipman, D. J. (1990) Basic local alignment search tool, *J. Mol. Biol. 215*, 403-410.

128. Thompson, J. D., Higgins, D. G. & Gibson, T. J. (1994) CLUSTAL W: improving the sensitivity of progressive multiple sequence alignment through sequence weighting, position specific gap penalties and weight matrix choice., *Nucl. Acids Res. 22*, 4673-80.

129. Holler, U., Konig, G. M. & Wright, A. D. (1999) Three New Metabolites from the Marine-Derived Fungi of the Genera *Coniothyrium* and *Microsphaeropsis*, *J. Nat. Prod. 62*, 114-118.

130. Kobayashi, J. & Ishibashi, M. (1999) Marine Natural Products and Marine Chemical Ecology, in *Comprehensive Natural Products Chemistry* (Mori, K., ed pp. 415-649, Elsevier Science B.V., Amsterdam.

131. Rahbaek, L., Sperry, S., Piper, J. E. & Crews, P. (1998) Deoxynortrichoharzin, a new polyketide from the saltwater culture of a sponge-derived *Paecilomyces* fungus, *J. Nat. Prod. 61*, 1571-3.

132. Keller, N. P. & Hohn, T. M. (1996) Metabolic pathway gene clusters in filamentous fungi., *Fungal Genet. Biol. 21*, 17-29.

133. Fulton, T. R., Ibrahim, N., Losada, M. C., Grzegorski, D. & Tkacz, J. S. (1999) A melanin polyketide synthase (PKS) gene from *Nodulisporium* sp. that shows homology to the pks1 gene of *Colletotrichum lagenarium.*, *Mol. Gen. Genet. 262*, 714-20.

134. Liras, P., Rodriguez_Garcia, A. & Martin, J. F. (1998) Evolution of the clusters of genes for beta-lactam antibiotics: a model for evolutive combinatorial assembly of new beta-lactams., *Int. Microbiol. 1*, 271-8.

135. Lawrence, J. G. & Roth, J. R. (1996) Selfish operons: horizontal transfer may drive the evolution of gene clusters., *Genetics. 143*, 1843-60.

136. Lumbsch, H. T. (2000) Phylogeny of filamentous ascomycetes, *Naturwissenschaften. 87*, 335-342.

137. Natvig, D. O. & May, G. (1996) Fungal evolution and speciation, *J. Genet. 75*, 441-452.

138. Peterson, R. H. & Hughes, K. W. (1999) Species and speciation in mushrooms, *Bioscience. 49*, 440-452.

139. Frisvad, J. C. & Filtenborg, O. (1990) Secondary metabolites as consistent criteria in *Penicillium* taxonomy and a synoptic key to *Penicillium* subgenus *Penicillium.*, in *Modern Concepts in Penicillium and Aspergillus Classification* (Samson, R. A. & Pitt, J. I., eds) pp. 373-384, Plenem Press, New York.

140. Gruner, J. & Traxler, P. (1977) Papulacandin, a new antibiotic, active especially against yeasts., *Experientia. 33*, 137.

141. Traxler, P., Gruner, J. & Auden, J. A. L. (1977) Papulacandins, a new family of antibiotics with antifungal activity, *J. Antibiot. 30*, 289-296.

142. Baguley, B. C., Rommele, G., Gruner, J. & Wehrli, W. (1979) Papulacandin B: an inhibitor of glucan synthesis in yeast spheroplasts, *Eur. J. Biochem. 97*, 345-351.

143. Murgui, A., Victoria Elorza, M. & Sentandreu, R. (1985) Effect of Papulacandin B and calcofluor white on the incorporation of mannoproteins in the wall of Candida albicans blastospores, Biochim. Biophys. Acta. 841, 215-222.

144. Perez, P., Varona, R., Garcia-Archa, I. & Duran, A. (1981) Effect of Papulacandin B and Aculeacin A on b-(1,3) glucan-synthase from Geotrichum lactis, FEBS Letters. 129, 249-252.

145. Perez, P., Garcia-Acha, I. & Duran, A. (1983) Effect of Papulacandin B on the cell wall and growth of Geotrichum lactis, J. Gen. Microbiol. 129, 245-250.

146. Kopecka, M. (1984) Lysis of growing cells of Saccharomyces cerevisiae induced by Papulacandin B, Folia Microbiol. 29, 115-119.

147. Kopecka, M. (1984) Papulacandin B: inhibitor of biogenesis of (1-3)-b-D-glucan fibrillar component of the cell wall of Saccharomyces cerevisiae protoplasts, Folia Microbiol. 29, 441-449.

148. Hector, R. F. (1993) Compounds active against cell walls of medically important fungi, Clin. Microbiol. Rev. Jan., 1-21.

149. Traxler, P., Fritz, H., Fuhrer, H. & Richter, W. J. (1980) Papulacandins, a new family of antibiotics with antifungal activity:
Structures of papulacandins A, B, C and D, J. Antibiot. 38, 967-978.

150. Danishefsky, S., Phillips, G. & Ciufolini, M. (1987) A fully synthetic route to the papulacandins. Stereo-specific spiroacetalization of a C-1-arylated methyl glycoside., Carbohydr. Res. 171, 317-27.

151. Parker, K. A. & Georges, A. T. (2000) Reductive Aromatization of Quinols: Synthesis of the C-Arylglycoside Nucleus of the Papulacandins and Chaetiacandin, Org. Lett. 2, 497-499.

152. Balachari, D. & O'Doherty, G. A. (2000) Sharpless Asymmetric Dihydroxylation of 5-Aryl-2-vinylfurans: Applicationto the Synthesis of the Spiroketal Moiety of Papulacandin D, Org. Lett. 2, 863-866.

153. Balachari, D. & O'Doherty, G. A. (2000) Enantioselective Synthesis of the Papulacandin Ring System: Conversion of the Mannose Diastereoisomer into a Glucose Stereoisomer, Org. Lett. 2, 4033-4036.

154. Traxler, P., Tosch, W. & Zak, O. (1987) Papulacandins- synthesis and biological activity of Papulacandin B derivatives, J. Antibiot. XL, 1146-1164.

155. Bartizal, K., Abruzzo, G., Trainor, C., Krupa, D., Nollstadt, K., Schmatz, D., Schwartz, R., Hammond, M., Balkovec, J. & Vanmiddlesworth, F. (1992) In vitro antifungal activities and in vivo efficacies of 1,3-beta-D-glucan synthesis inhibitors L-671,329, L-646,991, tetrahydroechinocandin B, and L-687,781, a papulacandin., *Antimicrob. Agents Chemother.* 36, 1648-57.

156. Debono, M. & Gordee, R. S. (1994) Antibiotics that inhibit fungal cell wall development, *Annu. Rev. Microbiol.* 48, 471-497.

157. Frost, D. J., Brandt, K., Capobianco, J. & Goldman, R. (1994) Characterization of (1,3)-beta-glucan synthase in *Candida albicans*: microsomal assay from the yeast or mycelial morphological forms and a permeabilized whole-cell assay., *Microbiology.* 140 (Pt 9), 2239-46.

158. Traxler, P., Fritz, H. & Richter, W. J. (1977) Zur struktur von Papulacandin B, einem neuen antifungischen antibiotikum, *Helv. Chim. Acta.* 60, 578-584.

159. Komori, T., Yamashita, M., Tsurumi, Y. & Kohsaka, M. (1985) Chaetiacandin, a novel Papulacandin I. Fermentation, isolation and characterization, *J. Antibiot.* 38, 455-459.

160. Komori, T. & Itoh, Y. (1985) Chaetiacandin, a novel Papulacandin II. Structure determination, *J. Antibiot.* 38, 544-546.

161. VanMiddlesworth, F., Nallin Omstead, M., Schmatz, D., Bartizal, K., Fromptling, R., Bills, G., Nollstadt, K., Honeycutt, S., Zweerink, M., Garrity, G. & Wilson, K. (1991) L-687,781, a new member of the Papulacandin family of b-1,3-D-glucan synthesis inhibitors I. Fermentation, isolation and biological activity, *J. Antibiot.* 44, 45-51.

162. Kaneto, R., Chiba, H., Agematu, H., Shibamoto, N., Yoshioka, T., Nishida, H. & Okamoto, R. (1993) Mer-WF3010, a new member of the Papulacandin family I. Fermentation, isolation and characterization, *J. Antibiot.* 46, 247-250.

163. Chiba, H., Kaneto, R., Agematu, H., Shibamoto, N., Yoshioka, T., Nishida, H. & Okamoto, R. (1993) Mer-WF3010, a new member of the Papulacandin family II. Structure determination, *J. Antibiot.* 46, 356-358.

164. Aoki, M., Andoh, T., Ueki, T., Mauyoshi, S., Sugawara, K. & Oki, T. (1993) BU-4794F, a new b-1,3-glucan synthase inhibitor, *J. Antibiot.* 46, 952-960.

165. Rommele, G., Traxler, P. & Wehrli, W. (1983) Papulacandins-the relationship between chemical structure and effect on glucan synthesis in yeast., *J. Antibiot. 36*, 1539-1542.

166. Okada, H., Nagashima, M., Suzuki, H., Nakajima, S., Kojiri, K. & Suda, H. (1996) BE-29602, a new member of the papulacandin family, *J. Antibiot. 49*, 103-106.

167. Chen, R. H., Tennant, S., Frost, D., O_Beirne, M. J., Karwowski, J. P., Humphrey, P. E., Malmberg, L. H., Choi, W., Brandt, K. D., West, P., Kadam, S. K., Clement, J. J. & McAlpine, J. B. (1996) Discovery of saricandin, a novel papulacandin, from a *Fusarium* species., *J. Antibiot. (Tokyo). 49*, 596-8.

168. Ramsey, U. P., Douglas, D. J., Walter, J. A. & Wright, J. L. C. (1998) Biosynthesis of Domoic Acid by the Diatom *Pseudo-nitzschia multiseries*, *Nat. Toxins. 6*, 137-146.

169. Quiros, L. M. & Salas, J. A. (1995) Biosynthesis of the macrolide oleandomycin by *Streptomyces antibioticus*. Purification and kinetic characterization of an oleandomycin glucosyltransferase., *J. Biol. Chem. 270*, 18234-9.

170. Quiros, L. M., Carbajo, R. J., Brana, A. F. & Salas, J. A. (2000) Glycosylation of macrolide antibiotics. Purification and kinetic studies of a macrolide glycosyltransferase from *Streptomyces antibioticus*., *J. Biol. Chem. 275*, 11713-20.

171. Moore, R. N., Bigam, G., Chan, J. K., Hogg, A. M., Nakashima, T. T. & Vederas, J. C. (1985) Biosynthesis of the Hypocholesterolemic Agent Mevinolin by *Aspergillus terreus*. Determination of the Origin of Carbon, Hydrogen, and Oxygen Atoms by ^{13}C NMR and Mass Spectrometry., *J. Am. Chem. Soc. 107*, 3694-3701.

172. Hendrickson, L., Davis, C. R., Roach, C., Nguyen, D. K., Aldrich, T., McAda, P. C. & Reeves, C. D. (1999) Lovastatin biosynthesis in *Aspergillus terreus*: characterization of blocked mutants, enzyme activities and a multifunctional polyketide synthase gene, *Chem. Biol. 6*, 429-39.

173. Alfatafta, A. A., Gloer, J. B., Scott, J. A. & Malloch, D. (1994) Apiosporamide, a new antifungal agent from the coprophilous fungus Apiospora montagnei., *Journal of Natural Products. 57*, 1696-702.

174. Yasumoto, T., Murata, M., Oshima, Y., Sano, M., Matsumoto, G. K. & Clardy, J. (1985) Diarrhetic Shellfish Toxins, *Tetrahedron. 41*, 1019-1025.

175. Lee, J., Igarashi, T., Fraga, S., Dahl, E., Hovgaard, P. & Yasumoto, T. (1989) Determination of diarrhetic shellfish toxins in various dinoflagellate species., *J. App. Phycol. 1*, 147-152.

176. Marr, J. C., Jackson, A. E. & McLachlan, J. L. (1991) Occurence of *Prorocentrum lima*, a DSP toxin-producing species from the Atlantic coast of Canada., *J. Appl. Phycol. 0*, 1-8.

177. Hu, T., Marr, J., deFrietas, W., Quilliam, M. A., Walter, J. A. & Wright, J. L. C. (1992) New diol esters isolated from cultures of the dinoflagellates *Prorocentrum lima and Prorocentrum concavum.*, *J. Nat. Prod. 55*, 1631.

178. Hu, T., Curtis, J. M., Walter, J. A. & Wright, J. L. C. (1995) Identification of DTX-4, a New Water-soluble Phosphatase Inhibitor from the Toxic Dinoflagellate *Prorocentrum lima*, *J. Chem. Soc., Chem. Commun.*, 597-599.

179. Hu, T., Curtis, J. M., Walter, J. A., McLachlan, J. L. & Wright, J. L. C. (1995) Two New Water-Soluble DSP Toxin Derivatives from the Dinoflagellate *Prorocentrum maculosum*: Possible Storage and Excretion Products., *Tetrahedron Lett. 36*, 9273-9276.

180. Hu, T., Doyle, J., Jackson, D., Marr, J., Nixon, E., Pleasance, S., Quilliam, M. A., Walter, J. A. & Wright, J. L. C. (1992) Isolation of a new diarrhetic shellfish poison from Irish mussels., *J. Chem. Soc. Chem. Commun. 39*, 39-41.

181. Bialojan, C. & Takai, A. (1988) Inhibitory effect of a marine-sponge toxin, okadaic acid, on protein phosphatases. Specificity and kinetics., *Biochemical Journal. 256*, 283-90.

182. Bialojan, C., Ruegg, J. C. & Takai, A. (1988) Effects of okadaic acid on isometric tension and myosin phosphorylation of chemically skinned guinea-pig taenia coli., *J. Physiol. 398*, 81-95.

183. Wilson, A. K., Takai, A., Ruegg, J. C. & de_Lanerolle, P. (1991) Okadaic acid, a phosphatase inhibitor, decreases macrophage motility., *Am. J. Physiol. 260*, L105-12.

184. Cohen, P. & Cohen, P. T. (1989) Protein phosphatases come of age., *J. Biol. Chem. 264*, 21435-8.

185. Haystead, T. A., Sim, A. T., Carling, D., Honnor, R. C., Tsukitani, Y., Cohen, P. & Hardie, D. G. (1989) Effects of the tumour promoter okadaic acid on intracellular protein phosphorylation and metabolism., *Nature. 337*, 78-81.

186. Tapia, R., Pena, F. & Arias, C. (1999) Neurotoxic and synaptic effects of okadaic acid, an inhibitor of protein phosphatases, *Neurochem. Res.* *24*, 1423-30.

187. Takai, A., Murata, M., Torigoe, K., Isobe, M., Mieskes, G. & Yasumoto, T. (1992) Inhibitory effect of okadaic acid derivatives on protein phosphatases. A study on structure-affinity relationship., *Biochem. J.* *284 (Pt 2)*, 539-44.

188. Rawlings, B. J. (2001) Type I polyketide biosynthesis in bacteria (part B)., *Nat. Prod. Rep.* *18*, 231-81.

189. Needham, J., McLachlan, J. L., Walter, J. A. & Wright, J. L. C. (1994) Biosynthetic Origin of C-37 and C-38 in the Polyether Toxins Okadaic Acid and Dinophysistoxin-1, *J. Chem. Soc., Chem. Commun*, 2599-2600.

190. Murata, M., Izumikawa, M., Tachibana, K., Fujita, T. & Naoki, H. (1998) Labeling pattern of okadaic acid from $^{18}O_2$ and $[^{18}O_2]$ acetate. Elucidation by collision-induced dissociation tandem mass spectrometry., *J. Am. Chem. Soc.* *120*, 147-151.

191. Izumikawa, M., Murata, M., Tachibana, K., Fujita, T. & Naoki, H. (2000) 18O-Labelling pattern of okadaic acid from H218O in dinoflagellate Prorocentrum lima elucidated by tandem mass spectrometry., *Eur. J. Biochem.* *267*, 5179-83.

192. Tillett, D., Dittmann, E., Erhard, M., von_Dohren, H., Borner, T. & Neilan, B. A. (2000) Structural organization of microcystin biosynthesis in *Microcystis aeruginosa* PCC7806: an integrated peptide-polyketide synthetase system., *Chem. Biol.* *7*, 753-64.